Genetic and Molecular Analysis of *Caenorhabditis elegans* *unc-69* Gene in Axonal Outgrowth and Presynaptic Differentiation

---

Dissertation

zur

Erlangung der naturwissenschaftlichen Doktorwürde
(Dr. sc. nat.)

vorgelegt der

Mathematisch-naturwissenschaftlichen Fakultät

der

Universität Zürich

von

Cheng-Wen Su

aus

Taiwan

Promotionskomitee

Prof. Dr. Michael O. Hengartner (Vorsitz)

Prof. Dr. Barry Dickson

Prof. Dr. Alex Hajnal

Prof. Dr. Martin Schwab

Zürich, 2005

To my family

Table of Contents

Zusammenfassung

Der Nematode *C. elegans* wurde in grossem Rahmen als Modellsystem eingesetzt, um die genetischen Voraussetzungen für die richtige Entwicklung und Funktion des Nervensystems zu ermitteln. Das *C. elegans*-Gen *unc-69* ist erforderlich für die Steuerung, das Auswachsen und die Bündelung der Axone und für die Synaptogenese. UNC-69 ist ein Protein aus 108 Aminosäuren mit einer kurzen Coiled-coil-Domäne. Während in starken *unc-69* Funktionsverlust-Mutanten die Axone nicht genügend wachsen und die Bündelung verloren geht, bewirkt das Allel *unc-69(ju69)*, welches die Funktion nur schwach reduziert, vor allem die falsche Lokalisierung von SNB-1::GFP, einem Markierer von synaptischen Vesikeln. UNC-69 ist spezifisch notwendig für das Auswachsen der Axone und die präsynaptische Differenzierung, zumal die Dendriten in *unc-69*-Mutanten normal wachsen und der Diazetylrezeptor ODR-10 zu den Zilien gelangt.

UNC-69 ist ein neuer Bindungspartner von UNC-76, einem Protein, welches in vielen Organismen für die Verlängerung und Bündelung der Axone und den axonalen Transport zuständig ist. UNC-69 und UNC-76 kolokalisieren in den Neuronen als Puncta und regulieren gemeinsam die Verlängerung der sensorischen Axone und die Lokalisierung von SNB-1::GFP. Allerdings können UNC-69 und UNC-76 in Würmern teilweise nicht kolokalisieren, in denen *unc-116* mutiert ist, das *C. elegans* Ortholog der schweren Kinesin-Kette, welches ebenfalls Defekte im Auswachsen der Axone und in der normalen präsynaptischen Differenzierung zur Folge hat. Möglicherweise reguliert der UNC-69/UNC-76-Komplex durch die Assoziation mit der schweren Kinesin-Kette den axonalen Transport. Ausserdem deuten meine Resultate darauf hin, dass Synapsenbildung und Wachstum der Axone eng gekoppelte

Prozesse sind, eine Funktion, die unter Umständen evolutionär weitgehend konserviert ist.

Summary

The nematode *C. elegans* has been used extensively as a model system to identify genetic requirements for proper nervous system development and function. The *C. elegans* gene *unc-69* is required for axon guidance, outgrowth, fasciculation and synaptogenesis. UNC-69 is a 108 amino acid protein with a short coiled-coil domain. Whereas axons fail to elongate and become defasciculated in strong *unc-69* loss-of-function mutants, the weak reduction-of-function allele *unc-69(ju69)* preferentially causes mislocalization of synaptic vesicle marker SNB-1::GFP. UNC-69 is specifically required for axonal outgrowth and presynaptic differentiation, as *unc-69* mutants do not show defects in dendritic growth or targeting the diacetyl receptor ODR-10 to cilia.

UNC-69 is a novel binding partner of UNC-76, a protein required for axon elongation, fasciculation and axonal transport in many organisms. UNC-69 and UNC-76 colocalize as puncta in neurons, and cooperate to regulate sensory axon extension and SNB-1::GFP localization. Moreover, UNC-69 and UNC-76 occasionally fail to colocalize in worms mutant for *unc-116*, the *C. elegans* orthologue of kinesin heavy chain, which is also defective in both axonal outgrowth and normal presynaptic differentiation. The UNC-69/UNC-76 protein complex might mediate cargo transport in the axons by associating with kinesin heavy chain. In addition, my results suggest that synapse formation and axonal growth are tightly coupled processes, and this function might be well evolutionarily conserved.

Even Borges couldn't imagine,

Grand *elegans exposé*,

Not your father's toy.

Chapter 1

Introduction

Overview of intracellular transport in neuronal development

Neurons are among the most highly differentiated cells in our body, and often show a complex and sophisticated morphology. However, the unique arborization of neuronal processes was not clearly observed until 1865. As described in Otto Deiters' famous posthumous lithography, two types of processes from a single nerve cell were categorized and named as "protoplasmic prolongations" and "axis cylinder", respectively [1, 2]. It was not until the late 1880's – 1890's that the term "neuron" was invented, along with "dendrites" and "axon," that were created to replace Deiters' earlier descriptions [3, 4].

Over the past 140 years, morphologists, embryologist as well as developmental biologists were all strived to understand the logic behind formation of these unusual neuronal processes. Multiple dendrites arise from a single neuron. In contrast, only one axon is produced from a single neuron. To become fully functional, the dendrites and axon need to be guided to their targets correctly. Not only that, they also have to establish proper contacts – synapses [5] – with their neighboring neurons or muscle cells. What is more surprising is that the whole nervous system is wired in a grossly invariant manner [6]. What are the instructive forces underpinning this elaborate neuronal connectivity?

A plethora of axonal guidance genes were found during the 1980's and 1990's, which encode proteins that are either attracting or repelling the dendrites or axon toward their destinations [7, 8]. Binding of these extracellular guidance cues to their corresponding receptors, which are enriched on the surface of the growth cone (a

motile structure at the tip of the neuronal processes), triggers signaling cascades that lead to cytoskeletal rearrangement inside the growth cones. What remains unclear is how cytoskeletal rearrangement coordinates with various intracellular events to advance the growth of neuronal processes. In addition to continuous transport of actin and tubulin oligomers, neurite extension requires a steady supply of new plasma membrane proteins and lipids to the growing tips. Axonal or dendritic transport is not passive diffusion. Rather, it requires various cytoskeleton-associated proteins that are capable of directional movement by hydrolyzing ATP. These ATPases, commonly known as motor proteins, are fundamental players of axonal and dendritic transport [9].

In this review I will focus on the mechanisms of intracellular transport in developing Deiters' "axis cylinder", the axon. I will first describe cellular mechanisms that allow short-range delivery/retrieval of proteins to and from the nerve terminals. I will then discuss the current knowledge about long-range microtubule-based axonal transport, and its relevance to axonal outgrowth and synaptogenesis. In particular, I will emphasize discoveries made in the nematode *C. elegans,* and the knowledge that was gained from studying basic neurobiology in such a tiny organism.

Part I:

Short-range trafficking in axonal guidance and synaptogenesis

1. Preface

The endosomal compartment receives vesicles endocytosed from the plasma membrane, as well as vesicles derived from the Golgi apparatus. Like the regulation of dendritic AMPA receptor targeting and turnover [10], many axonal proteins can be temporally and spatially targeted or retrieved. Most, if not all, of these regulations involve steering proteins into the endosomal pathway – an agile system that responds to stimuli expeditiously.

2. Commissureless regulates delivery of Roundabout receptors to the growth cones

The best characterized example for regulated delivery of axonal guidance receptors involves the *Drosophila* axonal guidance genes *commissureless (comm)* [11] and *roundabout (robo)* [12]. During the development of commissural axons in the *Drosophila* embryonic central nervous system (CNS), the level of the Robo receptor on the growth cones is low when the commissural axons are crossing the midline, where the repellent Slit [13, 14] is expressed. However, once the midline is crossed, the commissural axons raise the level of Robo receptor on the surface of the growth cones, preventing commissural axons from recrossing the midline [15]. Comm cell-autonomously downregulates Robo by sorting Robo receptor to late endosomes in the commissural axons [16, 17]. Thus, Comm function as a hijacker to prevent delivery of Robo to the growth cone surface during midline crossing.

How Comm sequesters Robo is still elusive. *In vitro* experiments suggested that Comm requires Nedd4-mediated ubiquitination to function [18]. However, these observations could not be replicated by *in vivo* experiments in *Drosophila* [17].

3. EphB-ephrinB bi-directional endocytosis mediates growth cone collapse

Another example of short-range protein trafficking in axonal guidance is the bi-directional endocytosis of EphB-ephrinB receptor-ligand protein complex [19, 20]. EphB receptor and its ligand ephrinB are transmembrane proteins that mediate axonal repulsion [21]. Physical contact between EphB2 receptor and its ligand, ephrinB1, elicits an intracellular signal that triggers bi-directional endocytosis of full-length EphB2-ephrinB1 protein complex, followed by growth cone retraction. The endocytosed receptor-ligand complex is transported retrogradely along the axon in a primary cultured neuron [19], and might serve additional signaling functions in the soma. Similarly, activation of EphB4 receptor leads to its localized endocytosis together with its full-length ligand ephrinB2 and to subsequent cell retraction. Interestingly, both events are Rac-dependent. [20].

4. Deep orange and Hook determine synapse size, possibly by regulating endocytic protein trafficking in *Drosophila*

An example of short-range cellular trafficking in synapse formation comes from studying the *Drosophila deep orange* and *hook* mutants. Deep orange (Dor) and Hook are endosomal protein that controls synapse size, but not synaptic vesicle cycling, at the larval neuromuscular junction [22]. Dor controls eye color in

Drosophila, and is similar to *S. cerevisiae* Vps18p, a protein required for delivering cargo to the vacuole, a lysosome-like compartment [23]. Dor is also found to promote fusion of Golgi-derived vesicles with Rab7-positive endosomes, before they fuse with tubular lysosomes [24]. Similarly, Hook is also found to be required for delivering proteins to the lysosomes in *Drosophila* [25, 26]. It is therefore suggested that synapse size is determined as a function of Dor- and Hook-regulated endocytic trafficking events, similar to Dor's function in mediating intracellular transport to lysosomes and pigment granules in photoreceptors. However, the precise mode of action of Dor and Hook in regulating synapse formation remains to be determined.

5. UNC-11 regulates synaptic vesicle size and proper localization of SNB-1 in *C. elegans*

unc-11 is homologous to the vertebrate AP180, which participates in clathrin-mediated endocytosis. *unc-11* mutants are defective in cholinergic, GABAergic, as well as glutamatergic transmission, as evidenced by their resistance to the acetylcholinesterase inhibitor aldicarb, their defects in enteric muscle contraction, and abnormal synaptic currents in their pharyngeal muscle cells, respectively [27, 28]. In *unc-11* mutants, the presynaptic vesicle marker SNB-1::GFP loses its characteristic punctate pattern and becomes diffused in the axons. In addition, ultrastructural analysis reveals synaptic vesicles enlargement in the *unc-11* mutants. It is therefore suggested that the synaptic defects in *unc-11* mutants arise from failure to control clathrin-mediated endocytosis. However, no defect of synaptic membrane recycling in *unc-11* mutants has yet been convincingly demonstrated. Since the defect of SNB-1::GFP mislocalization in *unc-11* mutants is epistatic to that in *unc-104* mutants (see

below), explanations other than a defect in endocytosis are plausible. Intriguingly, UNC-11 seems to be specifically required for sorting SNB-1 into synaptic vesicles.

The SNB-1::GFP diffusion phenotype in the *unc-11* mutants resembles the ODR-10::GFP diffusion phenotype in the *unc-101* mutants [29]. However, these two clathrin adaptor proteins function differently in the same neuron to target different proteins, and are unlikely to act in the same cellular processes [29].

Part II:

Long-range trafficking in axonal outgrowth and synapse formation – a *C. elegans* perspective

1. Preface

Axons are filled with cytoskeletons, including actin filaments, neurofilaments, as well as microtubules, which serve as routes for directional trafficking. Traditionally, axonal transport is classified into slow and fast axonal transports. Many vesicles and various membranous organelles move at a speed of ~400 mm day^{-1} in the axons, and this movement, termed fast axonal transport, is dependent on many motor proteins that walk along the microtubules [9]. In contrast, slow axonal transport, which measures at ~0.2-2.5 mm day^{-1}, is used to transport cytosolic as well as cytoskeletal proteins [9], and is thought to be motor protein-independent. However, in recent years the distinction between slow and fast axonal transports has broken down, as it became clear that slow axonal transport actually also requires motor proteins (for example see [30]; reviewed in [31]).

Since the discovery of dynein (*dyne,* force) and conventional kinesin (*kinesis,* movement) [32, 33], a great deal of effort has been devoted to studying these force-generating microtubule motors, their kinetics, their biochemical properties, and their relevance in axonal transport. Here I summarize our present knowledge of various molecular motors and their associated proteins that are involved in axonal transport in *C. elegans* (see below; summarized in Table 1).

2. Cytoplasmic dyneins

Isolated in 1987 [34], cytoplasmic dynein is a large protein complex consisting of two heavy chains, as well as several light chains, intermediate chains, and light

intermediate chains ([35]; for a detailed review, see [36]). *C. elegans* cytoplasmic dynein was purified as a microtubule-associated motor protein [37]. Although its biochemical properties resemble that of dynein, its microtubule translocating property *in vitro* resembles that of the conventional kinesin [37]. Nevertheless, recently a study has demonstrated an important role for *C. elegans* cytoplasmic dynein heavy chain DHC-1 [38, 39] and dynein light intermediate chain DLI-1 [39] in retrograde transport of synaptic cargoes including synaptobrevin, synaptotagmin, and UNC-104. Neuronal connectivity is grossly normal in *dhc-1* and *dli-1* mutants [38, 39].

2.1 Cytoplasmic dynein-associated proteins

The dynactin protein complex binds the dynein intermediate chain [40]. Dynactin is a multisubunit protein complex consisting of $p150^{Glued}$, dynamitin, and other proteins [41-43]. In *C. elegans*, $p150^{Glued}$ is encoded by *dnc-1,* while dynamitin is encoded by *dnc-2*. Partial loss-of-function of *dnc-1* and overexpression of *dnc-2* both cause SNB-1::GFP misaccumulation in the mechanosensory neurons [39].

The mammalian LIS1 protein (for type I lissencephaly) is essential for cortical nucleokinesis, and is a binding partner as well as an important regulator of cytoplasmic dynein (reviewed in [44]). In *C. elegans,* LIS-1 participates in dynein-dependent embryonic cell division events [45]. In addition, a nonsense mutation truncating the WD40 repeat domains of LIS-1 results in an alteration of SNB-1::GFP distribution in the D-type motor neurons: the SNB-1::GFP puncta are sometimes missing from a stretch of axon in the VNC, unevenly distributed, and irregular in size

[38]. However, GABAergic neuronal architecture is seemingly normal in *lis-1* mutants.

The KLC-associated protein UNC-16 (see below) is a potential binding partner of DLI-1 in *C. elegans* [46]. Thus, UNC-16 might serve as a coordinator for anterograde and retrograde axonal transport in *C. elegans* axons.

3. Kinesins

Kinesin was first purified in 1985 from the squid giant axon [33]. Since then, 45 different kinesin members were discovered by homology in mice and humans, and have been classified into 14 families [9]. However, many of their corresponding homologues in *C. elegans* are not characterized yet. Furthermore, only a few of them have been shown to be clearly involved in transport of axonal cargoes in *C. elegans* axons.

3.1 Kinesin-1

Kinesin-1 (conventional kinesin; KIF5) is a heterotetramer composed of two kinesin heavy chains (KHCs) and two kinesin light chains (KLCs) [9]. Kinesin-1 is a molecular motor for anterograde transport along the microtubules. Kinesin-1 transports various axonal and dendritic cargoes including mitochondria, lysosomes, endoplasmic reticulum (ER), oligomeric tubulins, RNA-containing granules, and vesicles containing synaptic receptor proteins [9, 35]. In *C. elegans,* KHC is encoded by a single gene *unc-116* [47], whereas KLC is encoded by two genes *klc-1* and *klc-2* [48].

3.1.1 UNC-116/KHC

unc-116 was cloned from a Tc5 insertion-based screen for mutants exhibiting abnormal backward but normal forward locomotion (*e2281*), as well as from a forward genetics screen for nervous system defect (*rh24*) [47]. UNC-116 is a 815 amino acid protein orthologous to KHC, a N-terminal kinesin motor [9], with the exception that it has a relatively short rodII region of the stalk domain (93 amino acids) compared to that in KHCs from *Drosophila* and squid (~230 amino acids) [47].

unc-116 mutants exhibit axonal outgrowth defects (Chapter 2) as well as presynaptic differentiation defects [46, 49, 50]: the synaptobrevin SNB-1::GFP, a synaptic vesicle marker, SYD-2::GFP, an active zone protein, UNC-16::GFP, the JNK-scaffolding protein, as well as UNC-14::GFP, a RUN-domain protein, are all mislocalized from the presynaptic regions in GABAergic motor neurons. Thus, the various presysnaptic protein mislocalization defects are likely a direct consequence of disruption of KHC-mediated cargo transport. In contrast, transport of ODR-10::GFP into dendrites appears normal in *unc-116* mutants [29].

Despite the SNB-1::GFP mislocalization, electron microscopy analysis reveals that synaptic vesicles are properly distributed in *unc-116(rh24)* mutants [47], analogous to the findings in *Drosophila khc* mutants [51]. Therefore, UNC-116/KHC might not be directly responsible for transporting synaptic vesicles to their appropriate destinations; the SNB-1::GFP mislocalization defects seen in *unc-116* mutants might be secondary to a more general defect in axonal transport. Alternatively, UNC-116/KHC may

utilize adaptor proteins like UNC-16 to regulate interaction between the synaptic vesicles and another kinesin motor, UNC-104/KIF1A (see below; see also discussion in [49]).

3.1.2 KLC-1 and KLC-2

KLC forms heterodimer with KHC by binding to the tail region of KHC via its coiled-coil region. The tetratricopeptide repeats (TPR) domain of KLC then serves as docking platform for various KLC-associating proteins [52].

C. elegans has two KLCs, KLC-1 and KLC-2 [48]. Only one of them, KLC-2, has been studied. KLC-2 was shown to be important for normal presynaptic differentiation in the GABAergic motor neurons in *C. elegans* [46]. The SNB-1::GFP mislocalization phenotype in L1 DD motor neurons in *klc-2* mutants is indistinguishable from that of *unc-116* mutants, supporting the notion that these two proteins regulate transport of the same set of synaptic proteins by forming the Kinesin-1 motor. However, the SNB-1::GFP mislocalization defects do not necessarily mean a direct cargo-motor relationship, as was previously ascribed for the *Drosophila klc* mutants [53].

3.2 Kinesin-3

In mammals, the Kinesin-3 family contains two subfamily members, Unc104/KIF1 and KIF13 [9]. KIF13 is not nervous system-specific, and transports cargoes like mannose-6-phosphate receptor [54] and DLG, the human homologue of the fly disc

large tumor suppressor protein [55]. In contrast, the monomeric motor Unc104/KIF1 preferentially transports synaptic vesicle precursors in mammalian neurons [56].

3.2.1 UNC-104/KIF1A

unc-104 was first found in *C. elegans* as a candidate kinesin motor gene [57]. Subsequently, UNC-104 was found to regulate transport of synaptic vesicles in *C. elegans* neurons: the number of synaptic vesicles decreases in the *unc-104(rh43)* mutants [58]. Furthermore, SNB-1::GFP fails to be transported into the axons, and is retained in the cell bodies in the *unc-104(e1265)* mutants [49], a phenotype totally different from the SNB-1::GFP mislocalization defects seen in the *C. elegans* Kinesin-1 *unc-116* and *klc-2* mutants [46]. UNC-104 also transports dense core vesicles required for peptidergic neurotransmission [59]. Interestingly, less SYD-2::GFP puncta can be seen in the axons [50], suggestive of a failure in active zone formation in *unc-104* mutants. The PH domain of UNC-104 is important for its *in vivo* activities [60].

UNC-104 seems to be specific for transport of synaptic vesicle and neuropeptidergic vesicles, since transport of Golgi, ER, and mitochondria appears normal in *unc-104* mutants [58]. Axonal outgrowth and guidance is largely normal in *unc-104* mutants except for the PVP, AVM/PVM and PDE axons [58], suggesting that UNC-104 possibly does not transport majority of the axonogenic vesicles. In addition, ODR-10 targeting is normal in *unc-104* mutants, suggesting that UNC-104 is possibly not required for dendritic transport [29]. However, UNC-104 is present in both axons and

dendrites in *C. elegans* neurons [61], raising intriguing questions regarding its true *in vivo* functions.

A recent report suggests that UNC-104 can dimerize [62], which would allow it to walk along the microtubules in a processive manner.

3.3 Kinesin-1-associated proteins in *C. elegans*

Kinesin-1 transports membranous organelles and vesicles via the help of several Kinesin-1-associated proteins that either function as cargo adaptors or regulators of cargo transport [9]. Since KLC and KHC together form the Kinesin-1 protein complex, traditional views regard them to function together to transport the same sets of cargoes. Indeed, KHC requires physical interaction with KLC to become fully active [46, 63]. However, Kinesin-1-associated proteins usually interact with either KLC or KHC [9, 64]. In addition, evidence that KHC could function independently of KLC in *Drosophila* embryos further indicates the possibility that KLC and KHC might function somewhat differently [65]. Several *C. elegans* proteins have been shown to associate with either KLC-2 or UNC-116/KHC, and might regulate different steps of axonal transport.

3.3.1 KLC-associated proteins

A. UNC-16

UNC-16 physically interacts with KLC-2's TPR domain [46]. In addition, UNC-16 binds the *C. elegans* JNK JNK-1, as well as its upstream activators JKK-1 and SEK-1 [49]. Thus, UNC-16 is a JNK-scaffolding protein. UNC-16 is homologous to the *Drosophila* Sunday Driver, as well as the mammalian JSAP1/JIP3 [49] (previously named mSYD2 [66]). *C. elegans* UNC-16 is required for proper targeting of several different axonal and dendritic proteins including SNB-1::GFP, the vesicular monoamine transporter CAT-1::GFP, and the AMPA-type glutamate receptor GLR-1, but not synaptotagmin [49]. In addition, *unc-16* partially suppresses the SNB-1::GFP retention defect in *unc-104* mutants, whereas *unc-116* could not suppress the *unc-104* mutant defects. It is not clear how this genetic interaction between *unc-16* and *unc-104* is achieved.

Worms mutant for the UNC-16-interacting proteins also show presynaptic differentiation defects: *jnk-1, jkk-1* and *sek-1* mutants all displayed subtle but synergistic defects in mislocalization of SNB-1::GFP [49]. Thus, UNC-16 might bring JNK-1, JKK-1 and SEK-1 into close proximity to execute their functions, and the JNK-signaling cascade might be necessary for proper targeting of the SNB-1-positive synaptic vesicles. Moreover, another UNC-16-binding protein, UNC-14, is also required for proper SNB-1::GFP localization (see below).

B. UNC-14

UNC-14 binds both UNC-16 and KLC-2 *in vitro*, and its interaction with UNC-16 depends on the presence of KLC-2 [46]. UNC-14 is a protein with a RUN (RPIP8, UNC-14 and NESCA) domain [67, 68]. As in the *unc-16* and *klc-2* mutants, in the

unc-14 mutants SNB-1::GFP is mislocalized. UNC-14::GFP becomes diffused and irregular in *unc-16, unc-116* and *klc-2* mutants [46], indicating that it is one of the cargo proteins that are transported by a Kinesin-1-dependent manner.

In addition to its effect on presynaptic differentiation, UNC-14 regulates axonal outgrowth together with a conserved serine/threonine kinase UNC-51 (see below) [69, 70].

C. UNC-51

UNC-51 has been shown to regulate both axonal outgrowth and SNB-1::GFP localization in the ASI sensory neurons in *C. elegans* [71, 72]. UNC-51 has a N-terminal serine/threonine kinase domain, and binds UNC-14 via its C-terminus. In addition, UNC-51 can oligomerize using its C-terminal region [71].

In both *unc-14* and *unc-51* mutants, abnormal membranous structures are found in the axons, indicating their roles in intracellular trafficking [73, 74]. However, like the *unc-116* mutants, synaptic vesicles still cluster normally in both *unc-14* and *unc-51* mutants. It is proposed that UNC-14 recruits UNC-51 to certain subcellular loci and activates it, where UNC-51 executes its functions by phosphorylating its substrates [69]. Since UNC-14 is recruited to Kinesin-1 [46], UNC-51 thus becomes a candidate regulator of Kinesin-1-dependent synaptic transport.

C. elegans UNC-51 can phosphorylate itself, as well as two other worm proteins, UNC-14 and VAB-8, both of which it physically interacts with [70]. UNC-51

regulates anteroposterior axonal outgrowth together with UNC-14 and VAB-8 [70]. VAB-8 is a kinesin motor-like protein, mutations in which preferentially cause posterior-directed axonal outgrowth and cell migration defects in *C. elegans* [75, 76]. Thus, VAB-8 might be recruited to posterior-directed cargoes, and possibly anchor them on the microtubules via its kinesin motor-like domain.

Recently, mammalian Unc51.1 protein has been shown to bind both SynGAP and Syntenin, a scaffolding protein and a binding partner of Rab5 [77]. SynGAP negatively regulates the activities of Ras and Rab5, a regulator of endocytosis. It is proposed that Unc51.1 promotes axon outgrowth by antagonizing the activity of SynGAP. It is not clear if *C. elegans* UNC-51 functions in a similar way to regulate axon outgrowth.

3.3.2 Potential KHC-associated proteins

A. UNC-76

Although the physical interaction between UNC-76 and UNC-116 has not been demonstrated in worms, the *Drosophila* homologue of UNC-76 has been shown to interact with the tail of *Drosophila* KHC [78]. UNC-76 is homologous to the mammalian FEZ proteins (for fasciculation and elongation protein, zygin zeta), which have been shown to interact with several different cytosolic proteins *in vitro* (Chapter 4). UNC-76 thus could possibly function as an adaptor by recruiting proteins essential for KHC-mediated cargo transport.

B. UNC-69 is a novel UNC-76-binding protein possibly required for KHC-mediated cargo transport

In this study, I identified UNC-69 as a novel UNC-76-interacting partner. UNC-69 is a 108 amino acid protein, and is homologous to mammalian SCOCO (short coiled-coil domain protein). Although *unc-69* is required for proper SNB-1::GFP localization, its phenotype in L1 DD neurons is different from that of the *unc-14, unc-16, unc-116,* and the *klc-2* mutants. UNC-69 and UNC-76 likely function in the same protein complex, and regulate both axonal outgrowth and presynaptic differentiation cooperatively. I propose that the UNC-69/UNC-76 protein complex constitutes a novel and important pathway for KHC-mediated axonal transport. Since so far most of the KHC-associated proteins identified in mammals are involved in dendritic transport [9], the discovery would most likely provide mechanistic insights into the regulation of KHC in the context of axonal transport.

References

1. Deiters OFK: **Untersuchungen über Gehirn und Rückenmark des Menschen und der Säugethiere.** Braunschweig: F. Vieweg u. Sohn; 1865.
2. Shepherd GM: **Neurobiology**, 3rd edn: Oxford University Press; 1994.
3. His W: **Über den Aufbau unseres Nervensystems.** *Berl Klin Wochenschr* 1893, **40**:41.
4. Kölliker RAv: **Handbuch der Gewebelehre des Menschen**, 6th edn. Leipzig: Engelmann; 1896.
5. Sherrington CS: **The Integrative Action of the Nervous System.** New Haven: Yale University Press; 1906.
6. Kozloski J, Hamzei-Sichani F, Yuste R: **Stereotyped position of local synaptic targets in neocortex**. *Science* 2001, **293**(5531):868-872.
7. Goodman CS: **Mechanisms and molecules that control growth cone guidance**. *Annu Rev Neurosci* 1996, **19**:341-377.
8. Furrer MP, Kim S, Wolf B, Chiba A: **Robo and Frazzled/DCC mediate dendritic guidance at the CNS midline**. *Nat Neurosci* 2003, **6**(3):223-230.
9. Hirokawa N, Takemura R: **Molecular motors and mechanisms of directional transport in neurons**. *Nat Rev Neurosci* 2005, **6**(3):201-214.
10. Malenka RC: **Synaptic plasticity and AMPA receptor trafficking**. *Ann N Y Acad Sci* 2003, **1003**:1-11.
11. Tear G, Harris R, Sutaria S, Kilomanski K, Goodman CS, Seeger MA: ***commissureless* controls growth cone guidance across the CNS midline in *Drosophila* and encodes a novel membrane protein**. *Neuron* 1996, **16**(3):501-514.

12. Kidd T, Brose K, Mitchell KJ, Fetter RD, Tessier-Lavigne M, Goodman CS, Tear G: **Roundabout controls axon crossing of the CNS midline and defines a novel subfamily of evolutionarily conserved guidance receptors**. *Cell* 1998, **92**(2):205-215.

13. Kidd T, Bland KS, Goodman CS: **Slit is the midline repellent for the Robo receptor in *Drosophila***. *Cell* 1999, **96**(6):785-794.

14. Brose K, Bland KS, Wang KH, Arnott D, Henzel W, Goodman CS, Tessier-Lavigne M, Kidd T: **Slit proteins bind Robo receptors and have an evolutionarily conserved role in repulsive axon guidance**. *Cell* 1999, **96**(6):795-806.

15. Rajagopalan S, Nicolas E, Vivancos V, Berger J, Dickson BJ: **Crossing the midline: roles and regulation of Robo receptors**. *Neuron* 2000, **28**(3):767-777.

16. Keleman K, Rajagopalan S, Cleppien D, Teis D, Paiha K, Huber LA, Technau GM, Dickson BJ: **Comm sorts robo to control axon guidance at the *Drosophila* midline**. *Cell* 2002, **110**(4):415-427.

17. Keleman K, Ribeiro C, Dickson BJ: **Comm function in commissural axon guidance: cell-autonomous sorting of Robo in vivo**. *Nat Neurosci* 2005, **8**(2):156-163.

18. Myat A, Henry P, McCabe V, Flintoft L, Rotin D, Tear G: ***Drosophila* Nedd4, a ubiquitin ligase, is recruited by Commissureless to control cell surface levels of the roundabout receptor**. *Neuron* 2002, **35**(3):447-459.

19. Zimmer M, Palmer A, Kohler J, Klein R: **EphB-ephrinB bi-directional endocytosis terminates adhesion allowing contact mediated repulsion**. *Nat Cell Biol* 2003, **5**(10):869-878.

20. Marston DJ, Dickinson S, Nobes CD: **Rac-dependent trans-endocytosis of ephrinBs regulates Eph-ephrin contact repulsion**. *Nat Cell Biol* 2003, **5**(10):879-888.

21. Kullander K, Klein R: **Mechanisms and functions of Eph and ephrin signalling**. *Nat Rev Mol Cell Biol* 2002, **3**(7):475-486.

22. Narayanan R, Kramer H, Ramaswami M: ***Drosophila*** **endosomal proteins hook and deep orange regulate synapse size but not synaptic vesicle recycling**. *J Neurobiol* 2000, **45**(2):105-119.

23. Sevrioukov EA, He JP, Moghrabi N, Sunio A, Kramer H: **A role for the *deep orange* and *carnation* eye color genes in lysosomal delivery in *Drosophila***. *Mol Cell* 1999, **4**(4):479-486.

24. Sriram V, Krishnan KS, Mayor S: ***deep-orange*** **and *carnation* define distinct stages in late endosomal biogenesis in *Drosophila melanogaster***. *J Cell Biol* 2003, **161**(3):593-607.

25. Kramer H, Phistry M: **Genetic analysis of *hook*, a gene required for endocytic trafficking in *Drosophila***. *Genetics* 1999, **151**(2):675-684.

26. Kramer H, Phistry M: **Mutations in the *Drosophila hook* gene inhibit endocytosis of the boss transmembrane ligand into multivesicular bodies**. *J Cell Biol* 1996, **133**(6):1205-1215.

27. Miller KG, Alfonso A, Nguyen M, Crowell JA, Johnson CD, Rand JB: **A genetic selection for *Caenorhabditis elegans* synaptic transmission mutants**. *Proc Natl Acad Sci U S A* 1996, **93**(22):12593-12598.

28. Nonet ML, Holgado AM, Brewer F, Serpe CJ, Norbeck BA, Holleran J, Wei L, Hartwieg E, Jorgensen EM, Alfonso A: **UNC-11, a *Caenorhabditis***

***elegans* AP180 homologue, regulates the size and protein composition of synaptic vesicles**. *Mol Biol Cell* 1999, **10**(7):2343-2360.

29. Dwyer ND, Adler CE, Crump JG, L'Etoile ND, Bargmann CI: **Polarized dendritic transport and the AP-1 mu1 clathrin adaptor UNC-101 localize odorant receptors to olfactory cilia**. *Neuron* 2001, **31**(2):277-287.

30. Xia CH, Roberts EA, Her LS, Liu X, Williams DS, Cleveland DW, Goldstein LS: **Abnormal neurofilament transport caused by targeted disruption of neuronal kinesin heavy chain KIF5A**. *J Cell Biol* 2003, **161**(1):55-66.

31. Brown A: **Axonal transport of membranous and nonmembranous cargoes: a unified perspective**. *J Cell Biol* 2003, **160**(6):817-821.

32. Gibbons IR, Rowe AJ: **Dynein: A Protein with Adenosine Triphosphatase Activity from Cilia**. *Science* 1965, **149**(3682):424-426.

33. Vale RD, Reese TS, Sheetz MP: **Identification of a novel force-generating protein, kinesin, involved in microtubule-based motility**. *Cell* 1985, **42**(1):39-50.

34. Paschal BM, Shpetner HS, Vallee RB: **MAP 1C is a microtubule-activated ATPase which translocates microtubules in vitro and has dynein-like properties**. *J Cell Biol* 1987, **105**(3):1273-1282.

35. Hirokawa N: **Kinesin and dynein superfamily proteins and the mechanism of organelle transport**. *Science* 1998, **279**(5350):519-526.

36. Vallee RB, Williams JC, Varma D, Barnhart LE: **Dynein: An ancient motor protein involved in multiple modes of transport**. *J Neurobiol* 2004, **58**(2):189-200.

37. Lye RJ, Porter ME, Scholey JM, McIntosh JR: **Identification of a microtubule-based cytoplasmic motor in the nematode *C. elegans***. *Cell* 1987, **51**(2):309-318.

38. Williams SN, Locke CJ, Braden AL, Caldwell KA, Caldwell GA: **Epileptic-like convulsions associated with LIS-1 in the cytoskeletal control of neurotransmitter signaling in *Caenorhabditis elegans***. *Hum Mol Genet* 2004, **13**(18):2043-2059.

39. Koushika SP, Schaefer AM, Vincent R, Willis JH, Bowerman B, Nonet ML: **Mutations in *Caenorhabditis elegans* cytoplasmic dynein components reveal specificity of neuronal retrograde cargo**. *J Neurosci* 2004, **24**(16):3907-3916.

40. Waterman-Storer CM, Karki SB, Kuznetsov SA, Tabb JS, Weiss DG, Langford GM, Holzbaur EL: **The interaction between cytoplasmic dynein and dynactin is required for fast axonal transport**. *Proc Natl Acad Sci U S A* 1997, **94**(22):12180-12185.

41. Gill SR, Schroer TA, Szilak I, Steuer ER, Sheetz MP, Cleveland DW: **Dynactin, a conserved, ubiquitously expressed component of an activator of vesicle motility mediated by cytoplasmic dynein**. *J Cell Biol* 1991, **115**(6):1639-1650.

42. Holzbaur EL, Hammarback JA, Paschal BM, Kravit NG, Pfister KK, Vallee RB: **Homology of a 150K cytoplasmic dynein-associated polypeptide with the *Drosophila* gene Glued**. *Nature* 1991, **351**(6327):579-583.

43. King SJ, Bonilla M, Rodgers ME, Schroer TA: **Subunit organization in cytoplasmic dynein subcomplexes**. *Protein Sci* 2002, **11**(5):1239-1250.

44. Tsai LH, Gleeson JG: **Nucleokinesis in Neuronal Migration**. *Neuron* 2005, **46**(3):383-388.

45. Cockell MM, Baumer K, Gonczy P: ***lis-1* is required for dynein-dependent cell division processes in *C. elegans* embryos**. *J Cell Sci* 2004, **117**(Pt 19):4571-4582.

46. Sakamoto R, Byrd DT, Brown HM, Hisamoto N, Matsumoto K, Jin Y: **The *C. elegans* UNC-14 RUN domain protein binds to the Kinesin-1/UNC-16 complex and regulates synaptic vesicle localization**. *Mol Biol Cell* 2004.

47. Patel N, Thierry-Mieg D, Mancillas JR: **Cloning by insertional mutagenesis of a cDNA encoding *Caenorhabditis elegans* kinesin heavy chain**. *Proc Natl Acad Sci U S A* 1993, **90**(19):9181-9185.

48. Fan J, Amos LA: **Kinesin light chain isoforms in *Caenorhabditis elegans***. *J Mol Biol* 1994, **240**(5):507-512.

49. Byrd DT, Kawasaki M, Walcoff M, Hisamoto N, Matsumoto K, Jin Y: **UNC-16, a JNK-signaling scaffold protein, regulates vesicle transport in *C. elegans***. *Neuron* 2001, **32**(5):787-800.

50. Yeh E, Kawano T, Weimer RM, Bessereau JL, Zhen M: **Identification of genes involved in synaptogenesis using a fluorescent active zone marker in *Caenorhabditis elegans***. *J Neurosci* 2005, **25**(15):3833-3841.

51. Gho M, McDonald K, Ganetzky B, Saxton WM: **Effects of kinesin mutations on neuronal functions**. *Science* 1992, **258**(5080):313-316.

52. Vale RD: **The molecular motor toolbox for intracellular transport**. *Cell* 2003, **112**(4):467-480.

53. Gindhart JG, Jr., Desai CJ, Beushausen S, Zinn K, Goldstein LS: **Kinesin light chains are essential for axonal transport in *Drosophila***. *J Cell Biol* 1998, **141**(2):443-454.

54. Nakagawa T, Setou M, Seog D, Ogasawara K, Dohmae N, Takio K, Hirokawa N: **A novel motor, KIF13A, transports mannose-6-phosphate receptor to plasma membrane through direct interaction with AP-1 complex**. *Cell* 2000, **103**(4):569-581.

55. Asaba N, Hanada T, Takeuchi A, Chishti AH: **Direct interaction with a kinesin-related motor mediates transport of mammalian discs large tumor suppressor homologue in epithelial cells**. *J Biol Chem* 2003, **278**(10):8395-8400.

56. Okada Y, Yamazaki H, Sekine-Aizawa Y, Hirokawa N: **The neuron-specific kinesin superfamily protein KIF1A is a unique monomeric motor for anterograde axonal transport of synaptic vesicle precursors**. *Cell* 1995, **81**(5):769-780.

57. Otsuka AJ, Jeyaprakash A, Garcia-Anoveros J, Tang LZ, Fisk G, Hartshorne T, Franco R, Born T: **The *C. elegans unc-104* gene encodes a putative kinesin heavy chain-like protein**. *Neuron* 1991, **6**(1):113-122.

58. Hall DH, Hedgecock EM: **Kinesin-related gene *unc-104* is required for axonal transport of synaptic vesicles in *C. elegans***. *Cell* 1991, **65**(5):837-847.

59. Zahn TR, Angleson JK, MacMorris MA, Domke E, Hutton JF, Schwartz C, Hutton JC: **Dense core vesicle dynamics in *Caenorhabditis elegans* neurons and the role of kinesin UNC-104**. *Traffic* 2004, **5**(7):544-559.

60. Klopfenstein DR, Vale RD: **The lipid binding pleckstrin homology domain in UNC-104 kinesin is necessary for synaptic vesicle transport in *Caenorhabditis elegans***. *Mol Biol Cell* 2004, **15**(8):3729-3739.

61. Zhou HM, Brust-Mascher I, Scholey JM: **Direct visualization of the movement of the monomeric axonal transport motor UNC-104 along neuronal processes in living *Caenorhabditis elegans***. *J Neurosci* 2001, **21**(11):3749-3755.

62. Tomishige M, Klopfenstein DR, Vale RD: **Conversion of Unc104/KIF1A kinesin into a processive motor after dimerization**. *Science* 2002, **297**(5590):2263-2267.

63. Rahman A, Kamal A, Roberts EA, Goldstein LS: **Defective kinesin heavy chain behavior in mouse kinesin light chain mutants**. *J Cell Biol* 1999, **146**(6):1277-1288.

64. Terada S, Hirokawa N: **Moving on to the cargo problem of microtubule-dependent motors in neurons**. *Curr Opin Neurobiol* 2000, **10**(5):566-573.

65. Palacios IM, St Johnston D: **Kinesin light chain-independent function of the Kinesin heavy chain in cytoplasmic streaming and posterior localisation in the *Drosophila* oocyte**. *Development* 2002, **129**(23):5473-5485.

66. Bowman AB, Kamal A, Ritchings BW, Philp AV, McGrail M, Gindhart JG, Goldstein LS: **Kinesin-dependent axonal transport is mediated by the sunday driver (SYD) protein**. *Cell* 2000, **103**(4):583-594.

67. Janoueix-Lerosey I, Pasheva E, de Tand MF, Tavitian A, de Gunzburg J: **Identification of a specific effector of the small GTP-binding protein Rap2**. *Eur J Biochem* 1998, **252**(2):290-298.

68. MacDonald JI, Kubu CJ, Meakin SO: **Nesca, a novel adapter, translocates to the nuclear envelope and regulates neurotrophin-induced neurite outgrowth**. *J Cell Biol* 2004, **164**(6):851-862.

69. Ogura K, Shirakawa M, Barnes TM, Hekimi S, Ohshima Y: **The UNC-14 protein required for axonal elongation and guidance in *Caenorhabditis elegans* interacts with the serine/threonine kinase UNC- 51**. *Genes Dev* 1997, **11**(14):1801-1811.

70. Lai T, Garriga G: **The conserved kinase UNC-51 acts with VAB-8 and UNC-14 to regulate axon outgrowth in *C. elegans***. *Development* 2004, **131**(23):5991-6000.

71. Ogura K, Wicky C, Magnenat L, Tobler H, Mori I, Muller F, Ohshima Y: ***Caenorhabditis elegans unc-51* gene required for axonal elongation encodes a novel serine/threonine kinase**. *Genes Dev* 1994, **8**(20):2389-2400.

72. Crump JG, Zhen M, Jin Y, Bargmann CI: **The SAD-1 kinase regulates presynaptic vesicle clustering and axon termination**. *Neuron* 2001, **29**(1):115-129.

73. Hedgecock EM, Culotti JG, Thomson JN, Perkins LA: **Axonal guidance mutants of *Caenorhabditis elegans* identified by filling sensory neurons with fluorescein dyes**. *Dev Biol* 1985, **111**(1):158-170.

74. McIntire SL, Garriga G, White J, Jacobson D, Horvitz HR: **Genes necessary for directed axonal elongation or fasciculation in *C. elegans***. *Neuron* 1992, **8**(2):307-322.

75. Wolf FW, Hung MS, Wightman B, Way J, Garriga G: ***vab-8* is a key regulator of posteriorly directed migrations in *C. elegans* and encodes a novel protein with kinesin motor similarity**. *Neuron* 1998, **20**(4):655-666.

76. Wightman B, Clark SG, Taskar AM, Forrester WC, Maricq AV, Bargmann CI, Garriga G: **The *C. elegans* gene *vab-8* guides posteriorly directed axon outgrowth and cell migration**. *Development* 1996, **122**(2):671-682.

77. Tomoda T, Kim JH, Zhan C, Hatten ME: **Role of Unc51.1 and its binding partners in CNS axon outgrowth**. *Genes Dev* 2004, **18**(5):541-558.

78. Gindhart JG, Chen J, Faulkner M, Gandhi R, Doerner K, Wisniewski T, Nandlestadt A: **The Kinesin-associated protein UNC-76 is required for axonal transport in the *Drosophila* nervous system**. *Mol Biol Cell* 2003, **14**(8):3356-3365.

Table

Table 1. Various molecular motors and their associating proteins in *C. elegans*, *Drosophila* and mice.

Name	Mice	*Drosophila*	*C. elegans*	Functions of *C. elegans* protein in the nervous system
Kinesin-1/Conventional kinesin				
Kinesin heavy chain/KHC	KIF5A KIF5B KIF5C	Khc	UNC-116	Axonal outgrowth; presynaptic SNB-1::GFP and SYD-2::GFP localization.
Kinesin light chain/KLC	KLC	Klc	KLC-1 KLC-2	Unknown. Presynaptic SNB-1::GFP localization.
Kinesin-1-associating proteins				
KHC-associating proteins	FEZ1 FEZ2	Unc-76	UNC-76	Axonal outgrowth; presynaptic SNB-1::GFP localization.
	SCOCO	Unc-69	UNC-69	Axonal outgrowth; presynaptic SNB-1::GFP localization.
KLC-associating proteins	JIP3/JSAP1 JIP1 JIP2	SYD	UNC-16	Synaptic protein localization.
	?	?	UNC-14	Axonal outgrowth; presynaptic SNB-1::GFP localization.
	Unc51.1 Unc51.2	?	UNC-51	Axonal outgrowth; presynaptic SNB-1::GFP localization.
	?	?	VAB-8	Posteriorly directed axonal outgrowth and cell migration.
Kinesin-3	KIF1A KIF1Bβ KIF1Bα, KIF1C KIF13A, KIF13B	?	UNC-104	Targeting SNB-1::GFP into axons; less presynaptic SYD-2::GFP puncta.

Table 1. Various molecular motors and their associating proteins in *C. elegans, Drosophila* and mice (continued).

Name	Mice	*Drosophila*	*C. elegans*	Functions of *C. elegans* protein in the nervous system
Cytoplasmic dynein	Dynein heavy chain	Dhc	DHC-1	Presynaptic SNB-1::GFP localization.
	Dynein light chains	Cdlc1/Ctp Cdlc2 Roadblock Dlc90F/Tctex-1	DLC-1	Unknown.
	Dynein intermediate chains	Short wing	C17H12.1	Unknown.
	Dynein light intermediate chains	?	DLI-1	Presynaptic SNB-1::GFP localization.
Cytoplasmic dynein-associating proteins				
	Dynactin			
	$p150^{Glued}$	Glued	DNC-1	Presynaptic SNB-1::GFP localization.
	Dynamitin	Dmn	DNC-2	Presynaptic SNB-1::GFP localization.
	LIS1	Lis1	LIS-1	Presynaptic SNB-1::GFP localization.

Chapter 2

Short coiled-coil domain-containing protein UNC-69 cooperates with UNC-76 to control axonal outgrowth and presynaptic differentiation in *C. elegans*

(manuscript in revision)

Preface

This chapter centers on two proteins, UNC-69 and UNC-76, which play essential roles in both synapse formation and axonal outgrowth in the nematode *C. elegans.* Not only are *unc-69* and *unc-76* mutants phenotypically similar, both UNC-69 and UNC-76 proteins also interact physically *in vitro* and colocalize as puncta in neuronal process in *C. elegans*. UNC-76 may require interaction with UNC-69 to function *in vivo*. *unc-69* and *unc-76* function in the same genetic pathway to control axonal outgrowth of the AWC class of sensory neurons, and cooperate to regulate size and position of SNB-1::GFP puncta, a marker of presynaptic regions. Subcellular distribution of both UNC-69 and UNC-76 requires UNC-116/kinesin heavy chain: in *unc-116(rh24)* mutants, UNC-69 and UNC-76 fail to colocalize in the same perinuclear structure in the soma and occasionally fail to be transported together into the axons. These studies reveal a novel mechanism for membrane traffic in mediating both synapse formation and axonal outgrowth. I hypothesize that UNC-69/UNC-76 protein complex might be required for post-Golgi transport of vesicles into the axons, and suggest that the mammalian homologues of UNC-69 and UNC-76, SCOCO and FEZ respectively, might function in a similar way during mammalian nervous system development.

Dr. Sydney Brenner initially isolated the *unc-69* mutants. Dr. Michael Hengartner studied the *unc-69* gene more than a decade ago in the laboratory of Dr. H. Robert Horvitz in Massachusetts Institute of Technology. At that time *unc-69* was merely known as one of the mutants in *C. elegans* that produces a ventral coiler phenotype due to defects in axonal outgrowth and guidance. Dr. Hengartner, collaborating with

Ms. Erika Hartwieg and Dr. Nancy Tsung, contributed to mapping, positional cloning of the *unc-69* gene and initial characterization of axonal guidance defects of the *unc-69* mutants. Ms. Hartwieg performed electron microscopy analysis of defasciculation defects of the *unc-69* mutants. Their results are presented in Figure 1, Figure 4A-B, Figure 4G-H, and Supplemental Table S1. Dr. Bruce Wightman in the laboratory of Dr. Gian Garriga in the University of California at Berkeley, analyzed axonal guidance defects of several types of neurons in *unc-69* mutants and part of his results are presented in Table 2. Dr. Suzanne Tharin, a former Ph.D. student in the Hengartner Laboratory, collaborating with Dr. Mona Spector in Cold Spring Harbor Laboratory, contributed to Figure 2B-C, Figure 3, Table 1-2, the yeast two-hybrid screen, as well as the initial *in vitro* homophilic binding assays of UNC-69 as described in the Supplemental Results. Dr. Yishi Jin in the University of California at Santa Cruz, isolated the *unc-69(ju69)* allele in a visual genetic screen for SNB-1::GFP mislocalization and her results are presented in Figure 5A-I. I extended the studies and found that UNC-69 is possibly not required for dendritic development and protein targeting within dendrites, and is likely involved specifically in axonal transport. I demonstrated that UNC-69 and UNC-76 proteins interact physically *in vitro* using a GST-pull down assay. Mr. David Meili, a former diploma student in the Hengartner Laboratory, subsequently contributed to serial deletion analysis of the *unc-76* gene and found a 19-amino acid stretch in UNC-76 that is necessary for UNC-76 to bind UNC-69 *in vitro.* Parts of his results are presented in Figure 6. I extended his studies and showed that these 19 amino acids are possibly essential for UNC-76's *in vivo* function. I then used various genetic and molecular approaches to show that UNC-69 and UNC-76 colocalize in axons (Figure 8A-F and J-L) and function together, possibly in a protein complex, to mediate axon extension and normal presynaptic

differentiation *in vivo* (Table 3 and Figure 7), and that the subcellular distribution of both UNC-69 and UNC-76 is altered in *unc-116* mutants (Figure 8G-I and M-W).

The birth of this manuscript, a long and laborious process, was not so much my own effort as to a collective and erudite effort of several people, who helped and guided me through the course of manuscript preparation. Special thank goes to Dr. Michael Hengartner, my boss, whose taste for perfection reflected not only in the phrases unambiguously chosen, but also in a number of experiments that were asked to be rigorously done. Dr. Suzanne Tharin, who finished most of the hard parts of *unc-69* characterization and to whom I am deeply grateful, provided me with lots of data and reagents. I thank Dr. Wan-Chih Chou, who helped me establish the GST pull-down assays, as well as Dr. Jason M. Kinchen, an intelligent 24 hour-helper and a pivotal force behind these studies. Mr. David Meili entitles special tribute for serial deletion analysis of the *unc-76* gene. Dr. Yishi Jin, by whom the synaptic trafficking project was initiated, provided timely advice and inspiration to these studies. I would like to thank Drs. Naoki Hisamoto at Nagoya University and Takao Inoue at University of Tokyo for their suggestions for generating low-copy extrachromosomal arrays. I also like to thank Drs. Mona Spector, Bruce Wightman, Alex Hajnal, Barry Dickson, Bob Horvitz, and many others for their critical reading and kind suggestions.

Short coiled-coil domain-containing protein UNC-69 cooperates with UNC-76 to regulate axonal outgrowth and presynaptic differentiation in *C. elegans*

Cheng-Wen Su,[1,3,*] Suzanne Tharin,[4,5,10,*] Yishi Jin,[6] Bruce Wightman,[7] Mona Spector,[5] David Meili,[1,2,11] Nancy Tsung,[8,12] Gian Garriga,[9] H. Robert Horvitz,[8] and Michael O. Hengartner[1,3]

[1]Institute for Molecular Biology, [2]Zoological Institute, University of Zurich, Winterthurerstrasse 190, CH-8057 Zurich, Switzerland

[3]Neuroscience Center Zurich, ETH and University of Zurich, Winterthurerstrasse 190, CH-8057 Zurich, Switzerland

[4]Program in Genetics, SUNY at Stony Brook, Stony Brook, NY 11794, USA

[5]Cold Spring Harbor Laboratory, Cold Spring Harbor, NY 11724, USA

[6]Howard Hughes Medical Institute, Department of Molecular, Cellular and Developmental Biology, Sinsheimer Laboratories, University of California, Santa Cruz, Santa Cruz, CA 95064, USA

[7]Biology Department, Muhlenberg College, Allentown, PA 18104, USA

[8]Howard Hughes Medical Institute, Department of Biology, Massachusetts Institute of Technology, Cambridge, MA 02139, USA

[9]Department of Molecular and Cell Biology, University of California, Berkeley, Berkeley, CA 94720, USA

[10]Present Address: Department of Neurosurgery, Brigham and Women's Hospital, Children's Hospital and Harvard Medical School, 300 Longwood Avenue, Boston, MA 02115, USA

[11]Present Address: Abteilung für Klinische Chemie und Biochemie, Universitäts-Kinderklinik, Steinwiesstrasse 75, CH-8032 Zürich, Switzerland

[12]Present Address: Clinigen, Inc., 400 W. Cummings Park #5700, Woburn, MA 01801, USA

[*]These authors contributed equally to this publication

e-mail addresses:

Cheng-Wen Su	cheng-wen.su@molbio.unizh.ch
Suzanne Tharin	STHARIN@PARTNERS.ORG
Yishi Jin	jin@biology.ucsc.edu
Bruce Wightman	wightman@muhlenberg.edu
Mona Spector	spectorm@cshl.org
David Meili	david.meili@kispi.unizh.ch
Nancy Tsung	nancy@clinigen.com
Gian Garriga	garriga@berkeley.edu
H.Robert Horvitz	horvitz@mit.edu
Michael O. Hengartner	michael.hengartner@molbio.unizh.ch

Correspondence: Michael O. Hengartner
Tel: +41 1 635-31 40
Fax: +41 1 635-68 64

1. Abstract

Background: The nematode *C. elegans* has been used extensively to identify genetic requirements for proper nervous system development and function. Key to this process is the direction of vesicles to the growing axons, which is required for growth cone extension and synapse formation in the developing neurons. However, the contribution and mechanism of membrane traffic in neuronal development are not fully understood.

Results: We show that the *C. elegans* gene *unc-69* is required for axon outgrowth, guidance, fasciculation and synaptogenesis. We identify UNC-69 as an evolutionarily conserved 108 amino acid protein with a short coiled-coil domain that physically interacts with UNC-76, mutations in which produce many similar defects to *unc-69(lf)*. Additionally, a weak reduction-of-function allele, *unc-69(ju69)*, preferentially causes mislocalization of the synaptic vesicle marker SNB-1. UNC-69 and UNC-76 colocalize as puncta in neuronal processes and cooperate to regulate axon extension and synapse formation.

Conclusions: We have identified a novel protein complex, composed of UNC-69 and UNC-76, which promotes axonal growth and normal presynaptic differentiation in *C. elegans*. As both proteins are conserved through evolution, we suggest that the mammalian homologues of UNC-69 and UNC-76, SCOCO and FEZ, may function similarly.

2. Background

At its simplest, a neuron is composed of three major structures, a central cell body and two networks of extensively branched membrane structures, the dendrite and the axon. The axon is deliberately formed in response to a wide variety of extracellular guidance and repulsion signals that direct migration to a fated location. Although many guidance and repulsion receptors have been identified on extending growth cones, little is known about how activation of receptors mediates coordinated neurite extension. In addition to signaling cues in the extracellular matrix, neurite elongation and growth cone extension depend on a concerted effort of vesicular transport and regulated membrane addition. For growth cones to extend, vesicles derived from the Golgi apparatus fuse with the plasma membrane by a process of regulated exocytosis [1]. Likewise, synapse formation also requires transport of pre- and post-synaptic components supplied in membranous organelles [2, 3]. These vesicles are not only transported but are also differentially sorted into dendrites or axons [4, 5]. To fulfill these tasks, intrinsic cytosolic factors are required to regulate transport of the vesicles [6] and to differentially control dendritic versus axonal growth and morphogenesis.

The nematode *C. elegans* has been extensively used to study vesicular transport in neuronal development. For example, the monomeric kinesin UNC-104/KIF1A, UNC-116/kinesin heavy chain (KHC), kinesin light chain KLC-2, and various cytoplasmic dynein complex components regulate various vesicle trafficking events [7-9]. In the absence of UNC-16, the worm homologue of JNK-scaffolding protein, SNB-1-containing synaptic vesicles and glutamate receptors dislodge from the pre- and post-synaptic terminals, suggestive of a role in intracellular trafficking [7]. Two

axonal outgrowth proteins, the serine/threonine kinase UNC-51 and RUN-domain-containing protein UNC-14, interact physically and are implicated in vesicular transport [10, 11]. Noticeably, although membranous structures with variable size accumulate within axons in *unc-51* [12, 13] and *unc-14* [13] mutants, synaptic vesicles are normally clustered in presynaptic terminals in these mutants [13]. UNC-14 associates with UNC-16 in the presence of KLC-2, whereas UNC-16 binds directly to the tetratricopeptide repeat (TPR) domain of KLC-2 [9]. Thus, KLC-2 is able to recruit UNC-16, UNC-14 and UNC-51, assembling the machinery on Kinesin-1 that regulates transport of various axonal and synaptic cargoes.

In contrast, *C. elegans* UNC-76 and its homologues appear to be required for both axonal outgrowth and synaptic transport via its association with the KHC of Kinesin-1. In worms mutant for *unc-76*, the nervous system is disorganized: the axons fail to extend, and axonal bundles are defasciculated [13, 14]. In *Drosophila,* Unc-76 binds KHC tail and is important for transporting synaptic cargoes in the axons [15]. The mechanism of UNC-76-mediated transport remains elusive, although there is some evidence that secondary modification by protein kinase Cζ (PKCζ) or polyubiquitination of fasciculation and elongation protein, zygin/zeta 1 (FEZ1), one of the mammalian UNC-76 homologues, contributes to its neurite outgrowth activity [16, 17].

In this study we report the cloning and characterization of UNC-69, a small evolutionarily conserved coiled-coil domain-containing protein and a novel binding partner of UNC-76 in *C. elegans*. While a weak reduction-of-function allele of *unc-69* results in a selective defect in mislocalization of a synaptic vesicle marker, strong

unc-69 mutants show extensive axonal outgrowth, fasciculation and guidance defects. UNC-69 preferentially directs membrane traffic within axons. We show that UNC-69 and UNC-76 participate in a common genetic pathway to control axon extension and cooperate to regulate size and position of synaptic vesicles in axons. Moreover, both proteins colocalize as puncta in neuronal processes. We propose that UNC-69 and UNC-76 form a conserved protein complex *in vivo* to regulate axonal transport of vesicles.

3. Results

3.1 *unc-69* encodes a conserved short coiled-coil domain-containing protein

unc-69 was identified in a large-scale behavioral screen for uncoordinated (Unc) mutants [18]. *unc-69* loss-of-function *(lf)* mutants move poorly, coil ventrally and are phenotypically similar to other coiler Unc mutants, many of which are defective in axonal outgrowth and guidance. Additionally, *unc-69* mutant hermaphrodites lay more eggs in the absence of food than wild-type worms do (Supp. Results and Supp. Table S1), suggesting a defect in the hermaphrodite-specific neurons (HSNs), which control egg-laying behavior.

Previous genetic data placed *unc-69* between *lin-12* and *tra-1* on chromosome III, 0.12 map units to the left of *ced-9* [19]. Using cosmid rescue, we were able to identify the predicted gene *T07A5.6a* (previously named *T07C4.10b*) as *unc-69* (Figure 1A). *unc-69* encodes a 108 amino acid protein and contains a short coiled-coil domain in its C-terminus (Figure 1B). While UNC-69 could possibly form a

homodimer via its coiled-coil domain, we failed to detect any homophilic interactions of UNC-69 (Supp. Results).

The original alleles of *unc-69*, *unc-69(e587)* and *unc-69(e602)*, are both nonsense mutations in the C-terminal half of the protein (Figure 1B). *unc-69(e602)* is a T-to-A transversion and replaces a leucine with an Amber stop codon at position 77. *unc-69(e587)* is a C-to-T transition changing a glutamine to an Amber stop codon at position 86; both of these mutations lie within the well-conserved coiled-coil domain. Both *unc-69(e602)* and *unc-69(e587)* are candidate genetic null alleles, as the axon extension and branching defects of ALM and AVM neurons were not significantly enhanced when either of these two alleles was placed *in trans* to the deficiency *nDf40* (Table 1). We also isolated a hypomorphic allele, *ju69*, which is a G-to-A transition at the start codon and changes the initiator methionine to an isoleucine. Theoretically, the M-to-I substitution should abolish translation initiation and hence synthesis of the UNC-69 protein. However, since the phenotype of *unc-69(ju69)* mutants is much weaker than that of the other two alleles, we suspect that a small amount of UNC-69 functional protein is still being produced, either by leaky translation initiation at the original site, translation initiation at an alternative mRNA start site, or through initiation at the internal in frame ATG site at residue 49, which leaves a potentially intact coiled-coil domain. We received a small deletion, *ok339*, which completely eliminates the *unc-69* locus. Unfortunately, this deletion also removes an essential neighboring gene and was therefore not studied further (see Supp. Results). Expressed sequence tag (EST) analysis suggested that the *unc-69* locus encodes two splice variants (Figure 1A and Supp. Results). Northern blot analysis of polyA+

RNA from mixed stage worms as well as from embryos revealed a 0.65 kb major transcript (Figure 1C), consistent with the predicted size of the *T07A5.6a* transcript.

3.2 UNC-69 is conserved from single cell eukaryotes to complex metazoan animals

We found that UNC-69 is highly conserved through evolution and encodes the *C. elegans* homologue of mammalian SCOCO (Short Coiled-Coil Protein), a protein recently found to interact with dominant negative ARF-like 1 (ARL1) protein in a yeast two-hybrid screen [20]. The *S. cerevisiae* UNC-69 homologue, Slo1p (SCOCO-like ORF protein), was shown to interact with Arl3p, a homologue of mammalian ARFRP1, another ARF-like protein, which is involved in ER-Golgi and post-Golgi transport [21, 22]. Uncharacterized UNC-69/SCOCO homologues can also be found in many other animal species (Figure 2A and Supp. Results).

All of the UNC-69 homologues are predicted to form a coiled-coil structure near their C-termini (underlined region in Figure 2A). In an alignment of the *S. cerevisiae*, *C. elegans*, *C. briggsae*, mosquito, fly, *Fugu*, zebrafish, *Xenopus*, mouse and human protein sequences, identity over the coiled-coil regions is 32.6% (Figure 2A). The identity in the coiled-coil region jumps to 73.9% if the yeast sequence is excluded. Except for yeast, an acidic region immediately upstream as well as a serine/threonine-rich and a basic region downstream of the coiled-coil domain appear also to be highly conserved. In contrast, the N-terminus of UNC-69 and its homologues is highly divergent, both in length and in primary amino acid sequence. The function of UNC-

69 proteins seems to be conserved, since expression of SCOCO as a transgene under the *unc-69* promoter restored locomotion to *unc-69* mutants (Figure 2C).

We also assessed the tissue distribution of human *SCOCO* transcripts by probing a human fetal tissue northern blot. This probe detected a single transcript of approximately 2.1 kb in all tissues examined (brain, lung, liver and kidney) (Figure 2B). Human *SCOCO* mRNA appeared to be enriched in fetal brain, possibly hinting at a role for SCOCO in mammalian nervous system development.

3.3 UNC-69 is expressed in the nervous system and other tissues from early embryogenesis to adulthood

We generated transgenic animals expressing either N- or C-terminal green fluorescent protein (*gfp*)-tagged *unc-69* fusion constructs under the control of endogenous *unc-69* promoter. Both of these translational fusion constructs rescued the Unc phenotype of *unc-69* mutants, suggesting that the fusion proteins were correctly expressed and biologically functional. UNC-69::GFP expression was first detectable in embryos (Figure 3A-B). In immature neurons, we observed expression of UNC-69::GFP in the processes and growth cones of developing neurites (arrowhead in Figure 3C). In older larvae and adults, UNC-69::GFP was expressed in neurons of the anterior, lateral, ventral and retro-vesicular ganglia in the head and in neurons of the preanal, dorso-rectal and lumbar ganglia in the tail. The fusion protein was also present in the ventral nerve cord (VNC), in the dorsal nerve cord (DNC), in the dorsal and ventral sublateral nerve cords, and in commissural axons (Figure 3D-F). The reporter was expressed in CAN, HSN, ALM, PLM, AVM, PVM, BDU, and SDQR neurons, as

evidenced by its localization to the cell bodies of these neurons. Expression of *unc-69* in these latter cells was confirmed using an *unc-69::LacZ::NLS* fusion (data not shown). Taken together, these results indicate that *unc-69* is expressed widely, perhaps ubiquitously, in the *C. elegans* nervous system.

Expression of UNC-69::GFP was also observed in non-neuronal cells. In larvae and adults, we observed occasionally UNC-69::GFP expression in body wall muscle (data not shown). We also observed UNC-69::GFP in the excretory canal, in the distal tip cells (DTCs), in the spermatheca and less frequently in hypoderm and gut (Figure 3E and data not shown). However, the expression in these non-neuronal cells was variable and might not reflect the endogenous expression pattern of *unc-69.*

3.4 UNC-69 is required for axonal outgrowth and guidance

The ventral coiler phenotype of *unc-69* mutants suggests a defect in nervous system development. Indeed, previous studies had reported axonal guidance defects of the D-type GABAergic motoneurons, the mechanosensory neurons as well as the HSNs in *unc-69* mutants [23, 24]. We confirmed these observations and extended them to other cell types (Table 1-2 and Figure 4A-F). Incorrect targeting of the DD and VD motor axons is likely to contribute to the Unc phenotype of *unc-69* mutants. In addition to outgrowth and guidance defects, we also observed ectopic branching of the DD/VD and the mechanosensory neurons in *unc-69* mutants (Figure 4D and 4F). In a few cases the axons had unusual large varicosities and occasionally meandered along the lateral body wall.

In examining other neuronal classes in *unc-69(e587)* mutants, we observed premature termination of axons of the FMRF-amide-positive neurons ALA, RID and AVKR, but not RMG (Table 2 and data not shown). We observed that 67% (20/30) of ALA axons terminated prematurely, and ALA axons sometimes branched prior to termination. AVKR had frequent axonal outgrowth and guidance defects: 85% (17/20) of AVKR axons terminated prematurely or crossed from the left VNC (VNCL) to the right VNC (VNCR). Taken together, these observations support a role for *unc-69* in ventral and dorsal axonal guidance as well as in axonal elongation within the fascicles.

3.5 UNC-69 is required for fasciculation in the dorsal and ventral nerve cords

Since *unc-69* mutants have midline crossover defects (Table 2), it is likely that axons running in the same fascicle lose cell-cell adhesion and fail to stay together. We constructed a series of electromicrograph (EM) cross-sections through the major nerve cords (DNC, VNCL and VNCR) that run antero-posteriorly in adult hermaphrodites. In wild-type animals, the composition of axons in any of these nerve cords is highly stereotyped, with four axons fasciculated to run in VNCL and the other ventral axons running within VNCR (Figure 4G) [25]. In *unc-69(e587)* and *unc-69(e602)* mutants, many fascicles split into two or more groups and in some cases defasciculated axons could be seen running alone along the hypodermal ridge. Moreover, some axons of both the DNC and VNCL appeared to be mislocalized and can be seen on the wrong side of the hypodermal ridge (Figure 4H and data not

shown). Anti-tubulin and anti-GABA staining confirmed the observed fasciculation defects in *unc-69(e587)* mutants (data not shown).

3.6 UNC-69 acts cell autonomously to control neurite outgrowth

Since *unc-69(lf)* mutants have axonal outgrowth defects of most of the neurons examined, we asked if the observed defects were caused by loss of *unc-69* function specifically in those neurons or in another tissue. We created *unc-69* transgenic lines expressing *unc-69(+)* specifically in the six touch neurons under the control of a *mec-7* promoter. We compared outgrowth and guidance defects of ALM and AVM in three such lines with that of *unc-69(lf)* mutants (Table 1). In all three transgenic lines, the percentage of ALM neurites that failed to send a branch into the nerve ring dropped significantly. The percentage of ALM neurites that failed to extend to full length also dropped significantly. Similar observations were made for AVM outgrowth and branching. Note that none of the transgenic lines completely rescued the ALM outgrowth and branching defects. This could be due to loss or silencing of the transgene carried on the extrachromosomal array, or reflect a requirement for *unc-69* in other neuronal and/or non-neuronal cells. Nevertheless, we conclude that UNC-69 promotes outgrowth and guidance largely, if not completely, in a cell-autonomous manner.

3.7 UNC-69 is required for normal presynaptic differentiation

The *C. elegans* synaptobrevin/vesicle-associated membrane protein (VAMP) homologue SNB-1 is a vesicular SNARE (v-SNARE) on synaptic vesicles (SVs).

Tagged SNB-1 can be used to follow SVs as they are transported to presynaptic regions [26]. We isolated an allele of *unc-69, ju69,* in a visual genetic screen for mislocalization of a SNB-1::GFP reporter in D-type GABAergic motor neurons. In wild-type worms, SNB-1::GFP expressed in the D neurons can be localized to discrete puncta along the VNC and DNC, at sites of neuromuscular junctions (Figure 5A and 5C). In *unc-69(ju69)* mutant nerve cords, SNB-1::GFP puncta were irregular in size and position, on average larger than in wild type, and often completely missing for extended stretches (Figure 5B and 5D-E). Additionally, we occasionally observed puncta that abnormally diffused from the nerve cords into the commissures (Figure 5D). The morphology of DD and VD neurons is grossly normal (Figure 5F-I) and only occasionally (<10%; n=50) did one commissure fail to exit the VNC. We made similar observations in touch neurons using the $P_{mec\text{-}4}$*::gfp* transgene *zdIs5* (data not shown).

While *unc-69(ju69)* mutant worms are Unc, they move much better than strong *unc-69* mutants. Thus, the locomotion defect observed in *unc-69(ju69)* mutants is likely a consequence of a defect in transport or localization of axonal cargoes rather than in axon guidance.

3.8 UNC-69 is not required for dendritic growth or targeting proteins into dendrites

To determine whether the outgrowth defects we observed in *unc-69* mutants were specific to axons, we examined the morphology of the AWC class of sensory neurons using the *kyIs140* [$P_{str\text{-}2}$*::gfp*] transcriptional reporter, which is normally

stochastically activated in either the right or left AWC neuron [27]. The bilaterally symmetric AWC neurons have a distinct bipolar structure, with a dendrite extending to the tip of the nose and an axon extending into the nerve ring (Figure 4I). In *unc-69(e587)* mutants, the axon of the AWC neuron often stopped prematurely (Figure 4J), and *str-2::gfp* expression was often silenced (see below). In contrast, the dendrite of the AWC neuron had no outgrowth defect, as 100% (136/136) of the AWC dendrites extended to their full length. In *unc-69(e587)* mutants, 73% (99/136) of AWC neurons had ectopic bulges/branches protruding from either the cell body or the axon (similar to what we observed in the mechanosensory neurons, Figure 4C). However, ectopic branches only rarely extended from dendrites (data not shown). Dendritic morphology was also normal in the ASI neurons (visualized by the *str-3::gfp* transgene), the AWB, AWC, ASG, ASI, ASK, and ASJ neurons (visualized by the *tax-2Δ::gfp* transgene) [28, 29], and the sensory neurons ASJ, ASH, ASI, ASK, ADL, and ADF (visualized by staining with the lipophilic dye DiI; data not shown). From the observations above, we conclude that UNC-69 is likely not required for either cilia formation or dendritic elongation within the amphid sensilla. Finally, an odorant receptor was still properly localized to the cilia (see below).

In vesicle trafficking mutants such as *unc-16 and unc-116,* markers for synaptic vesicles are also missorted into dendrites [7]. We wondered whether *unc-69* mutants also show such a general sorting defect, or whether *unc-69* might be more specifically required for efficient trafficking within the axons. At the L1 larval stage, the thirteen VD neurons are not yet born, and the six DD neurons are the only D-type GABAergic motor neurons present in the VNC. At this stage, the DD neurons receive their synaptic inputs from the DNC and output onto the ventral body wall muscles.

Therefore in wild-type L1s, the SNB-1::GFP puncta can only be seen along the VNC. In *unc-69(ju69)* mutants, the synaptic GFP was not significantly mislocalized to the DNC (3.4%; n=59; Figure 5J). In contrast, SNB-1::GFP puncta were frequently seen in the DNC in *unc-16(ju146)* mutant L1s (90.6%; n=32; Figure 5 J). We also made similar observations in worms carrying a *snb-1::gfp* transgene expressed in a pair of ASI sensory neurons, in which SNB-1::GFP was not significantly mislocalized to the ASI dendrites in *unc-69(ju69)* mutants (C.-W. S, Y. J. and M. O. H., unpublished data).

We next asked if UNC-69 plays any role in transporting proteins within the dendrites. We used an *odr-10::gfp* transgene that is expressed in the AWB neurons to answer this question [30]. ODR-10 is an odorant receptor for diacetyl, and is actively transported in vesicles from the cell bodies to the cilia at the end of the dendrites, where the GFP-fusion is deposited (Figure 5K). In dendritic targeting mutants, such as *unc-101* (which encodes the homologue of AP1 μ1 clathrin adaptor protein), ODR-10::GFP is not targeted to the AWB cilia [30] (Figure 5M); in contrast, in both *unc-69(ju69)* and *unc-69(e587)* mutants, ODR-10::GFP was still properly targeted (Figure 5L; data not shown). Taken together, our results suggest that dendritic development and transport of proteins into dendrites is not impaired in *unc-69* mutants. Thus, UNC-69 is possibly specifically required for axonal outgrowth and vesicular trafficking.

3.9 UNC-69 interacts physically with UNC-76

To identify potential UNC-69 interactors, we screened three *C. elegans* yeast two-hybrid (Y2H) libraries using full-length UNC-69 as bait. From these screens, we isolated at least 34 independent clones of UNC-76, a 385 amino acid protein that was previously shown to be involved in axonal outgrowth and fasciculation in *C. elegans* [12-14]. The *Drosophila* homologue of UNC-76 was identified as a kinesin heavy chain-binding protein and shown to be a regulator of axonal transport [15]. A mammalian homologue of UNC-76, FEZ1, is a substrate for PKCξ [16]. Worm, fly and mammalian UNC-76 proteins are not only conserved in primary amino acid sequences but also have several conserved regions (Figure 6D) predicted to be capable of forming coiled-coil domains [14, 15]. UNC-76 localizes to axons, and worms harboring mutations in *unc-76* are severely Unc and coil ventrally, phenotypes very similar to those observed in *unc-69* mutants [14].

We used an *in vitro* GST pull-down assay to verify the physical interaction between UNC-69 and UNC-76. As shown in Figure 6A, *in vitro* translated full-length UNC-76 (UNC-76FL) was pulled down efficiently by GST-UNC-69 but only minimally by GST-CBP, a eukaryotic transcription factor used as a negative control [31]. Conversely, *in vitro* translated adenoviral protein E1A efficiently bound to its cognate partner GST-CBP but not to GST-UNC-69. Therefore, the interaction between UNC-76 and UNC-69 is specific and most likely direct.

To narrow down the regions of interaction, we generated truncated proteins lacking various parts of UNC-76 (Figure 6B, D) and tested for their interaction with GST-UNC-69. We found that amino acids 281 to 299 of UNC-76 were necessary to interact with UNC-69 *in vitro*. Interestingly, this 19 amino acid region overlaps with

a region predicted to form a coiled-coil structure (amino acids 265-292; slashed region in Figure 6D), and lies within a region conserved from worms to humans (gray shaded region in Figure 6D).

3.10 UNC-76 may require interaction with UNC-69 to function *in vivo*

To corroborate the *in vitro* interactions with the *in vivo* function of UNC-76, we expressed YFP or CFP-tagged truncated UNC-76 proteins in *unc-76(e911)* mutant worms (Figure 6D) and assayed for rescue of the uncoordinated phenotype. Both N-terminally and C-terminally tagged full-length UNC-76::YFP or CFP::UNC-76 fusion proteins were functional and rescued *unc-76(e911)* mutants (Figure 6D). The CFP::UNC-76 Δα fusion protein failed to rescue *unc-76(e911)* mutants, suggesting that the N-terminal region of UNC-76 is required for its function *in vivo.* Bloom and Horvitz reported that amino acids 1-197 of UNC-76 are sufficient to direct proteins into the axons in *C. elegans* [14]. Since the axonal targeting sequence of UNC-76 includes the region deleted in UNC-76Δα, we speculated that CFP::UNC-76 Δα fusion proteins were not transported to axons. Indeed, the CFP signal was weak and seemed to congregate more around the soma (data not shown). In contrast, the CFP::UNC-76 Δγ fusion protein was both strongly expressed in soma and axons, but failed to rescue *unc-76(e911)* mutants, consistent with the hypothesis that binding to UNC-69 is critical for UNC-76 to function *in vivo*.

If coiled-coil structures are important for the UNC-76/UNC-69 interaction, any mutation that abolishes the coiled-coil structure would possibly also abolish physical interaction between the two proteins. To test these ideas, we mutagenized four

conserved residues in UNC-76: E275, L281, L287, and K291. Both UNC-76(E275A) and UNC-76(K291A) mutant proteins still bound UNC-69 *in vitro* (Figure 6D). Likewise, YFP fusions of these mutant proteins rescued *unc-76(e911)* mutants. In contrast, both UNC-76(L281P) and UNC-76(L287P) mutant proteins failed to bind UNC-69 *in vitro.* Surprisingly, UNC-76(L287P) was still able to rescue *unc-76(e911) in vivo* (Figure 6C, D; we did not test UNC-76(L281P) for rescue). These data suggest that a single amino acid substitution might not be potent enough to destroy the coiled-coil structure when UNC-76 protein is folded in its native state. Finally, we then created an internal deletion mutant, Δ19, which deletes amino acids 281-299 of UNC-76. The Δ19 mutant not only abolished binding of UNC-76 to UNC-69 *in vitro* but also abolished its ability to rescue *unc-76(e911) in vivo* (Figure 6C and 6D). Occasionally, mutant hermaphrodites carrying the *unc-76 Δ19::yfp* transgene were slightly rescued as young adults. In summary, amino acids 281-299 of UNC-76 likely contain or overlap with an UNC-69 binding site, and UNC-76 may require interaction with UNC-69 to function *in vivo*.

3.11 UNC-69 and UNC-76 act in the same pathway to control axon extension

Since both UNC-69 and UNC-76 are required for axon outgrowth and fasciculation, we asked whether they function in the same genetic pathway to regulate axon extension. We first tested whether overexpression of UNC-69 in *unc-76(lf)* mutants could bypass the *unc-76* mutant phenotype. We overexpressed a functional *unc-69::gfp* transgene as an extrachromosomal array in *unc-76(e911)* mutants but did not see any rescue in locomotion (three independent lines, data not shown). Likewise,

overexpression of a functional *unc-76::yfp* transgene failed to rescue the locomotion defect of *unc-69(e587)* mutants (data not shown).

We also performed a double mutant analysis to further address the question of whether *unc-69* and *unc-76* act in the same pathway. In *C. elegans,* expression of the odorant receptor gene *str-2* is randomly turned on in either the left or the right AWC sensory neuron (AWCL/R), but never in both [27]. In wild-type worms, this "1 AWC^{ON}" phenotype is determined by axonal contact and calcium signaling between AWCL and AWCR. In axonal guidance mutants like *unc-76, sax-3* and *vab-3*, the two AWC axons often fail to meet, and P_{str-2}*::gfp* expression is consequently silenced in both AWCs, giving rise to a "2 AWC^{OFF}" phenotype [27]. We used this system to assay for axon extension defects in the nerve ring in different *unc-69(lf)* and *unc-76(lf)* mutants as well as in *unc-69(lf); unc-76(lf)* double mutants.

In both strong loss-of-function mutants *unc-69(e602)* and *unc-69(e587)*, 30-34% of animals showed a 2 AWC^{OFF} phenotype. In contrast, the hypomorphic allele *unc-69(ju69)* resulted in only 1% of mutant worms (n=190) having P_{str-2}*::gfp* expression silenced in both AWCs (Table 3). This result was consistent with our previous observation that neuronal morphology is largely normal in *unc-69(ju69)* mutants. In agreement with previous studies [27], 47% of *unc-76(e911)* mutants (n=101) had the 2 AWC^{OFF} phenotype; *e911* was the strongest allele among all the nine alleles that we tested. For the other *unc-76* alleles, the 2 AWC^{OFF} phenotype varied from 6% to 30%. Interestingly, the strength of the AWC expression defect (which is an indication of axon extension defects) showed an inverse collinear relationship with the position of each mutation in the open reading frame: the most 5' mutation, *unc-76(n2457),*

showed the least defect in axon extension, whereas alleles located most C-terminally showed greater defects than alleles located close to the N-terminus (Table 3). Interestingly, we did not observe enhancement of axon extension defects in *unc-69(e602); unc-76(e911)* or *unc-69(e587); unc-76(e911)* double mutants (Table 3). In contrast, axon extension defects were greatly enhanced in *unc-76(e911); sax-3(ky123), unc-76(e911); unc-6(n102),* and slightly enhanced in *unc-76(e911); vab-3(e648)* double mutants (Table 3). These data support the notion that UNC-69 and UNC-76 interact genetically and act in the same pathway to control axon extension, at least in the case of the AWC sensory neurons.

3.12 UNC-69 and UNC-76 cooperate to promote presynaptic differentiation

We showed above that UNC-69 is required for localization of synaptic vesicles in axons. Does UNC-76 also play a role in this process, and if yes, does UNC-76 control presynaptic differentiation together with UNC-69? Unfortunately, all existing *unc-76* alleles have severe axonal outgrowth defects, making interpretations of the results of synaptic vesicle localization difficult. To bypass this problem and to reveal genetic interactions between *unc-69* and *unc-76*, we looked at localization of the synaptobrevin SNB-1::GFP puncta in *unc-69(lf)/+; unc-76(lf)/+* double heterozygotes (Figure 7). In wild-type adult hermaphrodites, SNB-1::GFP can be seen as evenly distributed puncta along the DNC [7] (Figure 7A and 7E). The GFP puncta distribution pattern in DNC was not significantly different in *unc-69(e587)/+* heterozygotes as compared to wild-type animals (Figure 7B). However, in both *unc-69(e587)/+; unc-76(e911)/+* and *unc-69(e587)/+; unc-76(n2457)/+* double heterozygous hermaphrodites, SNB-1::GFP puncta were occasionally more diffused,

larger, or completely absent within a stretch of DNC (Figure 7C-D and 7F); the absence of SNB-1::GFP puncta may be due to either transport or axon extension defects. In addition, *unc-69(e587)/+; unc-76(e911)/+* and *unc-69(e587)/+; unc-76(n2457)/+* double heterozygotes were occasionally slightly Unc in locomotion, resembling weak synaptic transmission mutants. The weak locomotion defect could be a direct or indirect effect of the synaptic vesicle mislocalization defect.

In summary, the *unc-69/+; unc-76/+* double heterozygotes show phenotypes that are similar, albeit significantly weaker, to those observed in *unc-69(ju69)* homozygotes. Genetic interactions of this type, commonly known as nonallelic (or unlinked) noncomplementation, are often observed with proteins that form heterodimers or function in a common protein complex (e.g., α- and β-tubulin; [32]). However, several other explanations are also possible (discussed in [33]). Thus, our observations are compatible with, but do not definitively prove, the hypothesis that UNC-69 and UNC-76 cooperate to control axonal transport.

3.13 UNC-69 and UNC-76 colocalize in puncta and possibly function together to mediate vesicular transport

To determine the subcellular localization of UNC-69 and UNC-76, we coinjected $P_{unc\text{-}69}$*::cfp::unc-69* and $P_{unc\text{-}76}$*::unc-76::yfp* constructs at low concentration (5 ng/μL) into *unc-76(e911)* mutant hermaphrodites, and selected rescued transgenic animals for examination. At low concentration, both CFP::UNC-69 and UNC-76::YFP often appeared as puncta along the DNC, in CAN neurons, as well as in other neuronal processes that run along the subdorsal and subventral tracts (Figure

8A-F). Less frequently, these puncta could also be found in commissures that connect the DNC to the VNC. The punctate pattern of UNC-76 can also be observed when worms are stained with anti-UNC-76 antisera [14], consistent with this being the endogenous expression pattern of UNC-76. Both CFP::UNC-69 and UNC-76::YFP puncta were of variable size but were usually large and immobile, even in the commissures. Interestingly, CFP::UNC-69 and UNC-76::YFP proteins also colocalized in round, perinuclear dots in the soma (Figure 8J-L). These observations strengthen our belief that UNC-69 and UNC-76 coexist in a complex to control synaptic vesicle trafficking and axonal outgrowth/fasciculation. The molecular nature of the observed UNC-69/UNC-76 puncta (multiprotein complexes? vesicles?) remains to be determined.

3.14 UNC-116/kinesin heavy chain is required for subcellular distribution of both UNC-69 and UNC-76

In *Drosophila*, Unc-76 binds KHC, which is the major component of the conventional kinesin motor required for axonal transport towards plus ends of the microtubules [15]. A similar biochemical interaction between UNC-76 and the *C. elegans* KHC orthologue UNC-116 [34], has not been reported so far. To determine whether UNC-69/UNC-76 are transported to axons by UNC-116, or by another kinesin, the KIF1A homologue UNC-104 [35], we compared subcellular localization of both CFP::UNC-69 and UNC-76::YFP in wild-type and in different kinesin mutant backgrounds.

In *unc-116(rh24)* mutants, UNC-76::YFP puncta were occasionally diffused and sometimes failed to be accompanied by CFP::UNC-69 puncta in a stretch of axon

(Figure 8G-I). In addition, both CFP::UNC-69 and UNC-76::YFP proteins often occupied distinct but partially overlapping perinuclear territories in the soma in *unc-116(rh24)* mutants (Figure $8M_I$-O_{III}). Whereas perinuclear CFP::UNC-69 dots increased in size in *unc-116(rh24)* mutants, perinuclear UNC-76::YFP either split into several smaller dots (as in Figure $8N_I$) or formed irregular reticular structure (as in Figure $8N_{III}$) in *unc-116(rh24)* mutants. The *unc-116(rh24)* mutants carry two missense mutations (I304M and E338K) at the end of the motor domain of KHC (amino acids 1-358; [34]). Thus, these mutations are likely to affect the processivity of KHC and cargo transport along the microtubules. The above data suggest that UNC-116/KHC might directly or indirectly contribute to transport of at least one of these two proteins into the axons.

We also generated functional integrated UNC-69::GFP and UNC-76::YFP transgenes that were stably overexpressed in the nervous system and studied their subcellular localization in different kinesin mutant backgrounds. The CAN neurons are a pair of bilaterally symmetric neurons that send processes antero-posteriorly along the excretory canal (Figure 8P; [36]). In wild-type animals, UNC-69::GFP and UNC-76::YFP could be observed both in the CAN soma and throughout the processes (Figure 8P and 8S). In worms mutant for *unc-104(e1265),* the *C. elegans KIF1A* homologue [35], subcellular distribution of UNC-69::GFP and UNC-76::YFP was not significantly altered (Figure 8Q and 8T). In *unc-116(rh24)* mutants, overexpression pattern of UNC-69::GFP and UNC-76::YFP were both significantly different from wild-type animals. The CAN neuron accumulated UNC-69::GFP in the vicinity of its cell body, which was swollen and deformed. In addition, there were ectopic branches near the cell body, and UNC-69::GFP also accumulated in these processes (Figure

8R). Unlike UNC-69::GFP, UNC-76::YFP appeared as giant dots along the CAN processes in *unc-116(rh24)* mutant, as if UNC-76::YFP was removed from the cytoplasm and concentrated in certain subcellular compartments (Figure 8U). Moreover, a CEH-23::UNC-$76_{1\text{-}197}$::GFP fusion protein [37] also appeared as large aggregates along CAN processes in *unc-116(rh24)* mutants (Figure 8W).

To sum up, our data show that the subcellular distribution of both UNC-69 and UNC-76 is altered in *unc-116(rh24)* mutants. However, axonal transport of UNC-69 and UNC-76 is still occurring in *unc-116(rh24)* mutants. Thus, different kinesin motors and/or additional factors likely contribute to transport of UNC-69 and UNC-76 along the axons.

4. Discussion

4.1 UNC-69 is required for presynaptic differentiation and axonal outgrowth

In this work we show that mutations that affect the small 108 amino acid protein UNC-69 abrogated a spectrum of processes, including synaptic vesicle targeting, axonal outgrowth, pathfinding, and fasciculation. While a weak reduction-of-function allele of *unc-69* results in a selective defect in synaptic vesicle localization, strong *unc-69* mutants show extensive axonal outgrowth, fasciculation and guidance defects. Both strong *unc-69(lf)* alleles, *unc-69(e602)* and *unc-69(e587)*, truncate the coiled-coil domain of UNC-69. In contrast, the hypomorphic allele *unc-69(ju69)* results in a missense mutation of the start codon and presumably interferes with translation

initiation. The lack of axonal outgrowth defects in the *unc-69(ju69)* mutants suggests that UNC-69 protein translation might not be totally abolished, and enough UNC-69 protein is still be produced to meet the requirement for growth cone extension. In contrast, the process of synaptic transport appears to be more sensitive to reduction of UNC-69 protein level. It is possible that *unc-69* mediates different cellular processes in parallel: axonal outgrowth, fasciculation and guidance on one hand, synaptic transport on the other. Alternatively, and perhaps more likely, the axonal outgrowth and fasciculation defects observed in strong *unc-69(lf)* mutants could be secondary to the transport defect, as UNC-69 might be required not only for transport of synaptic cargoes but also for the transport of axonogenic vesicles to growth cones.

UNC-69 is clearly different from most other molecules that have been implicated in axon outgrowth and guidance, which are either guidance cues, membrane receptors, or cell adhesion proteins [38, 39]. It is tempting to place *unc*-69 downstream of these molecules, acting possibly as an integrator or transducer of extracellular guiding signals.

4.2 UNC-69 and UNC-76 interact *in vivo*

We identified UNC-76 as an UNC-69-interacting protein. UNC-76 is required for axonal outgrowth and fasciculation in worms and its homologue in *Drosophila* is an axonal transport protein [14, 15]. We identified a 19-amino acid segment (aa 281-299) in UNC-76 that was necessary for its interaction with UNC-69, and possibly for its *in vivo* function. Our genetic experiments suggest that both UNC-69 and UNC-76 act in the same pathway to regulate axon extension. Additionally, we found that

UNC-76 and UNC-69 cooperate to regulate size and position of SNB-1::GFP puncta, a marker of presynaptic regions. Finally, we showed that UNC-69 and UNC-76 colocalize in neurons as puncta and that their normal subcellular distribution requires UNC-116/KHC. The physical interaction, subcellular colocalization, and similar mutant phenotypes all suggest that the UNC-69/UNC-76 protein complex acts as a functional unit that promotes transport of vesicles along axons.

4.3 UNC-69 and UNC-76 define a novel pathway for axonal transport

Proper SNB-1::GFP localization requires UNC-116/KHC, KLC-2, UNC-14, as well as UNC-16, the worm homologue of *Drosophila* Sunday Driver, which serves as a scaffold protein on the synaptic vesicles receiving regulatory signals from the JNK pathway [7, 9]. Both UNC-16 and UNC-14 are recruited to Kinesin-1 through their interaction with KLC-2 [9]. In all of these mutants, SNB-1::GFP is mislocalized from axons to dendrites. In contrast, SNB-1::GFP puncta were largely excluded from dendrites in *unc-69(ju69)* mutants, suggesting that UNC-69 is intrinsically different from these proteins. UNC-69 may function in a specific step of axonal transport, and is possibly not involved in polarized sorting. In addition, UNC-69 is unlikely to control general protein trafficking in neurons, as it was not required for dendritic transport of the transmembrane receptor ODR-10.

The implication of *Drosophila* Unc-76 as a KHC-binding protein further suggests that the UNC-69/UNC-76 protein complex constitutes an alternative pathway that regulates Kinesin-1-mediated transport. Instead of being recruited to Kinesin-1 by KLC-2, as is the case of UNC-16 and UNC-14, direct association of the UNC-

69/UNC-76 protein complex with the tail of KHC may provide additional regulation of intracellular trafficking of a different repertoire of cargoes.

Kinesin-1 transports various cargoes including Golgi, ER, mitochondria and synaptic membrane proteins, but not synaptic vesicles, in the nervous system [34, 40, 41]. In contrast, UNC-104/KIF1A preferentially transports synaptic vesicle precursors [35, 42]. Thus, the synaptic vesicle marker mislocalization defects in various Kinesin-1 mutants [7, 9, 43, 44] is likely secondary to a general defect of cargo trafficking within the axons. Since subcellular localization of UNC-69 and UNC-76 is altered in the KHC *unc-116(rh24)* mutants, but not in the *unc-104(e1268)* or *unc-104(rh43)* mutants (our unpublished observations), our data imply that UNC-69 and UNC-76 are possibly required for transporting membranous organelles other than synaptic vesicles. UNC-69 likely affects only a specific aspect of KHC-dependent vesicular transport, in contrast to the more general requirement for UNC-116/KHC.

4.4 UNC-69/UNC-76 protein complex in fasciculation

In this study we also revealed a possible requirement of vesicular trafficking for proper axonal fasciculation in *C. elegans*; in strong *unc-69* mutants axons were defasciculated. Fasciculation is poorly understood in *C. elegans*, though three other genes, *unc-34, unc-71 and unc-76,* are known to be required for this process [13]. UNC-34 is homologous to *Drosophila* Enabled (Ena), which acts downstream of attractive/repulsive guidance cues to regulate the actin cytoskeleton [45]. UNC-71 encodes an ADAM family metalloprotease that also controls axon guidance and cell migration in *C. elegans* [46]. Neither UNC-34 nor UNC-71 have been shown to

function in vesicular trafficking, suggesting that fasciculation defects can arise through multiple distinct mechanisms. Since in worms synapses are formed *en passant* along the axons, and the delivery of synaptic components requires UNC-69 and UNC-76, it is possible that proteins important for cell adhesion are also delivered along the surface of the axons in an UNC-69/UNC-76-dependent manner.

4.5 Implication of UNC-69 in mediating post-Golgi transport

UNC-69 is not predicted to have enzymatic activity, and possibly functions only by interacting with other coiled-coil domain-containing proteins. The budding yeast and mammalian homologues of UNC-69, Slo1p and SCOCO, have been shown to interact, respectively, with Arl3p and ARL1 – two related, Golgi-associated, GTP-binding ADP-ribosylation factor (ARF)-like proteins. Both Arl3p and ARL1 are involved in vesicular traffic, especially in post-Golgi transport [20, 21]. If this interaction is conserved in worms, UNC-69 might be recruited to Golgi by ARL-1 to regulate vesicular transport in the adult nervous system. Knock-down of the worm orthologue of mammalian ARL1, *arl-1*, by RNA interference (RNAi) results in an embryonic lethal phenotype. To assess a possible role of *arl-1* in the adult nervous system, we fed $P_{unc\text{-}25}$*::snb-1::gfp* transgenic L1 larvae with *arl-1* dsRNAs, but failed to observe any significant SNB-1::GFP mislocalization defects in adults (C.-W. S. and M. O. H., unpublished observations), possibly due to the low efficacy of feeding RNAi in knocking down genes expressed in mature neurons [47].

4.6 Model for UNC-69/UNC-76 protein complex in vesicular trafficking

We propose that UNC-69 and UNC-76 participate in a protein complex, which is localized to certain subcellular compartments in the cytoplasm to control vesicle formation from the Golgi, followed by tethering of these vesicles to the Kinesin-1 motor. Since multiple ectopic branches were consistently observed in both *unc*-69 and *unc-76* mutants, the UNC-69/UNC-76 protein complex might help target membrane addition precisely to the growth cones, thereby preventing unwanted membrane extension elsewhere along the axons. The location of the UNC-69/UNC-76 puncta may reflect nascent or established *trans*-Golgi network (TGN) exit sites [48]. Such Golgi outposts have not been carefully studied in *C. elegans* axons, although Golgi marker is seen as scattered dots around the cytoplasm in head muscles [49]. UNC-69/UNC-76 puncta could also reflect certain post-Golgi compartments that shuttle between their budding sites on *trans*-Golgi and their docking sites near the plasma membrane. As such, an UNC-69/UNC-76 protein complex might function at an intermediate step prior to vesicle maturation. Indeed, UNC-69/UNC-76 puncta were present along the commissures in addition to axons. Since commissures do not form synapses [36], these puncta could define a sorting compartment from which functional vesicles are formed. The UNC-69/UNC-76 puncta seemed to be stationary, possibly anchored through an as yet unidentified mechanism.

5. Conclusions

Our studies reveal an important role for the UNC-69/UNC-76 protein complex in axonal outgrowth, fasciculation and synapse formation. Our results suggest that the molecular basis of these various phenotypes is a defect in regulated axonal transport of vesicles. We conclude that UNC-69 and UNC-76 act as a functional unit to

regulate one or multiple steps of vesicle dynamics in the *C. elegans* nervous system. Finally, based on our transgenic rescue experiments, we suggest that mammals would also utilize the UNC-69/UNC-76 complex in a similar fashion to control synapse formation and axonal outgrowth. We expect further studies to shed light on this hitherto less noticed branch of axonal guidance.

6. Materials and Methods

C. elegans Strains and Genetics

C. elegans strains were maintained as described [18]. All strains were grown at 20°C, except *dpy-20(e1282ts)* and *lin-15(n765ts)* mutants, which were grown at 15°C prior to injection to improve viability, and at 25°C following injection to enhance selection of transgenic F1 animals. Wild-type worms were of the Bristol N2 strain.

Cloning of *unc-69*

All genetic mapping data were deposited into **WormBase** [http://www.wormbase.org]. *unc-69* is tightly linked to RFLP *nP55*, which is recognized by cosmid C15B3. The three overlapping cosmids C15B3, C41B4, and F11D2, but not the flanking cosmids C30B11 and F46H1, rescued the Unc phenotype of *unc-69(e587)* mutant. Subsequent subclonings identified a 1.2 kb EcoR I-Sac I rescuing genomic fragment, which contained a single gene comprised of three exons. A frameshift mutation was introduced into the *unc-69* open reading frame of the rescuing EcoR I-Sac I fragment by cutting and filling the unique Mlu I restriction site,

followed by religation of the blunt ends. The frameshifted construct failed to rescue *unc-69* mutant worms. To identify the molecular lesion(s) present in *unc-69* mutants, the *unc-69* locus from wild type and *unc-69* mutants was amplified using primers flanking the gene (GCTCCGCAGTACGTCTTCTAAGCCC and GCGAGAATGGAACAATCAATGGACG) and sequenced. In addition to the stop codon, *e602* also contains a silent (third base) G-to-A transition in lysine 107.

Egg-laying assay

Assays of egg-laying behavior were performed either in M9 [50] or on plates. For M9 assays, gravid hermaphrodites were individually transferred to microtiter wells containing either M9 or a 5 mg/mL solution of serotonin (5-HT, Sigma, St. Louis, MO) in M9 and the number of eggs laid after 60 minutes was determined. For plate assays, five gravid hermaphrodites were transferred onto fresh plates with or without food, and the total number of eggs laid after 90 minutes was determined.

Immunocytochemistry and fluorescence microscopy

Indirect immunofluorescence staining for serotonin and GABA were performed as previously described [51-53]. Anti-serotonin and anti-GABA antisera were generously provided by Dr. H. Steinbusch (Free University, Amsterdam, the Netherlands) and used at 1%. For fluorescence microscopy, animals were anaesthetized with either 30 mM NaN_3 or 5 mM levamisole and mounted on 4% agarose pads. Neuronal morphology was observed on a Zeiss Axioplan microscope equipped for epifluorescence, using the Zeiss filter set 488005 (excitation 395-440 nm

band-pass filter; emission 470 nm long pass filter). Alternatively, a Zeiss 510 or a Leica DMRE confocal laser-scanning microscope equipped with TCS SP2 AOBS and PL APO objectives was used.

Electron microscopy

Adult hermaphrodites were fixed in 0.8% glutaraldehyde, 0.7% OsO_4, 0.1 M cacodylate buffer for 1 hr on ice. Subsequently, samples were cut and postfixed in 2% OsO_4, 0.1 M cacodylate buffer, mounted into an agar block, dehydrated in series of alcohols, and embedded in a mixture of epon-araldite. Thin sections (50 nm) were cut on an Ultracut E and pictures were taken with a JEOL 1200X at 80 kV.

Dye filling

Adult worms were soaked in 10 μg/ml DiI (Molecular Probes) in M9, and incubated in the dark for 2 hours at 20°C, followed by several washes in M9 buffer. Staining was analyzed using appropriate filters.

cDNA screening and Northern blot

A rescuing 2.8 kb EcoR I genomic fragment was used to probe a *C. elegans* lambdaZAP cDNA library (gift of R. Barstead). From approximately 300,000 plaques, we isolated 4 cDNAs. The sequences present at the ends of the inserts were determined for all 4 clones, and the DNA sequence of the longest intact clone was determined (one strand only). A random-primed, ^{32}P-labeled *unc-69* cDNA was used

to probe a northern blot of wild-type polyA+ RNA. The blot was visualized and band intensities quantified using a Fuji Film phosphor imager. polyA+ RNA was isolated from purified embryos or mixed stages of wild-type strain N2 as described by Sambrook et al [54], except that FastTrack columns (Invitrogen, San Diego, CA) were used (according to the manufacturer's protocols) instead of standard oligo(dT) columns. Likewise, a human fetal multiple tissue Northern blot was probed with a portion of the *SCOCO* cDNA.

Molecular Biology

All manipulations were done following standard protocols [54]. A 1.5 kb *unc-69* genomic fragment containing 700 bp upstream and 300 bp downstream of the coding region was engineered through site-directed mutagenesis to construct various N- and C-terminal CFP/GFP fusions (pgfpu69, pu69gfp and pSU83). The rescuing ability of the constructs was tested for both N- and C-terminal GFP fusions. A full-length *unc-69* cDNA was cloned into pGEX-4T1 to generate a prokaryotic expression *unc-69-gst* construct. To generate a full-length *unc-76* major splicing form cDNA (pSU01), the EcoR I-Xba I fragment of p76-c4 [14] was replaced by the EcoR I-BamH I fragment of *yk784h09* and the Xba I-BamH I fragment of p76-c7, using three-way ligation. Progressive *unc-76* deletions were made either by a PCR-based method, or using ExoIII and S1 nucleases following Erase-a-Base® (Promega) and ExoIII/S1 Deletion Kit (Fermentas) protocols. To generate genomic *unc-76* constructs, an Asc I site was engineered 5' to the start ATG, and was used to insert a 1kb Kpn I-Asc I *unc-76* promoter region up to the start codon. Subsequently a Bgl II-Sph I genomic fragment encompassing exon 1 to 3 was used to replace the corresponding region of the cDNA.

An Asc I CFP cassette was inserted in-frame to create the N-terminal CFP fusion plasmid (pSU65). Likewise, a Not I site was engineered immediately 5' to the stop codon to allow creation of the C-terminal YFP fusion plasmid (pSU26).

Single amino acid changes were performed following QuikChange™ Site-Directed Mutagenesis Kit protocols (Stratagene). Sequences for each of the *unc-76* mutations are as follows: E275A: GAG→GCG; L281P: CTG→CCA; L287P: CTG→CCG; K291A: AAA→GCC. Mutations were confirmed by sequencing, and swapped back into the original plasmids before further subcloning.

All plasmids and construct sequences are available upon request.

Protein sequence analysis

Prediction of coiled-coil structures was carried out using the COILS verison 2.1 program [55]. The coiled-coil regions of UNC-69, UNC-76 and its homologues were assigned on the basis of a greater than 80% probability of forming coiled-coils according to this program. We used ClustalW or T-Coffee for multiple sequence alignment, and shaded the ClustalW alignment using BOXSHADE.

Yeast two-hybrid screens

Random- and dT-primed yeast two-hybrid phage libraries were generous gifts from Dr. R. Barstead (Oklahoma Medical Research Foundation, USA). A further random-primed library was provided by Dr. M. Vidal (Harvard Medical School, USA). *unc-*

69 cDNA was subcloned into pDBTrp and pDBLeu vectors (PROQUEST Two-Hybrid System, GibcoBRL), and cotransformed with the AD plasmids. Transformed yeast reporter strain Mav203 (GibcoBRL) was patched onto plates lacking Leu and Trp (LW plates), and then replica plated onto plates lacking Leu, Trp and His with 3-amino triazol (LWH/3AT plates), onto plates lacking Uracil (URA plates) and onto filters for β-Gal assays. Only clones that activated all three (His, Ura, LacZ) reporter genes were kept for further analysis. Plasmid DNAs were purified from positive clones and retested for interaction with the bait plasmid.

in vitro translation and GST pull-down assay

in vitro transcription and translation of *unc-76* was performed following protocols of the TNT Coupled Reticulocyte Lysate System (Promega) in the presence of ^{35}S-labeled methionine (Amersham). For pull-down experiments, purified recombinant GST and UNC-69-GST proteins were first immobilized on glutathione beads (Amersham). From 2 to 10 μg of immobilized proteins were incubated with 1 to 20 μl *in vitro* translated UNC-76 (depending on binding efficiency) in 1x interaction buffer (20 mM HEPES pH 7.9, 5 mM $MgCl_2$, 0.2% NP40, 0.2% BSA, 7.5% glycerol, protease inhibitor cocktail (Complete Mini®, Roche)) at 4°C for 1.5 to 2 hours. The beads were washed 3 times in washing buffer (100 mM KCl, 20 mM HEPES pH 7.9, 5 mM $MgCl_2$, 0.2% NP40, protease inhibitor cocktail (Complete Mini®, Roche)), resuspended in 20 μl 2x SDS sample buffer, boiled and analyzed by SDS-PAGE and autoradiography.

Germline transformations and array integration

For high copy overexpression, plasmids were injected into the germline of adult hermaphrodites [56] at 50 ng/µl together with 150 ng/µl rescuing *dpy-20(+)* or pL15-EK *lin-15(+)* genomic fragments. To generate low copy extrachromosomal arrays, plasmids were individually or co-injected each at 5 ng/µl together with 195 ng/µl pL15-EK. Transgenic progeny of injected animals were selected as non-Dpy or non-Muv animals at 25°C. Stably transmitting extrachromosomal arrays were integrated by γ-irradiation at 120 kV for 4.2 minutes.

7. List of abbreviations

ARF	ADP-ribosylation factor
ARL	ARF-like
CFP	Cyan fluorescent protein
DNC	Dorsal nerve cord
DTC	Distal tip cell
EM	Electromicrograph
EST	Expressed sequence tag
FEZ1	Fasciculation and elongation protein, zygin/zeta 1
FL	Full-length
GABA	γ-aminobutyric acid
GFP	Green fluorescent protein
GST	Glutathione S-transferase
HSN	Hermaphrodite specific neuron

KHC	Kinesin heavy chain
KLC	Kinesin light chain
lf	loss-of-function
MBP	Maltose-binding protein
ORF	Open reading frame
PKCζ	Protein kinase Cζ
RNAi	RNA interference
RUN	RPIP8, UNC-14, and NESCA
SCOCO	Short coiled-coil protein
SNARE	Soluble N-ethylmaleimide-sensitive factor attachment protein receptor
SV	Synaptic vesicle
TGN	*trans*-Golgi network
TPR	Tetratricopeptide repeat
ts	Temperature-sensitive
unc	Uncoordinated
VAMP	Vesicle-associated membrane protein
VNC	Ventral nerve cord
v-SNARE	vesicular SNARE
Y2H	Yeast two-hybrid
YFP	Yellow fluorescent protein

8. Acknowledgements

We thank A. Hajnal and J. M. Kinchen for critical reading of the manuscript, B. Dickson for thoughtful comments, and W.-C. Chou, L. Martin, P. Gisler and E.

Horvath for other help. We thank E. Hartwieg for assistance with the EM sections; D. Baillie for the *C. briggsae* genomic library; S. Clark for the *mec-4::gfp* plasmid; R. Barstead and M. Vidal for Y2H libraries; H. Steinbusch for antisera; R. Eckner for the E1A and CBP plasmids; Y. Kohara for cDNAs; and C. Bargmann for the *kyIs4* strain. Some strains were contributed by the *Caenorhabditis* Genetics Center (CGC), which is funded by the National Institutes of Health (NIH) Center for Research Resources. We would also like to thank G. Moulder at the *C. elegans* Gene Knockout Consortium for providing us with the *unc-69(ok339)* deletion strain. This work was funded by grants from the Rita Allen Foundation, March of Dimes, Ernst Hadorn Foundation, and Swiss National Science Foundation to M.O.H. The work at MIT was supported by NIH Grant GM24663 to H.R.H. H.R.H. and Y.J. are investigators of the Howard Hughes Medical Institute. C.-W.S. is supported by the Ernst Hadorn Foundation and a Zentrum für Neurowissenschaften Zürich (ZNZ) Ph.D. fellowship.

References

1. Martinez-Arca S, Coco S, Mainguy G, Schenk U, Alberts P, Bouille P, Mezzina M, Prochiantz A, Matteoli M, Louvard D *et al*: **A common exocytotic mechanism mediates axonal and dendritic outgrowth**. *J Neurosci* 2001, **21**(11):3830-3838.
2. Washbourne P, Bennett JE, McAllister AK: **Rapid recruitment of NMDA receptor transport packets to nascent synapses**. *Nat Neurosci* 2002, **5**(8):751-759.
3. Ahmari SE, Buchanan J, Smith SJ: **Assembly of presynaptic active zones from cytoplasmic transport packets**. *Nat Neurosci* 2000, **3**(5):445-451.
4. Burack MA, Silverman MA, Banker G: **The role of selective transport in neuronal protein sorting**. *Neuron* 2000, **26**(2):465-472.
5. Horton AC, Ehlers MD: **Neuronal polarity and trafficking**. *Neuron* 2003, **40**(2):277-295.
6. Vale RD: **The molecular motor toolbox for intracellular transport**. *Cell* 2003, **112**(4):467-480.
7. Byrd DT, Kawasaki M, Walcoff M, Hisamoto N, Matsumoto K, Jin Y: **UNC-16, a JNK-signaling scaffold protein, regulates vesicle transport in *C. elegans***. *Neuron* 2001, **32**(5):787-800.
8. Koushika SP, Schaefer AM, Vincent R, Willis JH, Bowerman B, Nonet ML: **Mutations in Caenorhabditis elegans cytoplasmic dynein components reveal specificity of neuronal retrograde cargo**. *J Neurosci* 2004, **24**(16):3907-3916.

9. Sakamoto R, Byrd DT, Brown HM, Hisamoto N, Matsumoto K, Jin Y: **The *C. elegans* UNC-14 RUN domain protein binds to the Kinesin-1/UNC-16 complex and regulates synaptic vesicle localization**. *Mol Biol Cell* 2004.

10. Ogura K, Shirakawa M, Barnes TM, Hekimi S, Ohshima Y: **The UNC-14 protein required for axonal elongation and guidance in *Caenorhabditis elegans* interacts with the serine/threonine kinase UNC- 51**. *Genes Dev* 1997, **11**(14):1801-1811.

11. Lai T, Garriga G: **The conserved kinase UNC-51 acts with VAB-8 and UNC-14 to regulate axon outgrowth in *C. elegans***. *Development* 2004, **131**(23):5991-6000.

12. Hedgecock EM, Culotti JG, Thomson JN, Perkins LA: **Axonal guidance mutants of *Caenorhabditis elegans* identified by filling sensory neurons with fluorescein dyes**. *Dev Biol* 1985, **111**(1):158-170.

13. McIntire SL, Garriga G, White J, Jacobson D, Horvitz HR: **Genes necessary for directed axonal elongation or fasciculation in *C. elegans***. *Neuron* 1992, **8**(2):307-322.

14. Bloom L, Horvitz HR: **The *Caenorhabditis elegans* gene *unc-76* and its human homologs define a new gene family involved in axonal outgrowth and fasciculation**. *Proc Natl Acad Sci U S A* 1997, **94**(7):3414-3419.

15. Gindhart JG, Chen J, Faulkner M, Gandhi R, Doerner K, Wisniewski T, Nandlestadt A: **The Kinesin-associated protein UNC-76 is required for axonal transport in the *Drosophila* nervous system**. *Mol Biol Cell* 2003, **14**(8):3356-3365.

16. Kuroda S, Nakagawa N, Tokunaga C, Tatematsu K, Tanizawa K: **Mammalian homologue of the *Caenorhabditis elegans* UNC-76 protein**

involved in axonal outgrowth is a protein kinase C zeta-interacting protein. *J Cell Biol* 1999, **144**(3):403-411.

17. Okumura F, Hatakeyama S, Matsumoto M, Kamura T, Nakayama KI: **Functional regulation of FEZ1 by the U-box-type ubiquitin ligase E4B contributes to neuritogenesis**. *J Biol Chem* 2004, **279**(51):53533-53543.

18. Brenner S: **The genetics of *Caenorhabditis elegans***. *Genetics* 1974, **77**(1):71-94.

19. Hengartner MO, Horvitz HR: ***C. elegans* cell survival gene *ced-9* encodes a functional homolog of the mammalian proto-oncogene *bcl-2***. *Cell* 1994, **76**(4):665-676.

20. Van Valkenburgh H, Shern JF, Sharer JD, Zhu X, Kahn RA: **ADP-ribosylation factors (ARFs) and ARF-like 1 (ARL1) have both specific and shared effectors: characterizing ARL1-binding proteins**. *J Biol Chem* 2001, **276**(25):22826-22837.

21. Panic B, Whyte JR, Munro S: **The ARF-like GTPases Arl1p and Arl3p act in a pathway that interacts with vesicle-tethering factors at the Golgi apparatus**. *Curr Biol* 2003, **13**(5):405-410.

22. Huang CF, Buu LM, Yu WL, Lee FJ: **Characterization of a novel ADP-ribosylation factor-like protein (yARL3) in *Saccharomyces cerevisiae***. *J Biol Chem* 1999, **274**(6):3819-3827.

23. Siddiqui SS: **Mutations affecting axonal growth and guidance of motor neurons and mechanosensory neurons in the nematode *Caenorhabditis elegans***. *Neurosci Res Suppl* 1990, **13**(90):S171-190.

24. Wightman B, Baran R, Garriga G: **Genes that guide growth cones along the *C. elegans* ventral nerve cord**. *Development* 1997, **124**(13):2571-2580.

25. White JG, Southgate E, Thomson JN, Brenner S: **The structure of the ventral nerve cord of *Caenorhabditis elegans***. *Philos Trans R Soc Lond B Biol Sci* 1976, **275**(938):327-348.

26. Nonet ML: **Visualization of synaptic specializations in live *C. elegans* with synaptic vesicle protein-GFP fusions**. *J Neurosci Methods* 1999, **89**(1):33-40.

27. Troemel ER, Sagasti A, Bargmann CI: **Lateral signaling mediated by axon contact and calcium entry regulates asymmetric odorant receptor expression in *C. elegans***. *Cell* 1999, **99**(4):387-398.

28. Peckol EL, Zallen JA, Yarrow JC, Bargmann CI: **Sensory activity affects sensory axon development in *C. elegans***. *Development* 1999, **126**(9):1891-1902.

29. Coburn CM, Bargmann CI: **A putative cyclic nucleotide-gated channel is required for sensory development and function in *C. elegans***. *Neuron* 1996, **17**(4):695-706.

30. Dwyer ND, Adler CE, Crump JG, L'Etoile ND, Bargmann CI: **Polarized dendritic transport and the AP-1 mu1 clathrin adaptor UNC-101 localize odorant receptors to olfactory cilia**. *Neuron* 2001, **31**(2):277-287.

31. Eckner R, Yao TP, Oldread E, Livingston DM: **Interaction and functional collaboration of p300/CBP and bHLH proteins in muscle and B-cell differentiation**. *Genes Dev* 1996, **10**(19):2478-2490.

32. Stearns T, Botstein D: **Unlinked noncomplementation: isolation of new conditional-lethal mutations in each of the tubulin genes of *Saccharomyces cerevisiae***. *Genetics* 1988, **119**(2):249-260.

33. Belanger KD, Kenna MA, Wei S, Davis LI: **Genetic and physical interactions between Srp1p and nuclear pore complex proteins Nup1p and Nup2p**. *J Cell Biol* 1994, **126**(3):619-630.

34. Patel N, Thierry-Mieg D, Mancillas JR: **Cloning by insertional mutagenesis of a cDNA encoding *Caenorhabditis elegans* kinesin heavy chain**. *Proc Natl Acad Sci U S A* 1993, **90**(19):9181-9185.

35. Hall DH, Hedgecock EM: **Kinesin-related gene *unc-104* is required for axonal transport of synaptic vesicles in *C. elegans***. *Cell* 1991, **65**(5):837-847.

36. White JG, Southgate E, Thomson JN, Brenner FRS, S.: **The structure of the nervous system of the nematode *Caenorhabditis elegans***. *Phil Trans R Soc Lond* 1986, **B 314**:1-340.

37. Zallen JA, Kirch SA, Bargmann CI: **Genes required for axon pathfinding and extension in the *C. elegans* nerve ring**. *Development* 1999, **126**(16):3679-3692.

38. Yu TW, Bargmann CI: **Dynamic regulation of axon guidance**. *Nat Neurosci* 2001, **4 Suppl**:1169-1176.

39. Kiryushko D, Berezin V, Bock E: **Regulators of neurite outgrowth: role of cell adhesion molecules**. *Ann N Y Acad Sci* 2004, **1014**:140-154.

40. Hirokawa N: **Kinesin and dynein superfamily proteins and the mechanism of organelle transport**. *Science* 1998, **279**(5350):519-526.

41. Gho M, McDonald K, Ganetzky B, Saxton WM: **Effects of kinesin mutations on neuronal functions**. *Science* 1992, **258**(5080):313-316.

42. Okada Y, Yamazaki H, Sekine-Aizawa Y, Hirokawa N: **The neuron-specific kinesin superfamily protein KIF1A is a unique monomeric motor for**

anterograde axonal transport of synaptic vesicle precursors. *Cell* 1995, **81**(5):769-780.

43. Hurd DD, Saxton WM: **Kinesin mutations cause motor neuron disease phenotypes by disrupting fast axonal transport in *Drosophila***. *Genetics* 1996, **144**(3):1075-1085.

44. Gindhart JG, Jr., Desai CJ, Beushausen S, Zinn K, Goldstein LS: **Kinesin light chains are essential for axonal transport in *Drosophila***. *J Cell Biol* 1998, **141**(2):443-454.

45. Yu TW, Hao JC, Lim W, Tessier-Lavigne M, Bargmann CI: **Shared receptors in axon guidance: SAX-3/Robo signals via UNC-34/Enabled and a Netrin-independent UNC-40/DCC function**. *Nat Neurosci* 2002, **5**(11):1147-1154.

46. Huang X, Huang P, Robinson MK, Stern MJ, Jin Y: **UNC-71, a disintegrin and metalloprotease (ADAM) protein, regulates motor axon guidance and sex myoblast migration in *C. elegans***. *Development* 2003, **130**(14):3147-3161.

47. Feinberg EH, Hunter CP: **Transport of dsRNA into cells by the transmembrane protein SID-1**. *Science* 2003, **301**(5639):1545-1547.

48. Griffiths G, Simons K: **The *trans* Golgi network: sorting at the exit site of the Golgi complex**. *Science* 1986, **234**(4775):438-443.

49. Rolls MM, Hall DH, Victor M, Stelzer EH, Rapoport TA: **Targeting of rough endoplasmic reticulum membrane proteins and ribosomes in invertebrate neurons**. *Mol Biol Cell* 2002, **13**(5):1778-1791.

50. Sulston J, Hodgkin J: **Methods**. In: *The Nematode Caenorhabditis elegans.* Edited by Wood WB. Cold Spring Harbor, New York: Cold Spring Harbor Laboratory Press; 1988: 587-606.

51. Desai C, Garriga G, McIntire SL, Horvitz HR: **A genetic pathway for the development of the *Caenorhabditis elegans* HSN motor neurons**. *Nature* 1988, **336**(6200):638-646.

52. McIntire SL, Jorgensen E, Horvitz HR: **Genes required for GABA function in *Caenorhabditis elegans***. *Nature* 1993, **364**(6435):334-337.

53. McIntire SL, Jorgensen E, Kaplan J, Horvitz HR: **The GABAergic nervous system of *Caenorhabditis elegans***. *Nature* 1993, **364**(6435):337-341.

54. Sambrook J, Fritsch EF, Maniatis T: **Molecular cloning: a laboratory manual.** Cold Spring Harbor, New York: Cold Spring Harbor Laboratory Press; 1989.

55. Lupas A, Van Dyke M, Stock J: **Predicting coiled coils from protein sequences**. *Science* 1991, **252**(5010):1162-1164.

56. Mello CC, Kramer JM, Stinchcomb D, Ambros V: **Efficient gene transfer in *C.elegans*: extrachromosomal maintenance and integration of transforming sequences**. *Embo J* 1991, **10**(12):3959-3970.

Figures

Figure 1. *unc-69* locus encodes a 108 amino acid protein with a short coiled-coil domain.

(A) Genetic and physical maps of chromosome III in the vicinity of the *unc-69* locus. *unc-69* is close to and left of *ced-9*. Cosmids and subclones able to rescue the locomotion defect of *unc-69(e587)* mutants are shown in bold. B: BamH I; H: Hind III; M: Mlu I; P: Pst I; R: EcoR I; S: Sac I. Introduction of a frameshift mutation at the BamH I site in the second exon (denoted by x) abrogated rescue by the minimal Pst I-Sac I rescuing fragment. Both splice variants, *T07A5.6a* and *T07A5.6b*, are contained within this fragment. (B) UNC-69 protein sequence. The boxed region is predicted to form a coiled-coil domain. Arrows indicate the positions of the three known *unc-69* mutations. Additional amino acids encoded by *T07A5.6b* are shown in italic letters (see Supp. Results). (C) Northern analysis of *unc-69* revealed a single major, 0.65 kb transcript (arrow).

Su et al. Figure 1

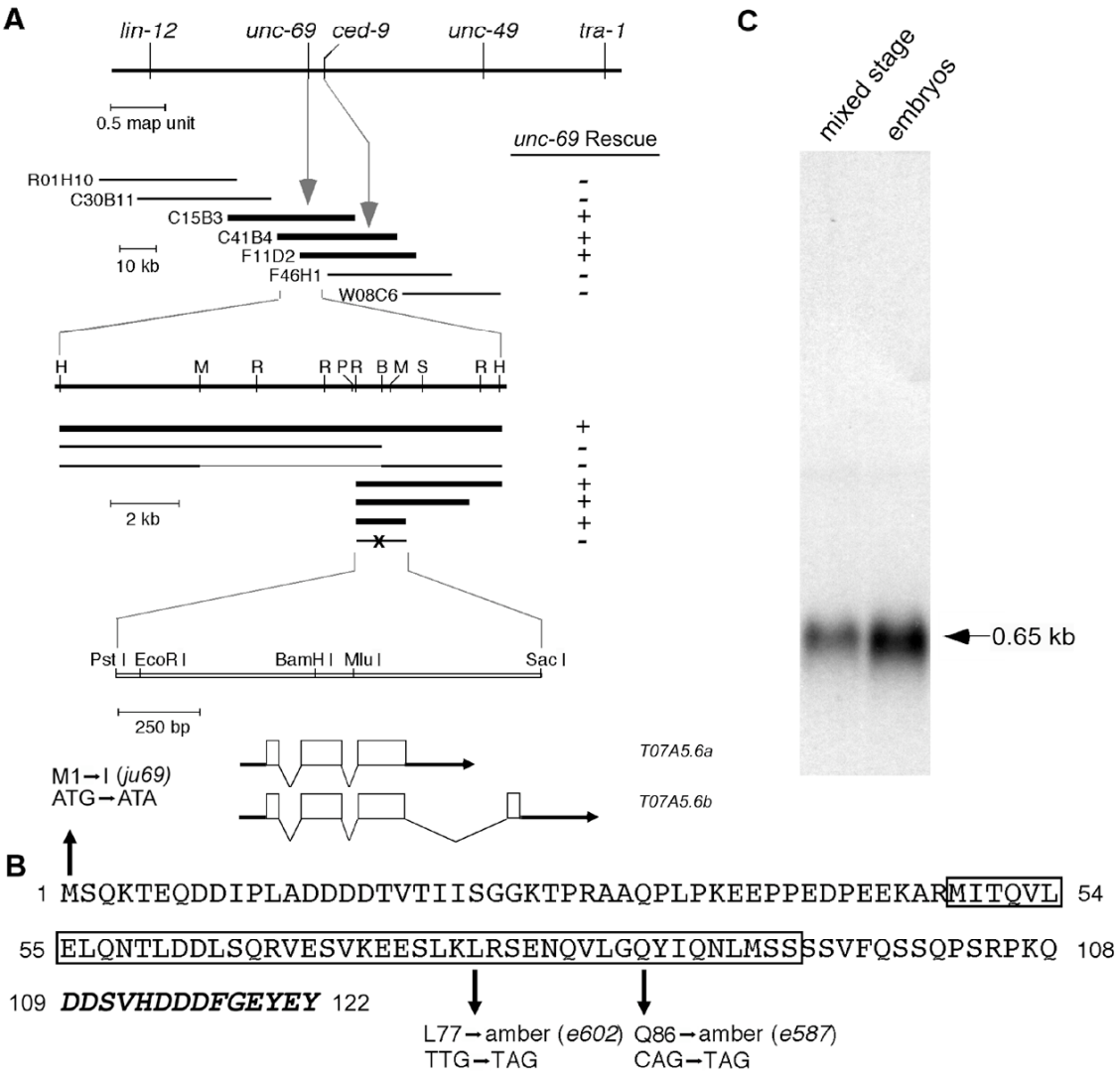

Figure 2. UNC-69 is homologous to mammalian SCOCO.

(A) Sequence alignment of UNC-69/SCOCO proteins from *S. cerevisiae*, *C. elegans*, *C. briggsae*, mosquito, *Drosophila*, *Fugu*, zebrafish, *Xenopus*, mouse and human. Residues identical in all ten sequences are shaded black; similar residues are shaded gray. The underlined region is predicted in all cases to form a coiled-coil domain. The region boxed in green is acidic, and the region boxed in purple is serine/threonine-rich. The bracket indicates the C-terminal basic region. Asterisks mark mutations in *unc-69*. (B) mRNA of the human *unc-69* homologue *SCOCO* is enriched in fetal brain and is also present in fetal kidney, liver and lung. (C) Expression of human *SCOCO* rescues the locomotion defect of *unc-69* mutant. Movement of the wild type (WT), mutants, and transgenic L4 hermaphrodites was scored as complete sine waves per minute. For each genotype n=10. Error bars represent S.E.M.

Su et al. Figure 2

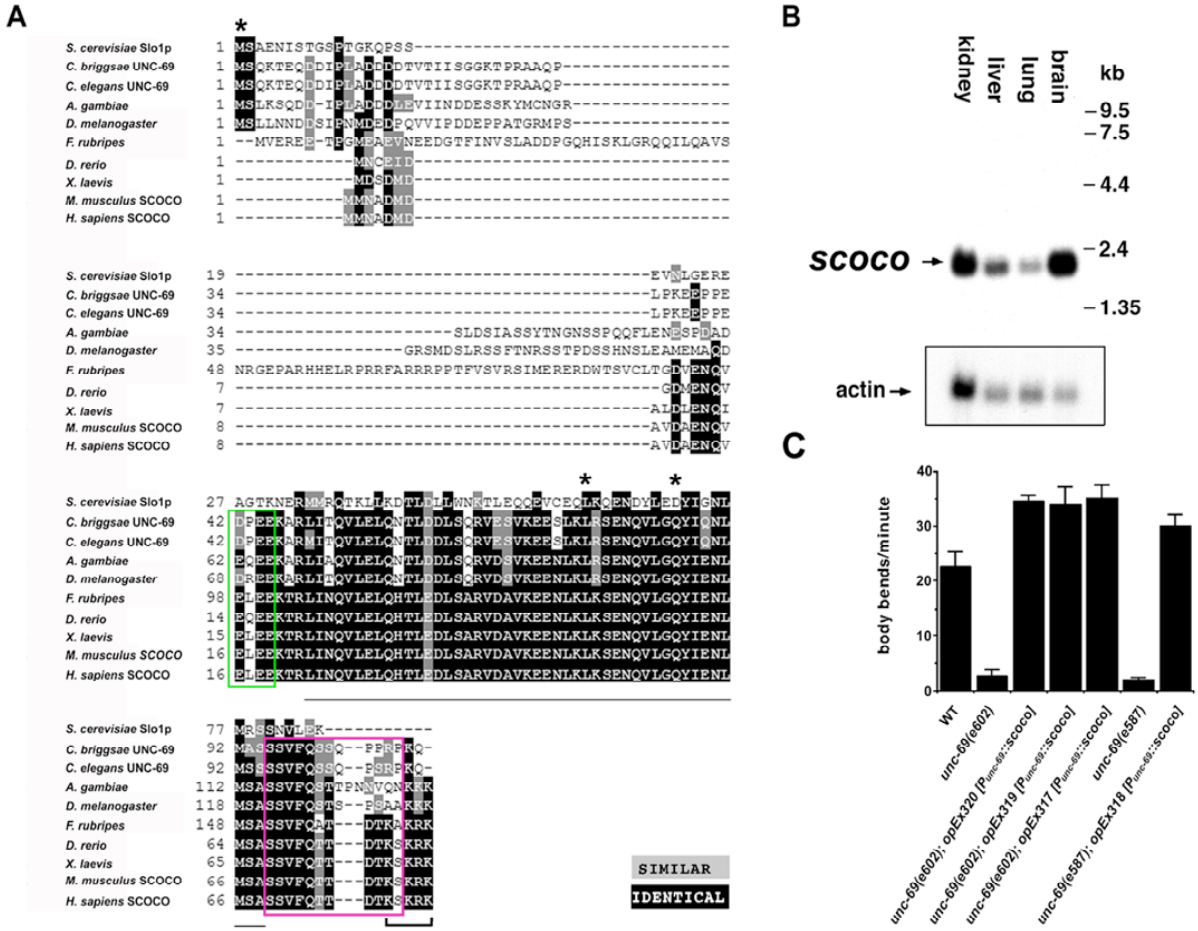

Figure 3. UNC-69::GFP is expressed in neurons.

Confocal micrographs of mosaic animals expressing a rescuing C-terminal UNC-69::GFP fusion. Panel (A) is a 1 μm optical section. All other panels are projections of optical series. (A) Late gastrula (large arrowhead) and early comma-stage embryo (arrow) with widespread expression of UNC-69::GFP. Embryos were still inside the mother. Small arrowheads indicate the maternal VNC. v indicates maternal vulva. (B) 2-fold embryo with strong UNC-69::GFP expression in VNC neurons (between arrowheads). (C) 3-fold embryo expressing UNC-69::GFP in a growth cone (arrowhead). Arrow indicates neuronal cell body. (D) L1 larva expressing UNC-69::GFP in neurons and axons in the head (arrow), VNC (small arrowheads) and tail (large arrowhead). Asterisk indicates reporter expression in labial sensory neuronal processes of an adjoining adult animal. (E) L3 larva expressing UNC-69::GFP in the CAN neuron (large arrow), excretory canal (small arrowheads) and in commissural axons (e.g. small arrow). (F) L4 larva expressing UNC-69::GFP in CAN (large arrow), HSN (large arrowhead) and ALM (small arrowhead). Small arrows indicate commissures. All scale bars = 10 μm. In all cases, anterior is to the left and dorsal is up.

Su et al. Figure 3

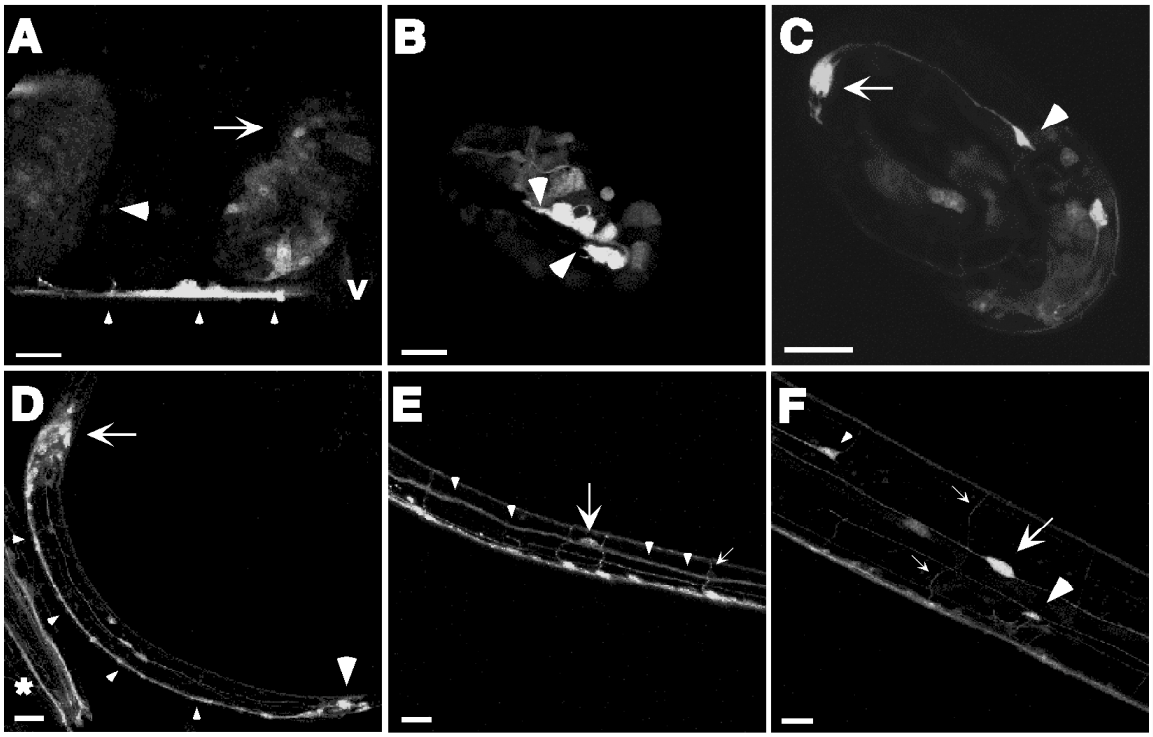

Figure 4. Axonal outgrowth, guidance, branching and fasciculation defects in *unc-69* mutants.

(A-B) HSN migration defect. In wild-type animals (A), the HSN axons migrate ventrally until they reach the VNC, which they join and follow rostrally towards the head (arrow in A). In *unc-69* mutants (B), HSN axons occasionally fail to grow ventrally and instead project laterally along the body wall (arrow in B). Animals were stained with anti-serotonin antibodies to visualize the HSN neurons. Arrowheads indicate the vulva. Dotted lines mark the ventral margin of the body walls. (C-D) Commissures of D-type GABAergic neurons routinely reach the DNC in wild-type animals (C), but often fail in *unc-69(e587)* animals (D) and prematurely bifurcate (arrow). D-type GABAergic neurons were visualized by the *unc-47::gfp* transgene *oxIs12*. Asterisk in D marks a gap in the DNC. There are also often ectopic sprouts from the commissures (arrowheads in D) in *unc-69(e587)* mutants. (E-F) Images of single ALM touch neuron in wild-type (E) and *unc-69(e602)* (F) animals. Many ectopic neurites branched out from the soma and the axonal shaft of the ALM neuron in *unc-69(e602)* mutant (arrowheads). (G-H) Tracings of representative electron micrographs of sections through DNC and VNC. In the wild type (G), the position and content of the three major fascicles are highly stereotyped (black arrows). In *unc-69(e587)* mutants (H), defasciculated axons can often be found migrating separately along the body wall (open arrows). (I-J) Morphology of bipolar AWC sensory neuron in wild-type (I) and *unc-69(e587)* (J) animals. Dendrites of AWC neurons in both animals reach the nose (arrows). Axonal shape is normal in wild-type worms (arrowhead in I), but abnormal in *unc-69(e587)* mutants, with ectopic bulges

occasionally extending from the soma (arrowhead in J). In all panels anterior is to the left and dorsal is up. All scale bars = 10 μm.

Su et al. Figure 4

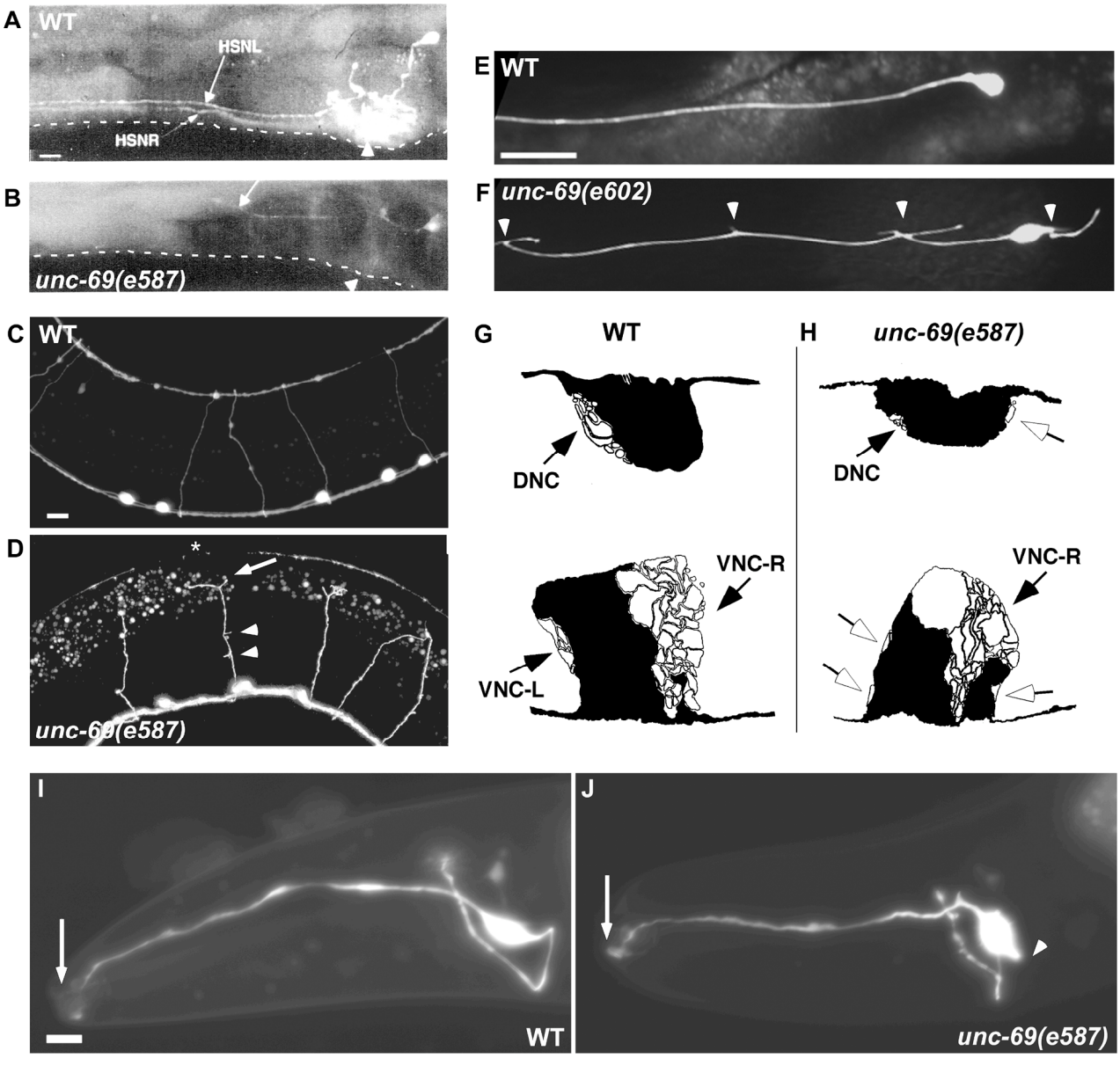

Figure 5. *unc-69* affects axonal but not dendritic trafficking.

(A and C) SNB-1::GFP exists as evenly spaced puncta along the VNC (A) and DNC (C) in wild-type animals. (B, D, and E) In *unc-69(ju69)* mutants, SNB-1::GFP puncta are on average bigger and often are absent from the VNC (arrowhead in B) and the DNC (arrowheads in D and E). In addition, SNB-1::GFP sometimes diffuse into the commissure (arrow in D). A, B and E are lateral views and C-D are dorsal views of adult hermaphrodites. (F-I) As in wild-type animals (F and H), neuronal morphology is grossly normal in *unc-69(ju69)* mutants, and commissures still routinely reach the DNC (G and I). D-type GABAergic neuron morphology is visualized by the P_{unc-25}*::gfp* transgene *juIs76.* (F-G) are lateral views, (H-I) are dorsal views. (J) SNB-1::GFP is not significantly mislocalized into DD dendrites in *unc-69(ju69)* mutants. Animals carrying an *snb-1::gfp* transgene are scored at the L1 larval stage. Whereas 90% of *unc-16(ju146)* L1s (n=32) show dorsal GFP, 0% of wild-type L1s (n=47) and 3% *unc-69(ju69)* L1s (n=59) show dorsal GFP. Error bars represent S.E.M. (K-M) The diacetyl odorant receptor ODR-10::GFP is targeted efficiently into AWB cilia both in the wild-type worms (K) and in *unc-69(ju69)* mutants (L). In contrast, ODR-10::GFP becomes diffused in the dendritic targeting mutant *unc-101* (M). Arrow indicates the cilia, and arrowheads indicate packets of ODR-10::GFP that shuttle in the dendrites. Anterior is to the left, and dorsal is up.

Su et al. Figure 5

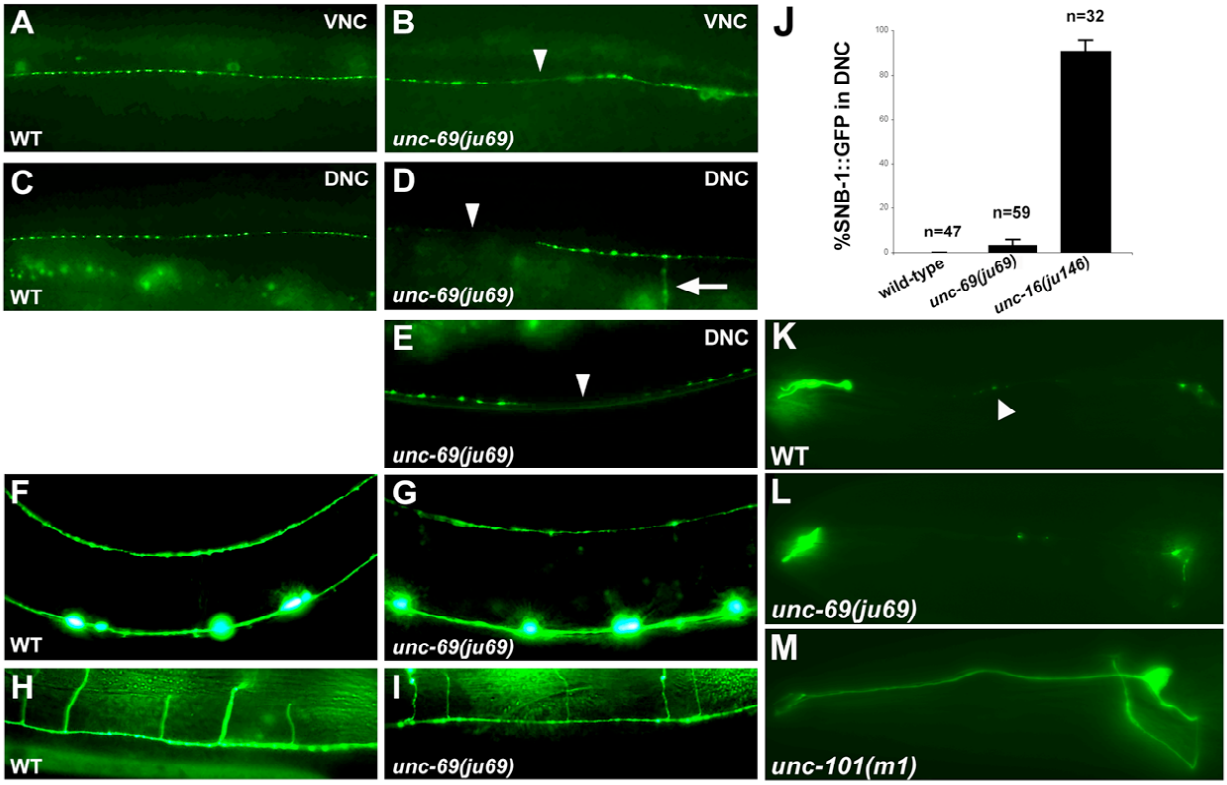

Figure 6. UNC-69 physically interacts with UNC-76.

(A) Full-length UNC-76 (UNC-76 FL) specifically binds to full-length GST-UNC-69, but not GST-CBP. The E1A/CBP interaction was used as a positive control. (B) Serial deletions of UNC-76: a portion of the C-terminal region (deleted in UNC-76 Δγ, but contained within UNC-76 B3 and A3) is necessary for interaction with GST-UNC-69. (C) Point mutation L287P or a small 19-amino-acid deletion (UNC-76 Δ19), which deletes amino acids 281-299, totally abolishes the ability of UNC-76 to bind GST-UNC-69. (D) Summary of the deletion analysis, as well as the results of rescuing experiments. Note that UNC-76 Δ19 not only loses its binding ability but also its rescuing activity for the *unc-76(e911)* mutants. The 19 amino acid region (green box) lies within a conserved region (gray box) and overlaps with a region we predicted to form a coiled-coil domain (slashed box). A previously described axonal targeting sequence [14] is colored in red. The positions of different *unc-76* alleles are indicated.

Su et al. Figure 6

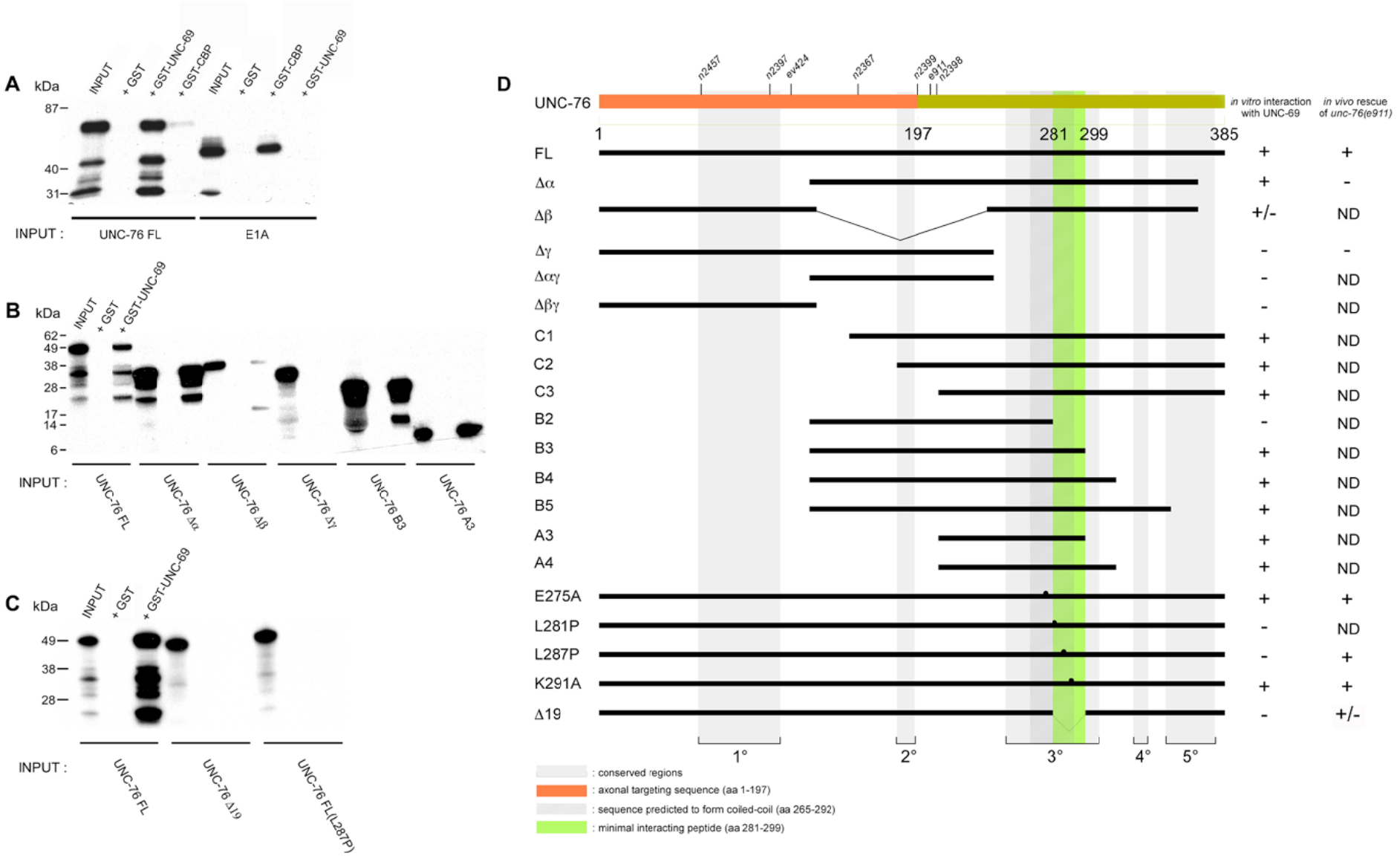

Figure 7. UNC-69 and UNC-76 cooperate to regulate size and position of synaptic vesicles.

(A-D) Lateral view of adult hermaphrodites 52-54 hours post hatching, single section. (E-F) Lateral view of the DNC of adult hermaphrodites 52-54 hours post hatching, flattened images of confocal z-stack. Anterior is to the left, and dorsal is up. (A and E) SNB-1::GFP is evenly distributed along the DNC in wild-type animals. (B) Removing one copy of *unc-69* does not affect SNB-1::GFP distribution. (C-D and F) SNB-1::GFP becomes diffused and the puncta becomes larger (arrows) in *unc-69(e587)/+; unc-76(e911)/+* and *(unc-69(e587)/+; unc-76(n2457)/+* double heterozygotes. Occasionally, SNB-1::GFP is missing altogether from a stretch of the DNC (bracket in D). The genotypes are as follows: (A and E) *juIs1 [P_{unc-25}::snb-1::gfp]*, (B) *qC1/unc-69(e587); juIs1,* (C) *qC1/unc-69(e587); nT1[qIs51]/juIs1; nT1[qIs51]/unc-76(e911),* (D and F) *qC1/unc-69(e587); nT1[qIs51]/juIs1; nT1[qIs51]/unc-76(n2457).* Scale bars = 10 μm.

Su et al. Figure 7

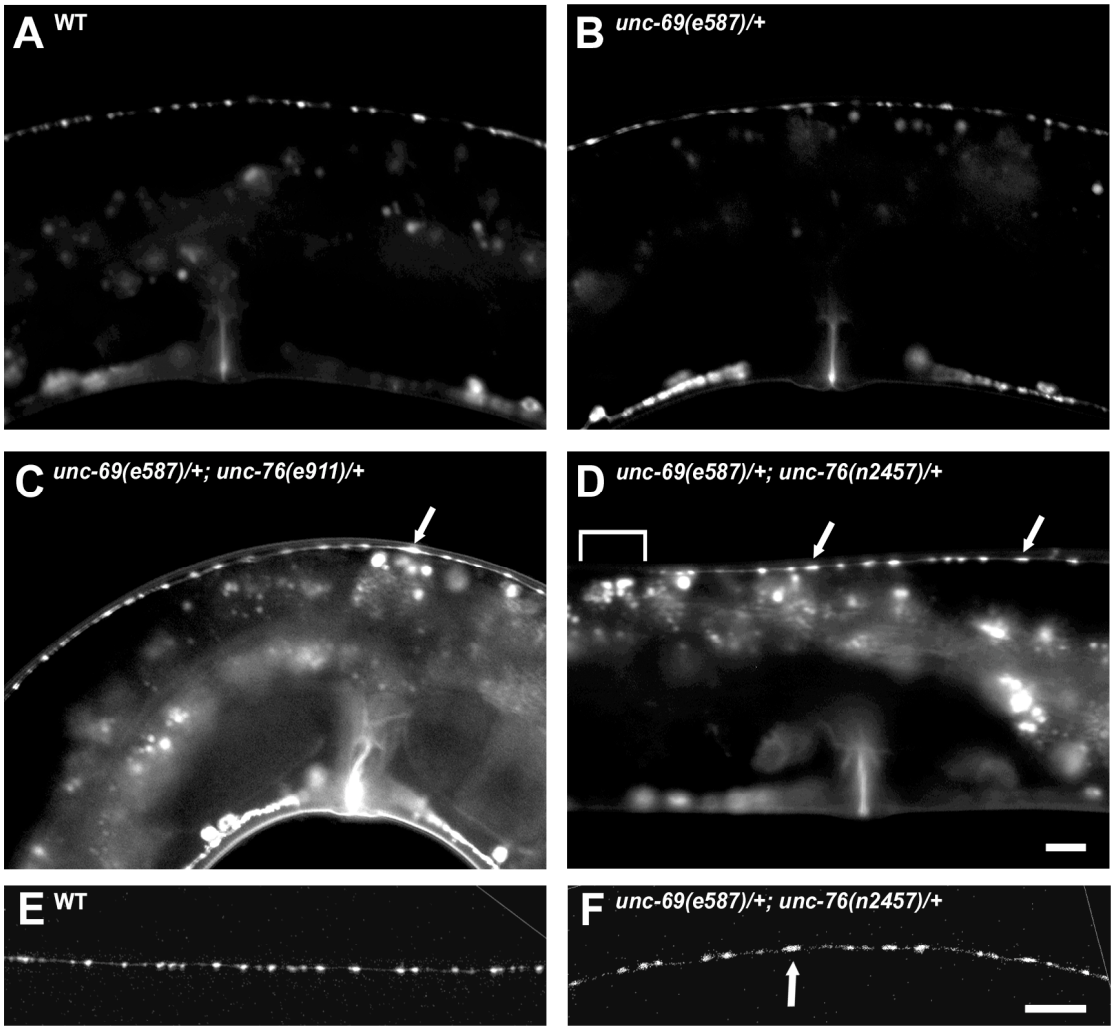

Figure 8. UNC-69 and UNC-76 colocalize as puncta in neuronal processes.

(A-O) Functional $P_{unc\text{-}69}$*::cfp::unc-69* and $P_{unc\text{-}76}$*::unc-76::yfp* constructs were coinjected at 5 ng/μl each into *unc-76(e911)* mutants, and worms rescued for locomotion were selected. Note that *unc-76(e911)* mutation was removed from the background in (G-O). (D-O) are deconvolved single layer images. (A-C) Lateral view of an adult hermaphrodite from one line of transgenic animals. Both CFP::UNC-69 and UNC-76::YFP form discrete, large puncta in the DNC, as well as in the commissure (arrow). Vignette in (C) shows an enlarged image of colocalized puncta in the DNC from the rectangle. (D-F) Lateral view of an adult hermaphrodite from a second line of transgenic animals. Note that CFP::UNC-69 and UNC-76::YFP are both cytoplasmic and punctal, and the puncta are present in lateral and sublateral processes. (G-I) In *unc-116(rh24)* mutants, UNC-76::YFP puncta became diffuse in a stretch of axon in the VNC, and failed to colocalize with CFP::UNC-69 (arrows in H-I). (J-L) CFP::UNC-69 and UNC-76::YFP colocalize in perinuclear structures in the soma of a neuron in the tail ganglia. (M-O) In *unc-116(rh24)* mutants both UNC-76::YFP and CFP::UNC-69 often appear as non- or partially overlapping aggregates in the soma of a preanal (MI-OI) and two tail ganglion neurons (MII-OIII). (P-U) Expression pattern of *opIs124 (*$P_{unc\text{-}69}$*::unc-69::gfp*) (P-R) and *opIs130 (*$P_{unc\text{-}76}$*::unc-76::yfp*) (S-U). Both transgenes were integrated into the genome to ensure stable gene expression. All pictures show the CAN neuron soma (arrowhead) and its vicinity. (P and S) In wild-type worms, the CAN neuron extended its bipolar processes along the excretory canal, and the CAN neurites were filled with UNC-69::GFP and UNC-76::YFP. Note that puncta cannot be seen in these integrants due to overexpression of the transgenes. (Q) In *unc-104(e1265)* mutants, UNC-69::GFP

accumulated near the CAN soma as well as in its neuronal processes (asterisk), giving it a notched appearance. (T) UNC-76::YFP localization appeared to be grossly normal in *unc-104(e1265)* mutants. (R and U) In *unc-116(rh24)* mutants, both UNC-69::GFP and UNC-76::YFP accumulated in CAN neurites (asterisk). UNC-69::GFP accumulation was prominent near the CAN soma and was accompanied by ectopic branches. In contrast, UNC-76::YFP aggregated and was evenly distributed along the CAN processes. Scale bar = 20 μm. (V and W) CAN neuron visualized by an integrated transgene *kyIs4* ($P_{ceh\text{-}23}$*::ceh-23::unc-76*$_{1\text{-}197}$*::gfp)*. (V) In wild-type worms, GFP appeared as string of dots, reminiscent of endogenous UNC-76 expression pattern. (W) In *unc-116(rh24)* mutants, GFP dots became larger and more dispersed. (X and Y) CAN neuron visualized by an extrachromosomal array *opEx901* ($P_{unc\text{-}69}$*::gfp)*. Unlike the UNC-69::GFP fusion (R), GFP itself was not significantly accumulated around CAN soma in *unc-116(rh24)* mutants (Y), although ectopic branches were frequently observed. (P-Y) are confocal z-stack images. Anterior is to the left in (A-I) and (P-Y). Anterior is up and ventral is to the right in (J-O). All scale bars except in (P-U): 10 μm.

Su et al. Figure 8

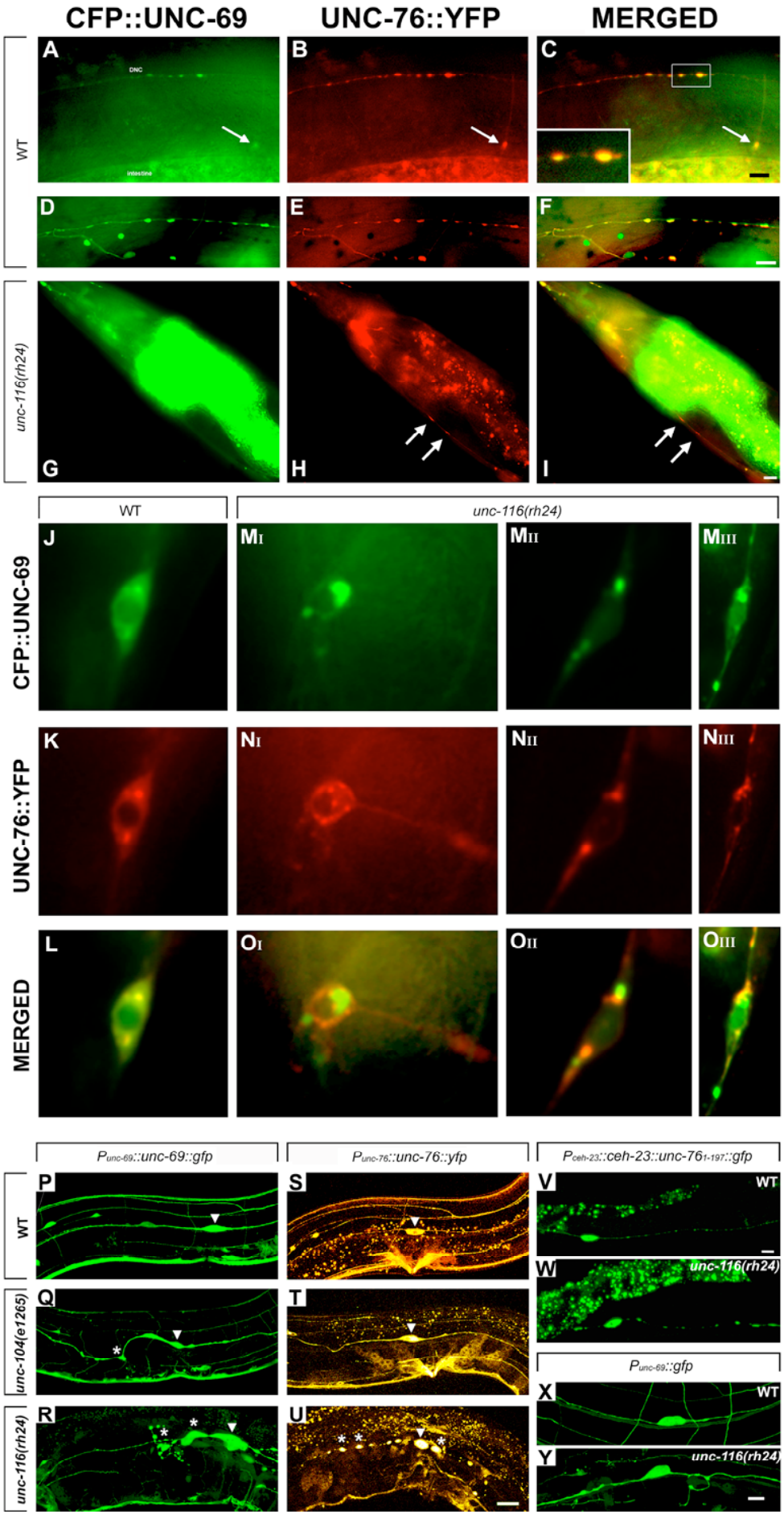

Supplemental Figure S1. Extent of the *ok339* deletion.

ok339 deletes a 2.65kb genomic region containing both verified splice variants of *unc-69,* as well as the predicted single-exon gene *T07A5.5*. Deletion breakpoints: 5'-TAAATTAGGG/tagagacgaa … 2.65kb … gtcacggtgt/TCACACGTTT-3'.

Su et al. Supplemental Figure S1

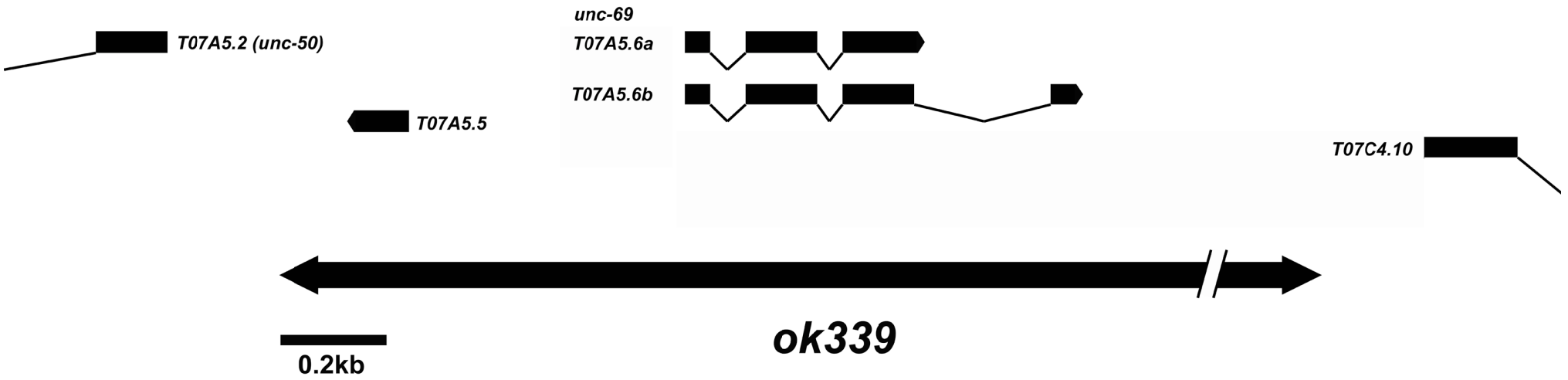

Tables

Table 1. Axon outgrowth and guidance defects in *unc-69* mutants.

(A)

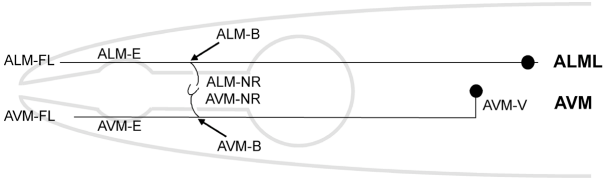

(B)

	ALM% defect				
Genotype	B	NR	E	FL	*n*
Wild type	0	0	0	12	113
unc-69(e602)	12	36	77	84	77
unc-69(e587)	15	45	85	89	80
unc-69(e602) (m+z-)	0	4.3	39	91	70
unc-69(e602)/nDf40 (m+z-)	0	7.2	20	72	69
unc-69(e587) (m+z-)	1.4	7.2	43	87	69
unc-69(e587)/nDf40 (m+z-)	0	8.3	20	82	60
*unc-69(e602)**	19	48	62	95	113
*unc-69(e602); opEx[P_{mec-7}::unc-69]**	1	12	2	5	81
*unc-69(e602); opEx[P_{mec-7}::unc-69]**	5	9	6	10	79
*unc-69(e602); opEx[P_{mec-7}::unc-69]**	8	29	0	10	85

(C)

	AVM% defect					
Genotype	B	NR	E	FL	V	*n*
Wild type	0	0	1	8	0	106
unc-69(e602)	32	27	72	73	2.7	77
unc-69(e587)	64	70	86	87	0	80
unc-69(e602) (m+z-)	1.4	4.3	57	86	0	70
unc-69(e602)/nDf40 (m+z-)	0	0	56	80	0	69
unc-69(e587) (m+z-)	2.9	8.8	56	85	0	69
unc-69(e587)/nDf40 (m+z-)	0	3.6	76	95	0	60
*unc-69(e602)**	46	67	93	100	ND	113
*unc-69(e602); opEx[P_{mec-7}::unc-69]**	0	4	4	4	ND	81
*unc-69(e602); opEx[P_{mec-7}::unc-69]**	8	12	12	23	ND	79
*unc-69(e602); opEx[P_{mec-7}::unc-69]**	11	21	12	13	ND	85

Neurite outgrowth and guidance defects of mechanosensory touch neurons in *unc-69* mutants. Morphology of neurites of ALM (B) and AVM (C) neurons (as in the schematic in A) was scored in different *unc-69* mutants, in *unc-69/nDf40* heterozygotes, as well as in mosaic animals carrying a functional *unc-69* transgene under the control of the *mec-7* promoter, which directs expression in the six touch neurons. All worms scored had a P_{mec-4}*::gfp* transgene *zdIs5* in the background to allow visualization of the neurite morphology. One ALM neurite was scored per animal. B: failure to form proper branch at the nerve ring; NR: failure of nerve ring branch to fully extend; E: failure to elongate past the branch point; FL: failure to extend fully; V: ventral guidance defect. (m+z-): homozygous mutant animals derived from heterozygous mothers. *: these strains also carry a *lin-15(n765)* mutation in the background. All *opEx* transgenes also carry a wild-type copy of *lin-15(+)* as a coinjection marker. ND: not done. *n:* number of worms scored.

Table 2. Axon outgrowth and guidance defects of HSN, DD/VD, ALA and AVK neurons.

Axon guidance phenotype	% defect in *unc-69(e587)* mutants	*n*
HSN		
Ventral outgrowth	16	70
Midline crossover (HSNL)	38	40
Failure to reach nerve ring	99	59
DD/VD		
Dorsal outgrowth	33	45
ALA		
Premature termination	67	30
AVKR		
Premature termination/crossover	85	20

Morphology of HSN neurons was visualized using antibodies against serotonin. Morphology of DD/VD neurons was visualized using antibodies against GABA. Morphology of ALA and AVKR neurons was visualized using antibodies against FMRF-amide. See Materials and Methods for details. *n:* number of animals scored.

Table 3. *unc-69* and *unc-76* function in the same genetic pathway to control AWC axon extension.

Genotype	2 AWC^{OFF}(%)	1 AWC^{ON}(%)	2 AWC^{ON}(%)	*n*
Wild type	1	99	0	398
unc-69(ju69)	1	99	0	190
unc-69(e602)	34	66	0	119
unc-69(e587)	30	70	0	194
unc-76(rh116)	11	89	0	83
unc-76(n2457)	6	94	0	102
unc-76(n2397)	8	92	0	64
unc-76(ev424)	10	90	0	68
unc-76(n2367)	30	70	0	84
unc-76(n2399)	25	75	0	67
unc-76(e911)	47	53	0	101
unc-76(e911); lon-2(e678)	31	69	0	91
unc-76(n2398)	28	72	0	184
unc-69(e602); unc-76(n2457)	35	65	0	106
unc-69(e602); unc-76(e911)	48	52	0	118
unc-69(e587); unc-76(n2457)	33	67	0	108
unc-69(e587); unc-76(e911)	31	69	0	143
Other axonal guidance mutants				
sax-3(ky123)	64	33	3	112
lon-2(e678) unc-6(n102)	38	62	0	65
vab-3(e648)	54	40	6	68
unc-76(e911); sax-3(ky123)	95	5	0	22
unc-76(e911); lon-2(e678) unc-6(n102)	73	27	0	152
unc-76(e911); vab-3(e648)	63	27	10	62

All animals scored had *kyIs140* ($P_{str\text{-}2}$*::gfp)* in the background, which turns on its expression in only one of the two AWC neurons (1 AWC^{ON}) in wild-type animals. In axon guidance mutants, $P_{str\text{-}2}$*::gfp* expression is silenced in both AWCs (2 AWC^{OFF}) due to failure of axonal contact. All *unc-69* and *unc-76* alleles except *unc-76(rh116)* are arranged in order according to their physical position (5' to 3') in the open reading frame. *n:* number of animals scored.

Supplemental Results

unc-69(ok339) deletion

unc-69(ok339) deletes a 2.65 kb genomic fragment encompassing the whole *unc-69* transcription unit as well as flanking sequences both 5' and 3' of the gene (Supplemental Figure S1). Thus, this deletion is certain to represent a null allele of *unc-69*. *unc-69(ok339)* homozygotes are Unc and arrest during L1 to L2 transition (Supp. Table S2). We found that *ok339* also deletes *T07A5.5* (predicted to encode the *C. elegans* homologue of the Ost4p subunit of the *S. cerevisiae* oligosaccharyltransferase) and ends but 200 bp 5' of the *unc-50* coding region (unpublished). We reasoned that the *ok339* arrest phenotype could either be due to loss of *T07A5.5*, or a synthetic phenotype due to the simultaneous loss of both *unc-50* and *unc-69* function. Indeed, *unc-69(ok339)* mutant worms were resistant to 25mM levamisole, a hallmark of *unc-50* mutations. Furthermore the *ok339* deletion failed to complement *unc-50(e306)* mutants (data not shown). We balanced *unc-69(ok339)* with *qC1*, and microinjected a 6.7 kb Hind III-EcoR I genomic fragment (*pUnc50-10*) carrying wild-type copies of both *unc-50* and *T07A5.5* into the deletion carrying strain. Transgenic worms homozygous for *unc-69(ok339)* grew to adulthood but were sterile (3 independent lines). It is likely that the sterility is due to lack of germline expression of *T07A5.5* off the extrachromosomal array. For this reason, we did not pursue usage of *unc-69(ok339)* in our studies.

The *unc-69* locus encodes multiple splice variants

We found a splice variant of *unc-69* by sequencing EST clones provided by Yuji Kohara (National Institute of Genetics, Japan), which we termed *T07A5.6b* (GenBank accession number AY919833). This splice variant (encoded by *yk508g10*) adds another 14 amino acids (DDSVHDDDFGEYEY) to the C-terminus of UNC-69. The small peptide is enriched in acidic amino acid residues, and makes the C-terminus quite acidic (Figure 1A and B). Wormbase also predicts the existence of splice variant *T07C4.10a*, which could encode a 1138 amino acid protein. We have failed to obtain any experimental evidence to support the existence of this latter splice variant. It is likely that *T07C4.10a* is either expressed at a very low level or is improperly predicted. Therefore we removed the *unc-69* coding sequence from *T07C4.10a* and renamed the remaining coding sequence as *T07C4.10* (Supp. Figure S1; also see **WormBase** [http://www.wormbase.org] release WS140).

UNC-69 homologues

A *C. elegans unc-69* cDNA was used to probe a *C. briggsae* genomic library (gift of D. Baillie) in lambda Charon4 under low stringency conditions (hybridization at 55 °C in 6x SSPE, 0.5% SDS, washing at 55 °C, twice in 2x SSPE, 0.5% SDS, and twice in 0.5x SSPE, 0.5% SDS). Positive phage were purified and EcoR I insert fragments were subcloned into pBluescript, and their DNA sequence determined. We also identified hybridizing bands in *C. vulgaris, C. remanei,* and *Ascaris suum.* Additional UNC-69-like proteins were found in the expressed sequence tag (EST) database of rat (CB577413) and chimpanzee (AU298017). Partial UNC-69 sequences were also found in chick EST collections (BU311615). Surprisingly, the primary amino acid sequences or rat, mouse, chimpanzee and human are 100% identical.

Homophilic interaction of UNC-69

In many proteins, a coiled coil domain mediates homophilic dimer- or trimer-formation. We thus used the Y2H system to assay UNC-69's ability to interact with itself. We created yeast GAL4 DNA binding domain (DB)- and activation domain (AD)-UNC-69 fusion constructs, and transformed them into the yeast reporter strain HF7c. A very weak expression of the His reporter, as assayed by growth on LTH-plates, was consistently observed just above background level. However the interaction was not strong enough to activate the LacZ reporter above background level (data not shown).

We also assayed for a homophilic interaction of UNC-69 *in vitro* in several different ways. Maltose-binding protein (MBP)-tagged and GST-tagged UNC-69 were expressed in bacteria and used in pull-down assays using column of beads against either one or the other of the fusion proteins followed by western analysis. We were not able to observe any interaction between GST-UNC-69 and MBP-UNC-69 (data not shown). We also *in vitro* translated S-tagged and T7-tagged UNC-69 proteins separately, mixed the proteins at room temperature, immunoprecipitated with anti-T7 beads followed by western blots using antibodies against the S-tag. No interaction between T7-UNC-69 and S-UNC-69 was observed, even when the conditions were extremely mild. Finally we failed to observe any homophilic interaction of UNC-69 when T7-UNC-69 and S-UNC-69 were cotranslated *in vitro* (data not shown). These results suggest that UNC-69 likely does not interact with itself.

Supplemental Table S1. *unc-69* mutants lay more eggs in the absence of food than wild-type animals

Genotype	Eggs laid (M9 assay)			Eggs laid (plate assay)		
	M9	M9 + 5 mg/ml 5-HT	*n*	- Food	+ Food	*n*
Wild type	0	26	5	0	30	5
unc-69(e587)	13	ND	5	16	28	5
unc-69(e602)	14	ND	5	5	11	5

Total number of eggs laid in 60 min. (M9 assay) or 90 min. (plate assay) was determined. *n*, number of animals tested. ND, not done.

Supplemental Table S2. *unc-69(ok339)* mutants arrest development as L1 larvae

Genotype	Eggs laid per animal	Progeny		*n*
		Hatching (%)	L1 arrest (%)*	
qC1/unc-69(ok339)	157±26	99.9±0.9	24.2±4.1	9

*L1 arrest (%) represents per cent of hatched progeny that failed to develop past the first larval (L1) stage within six days of hatching (wild-type larvae remain in the L1 stage for about 12 hours at 20 °C). L1 arrested larvae were confirmed to be *unc-69(ok339)* homozygotes by nested PCR. Data are mean±s.d. *n*, number of broods analyzed.

Chapter 3

Isolation, characterization and mapping of *unc-69* suppressors

1. **Introduction**

As with many other scientific discoveries, the realization that UNC-69 cooperates with UNC-76 in regulating vesicular transport in *C. elegans* axons is just one chapter in an unfolding story. There are many new questions to be answered: what triggers the vesicles to move along the axons, and what signals them to stop? How do vesicles select their targets? How are the processes of neuritogenesis and synaptogenesis coupled? And to what extent do UNC-69 and UNC-76 participate in each of these processes? Unfortunately, so far genetic studies have provided only limited information regarding the genes that might function upstream and downstream of the UNC-69/UNC-76 protein complex. We also know very little about the biochemical functions of the UNC-69 and UNC-76 proteins themselves.

Genetic suppressor screens have often provided an effective way to identify additional components in a signaling pathway or protein complex. A EMS-based mutagenesis screen for suppression of locomotion defects of the *unc-69* mutants, had previously been performed by Dr. Suzanne Tharin and Miss Heather Waring in Dr. Michael Hengartner's laboratory in Cold Spring Harbor Laboratory. The aim of the suppressor screen was to identify potential negative regulators of the UNC-69-dependent axonal guidance pathway(s), as well as potential positive regulators that, when constitutively activated, could bypass the requirement for UNC-69. From their screen, three alleles, *op101, op209* and *op213,* were isolated as *unc-69(e602)* suppressors. Unfortunately, one of them, *op213*, was lost and the other two alleles only weakly or partially suppressed the Unc phenotype of the *unc-69(e602)* mutants.

Nevertheless, these preliminary results suggested that an *unc-69* suppressor screen might be a productive endeavor.

To identify genes that might function together with or in parallel to *unc-69,* I carried out a large-scale forward genetics screen based on suppression of the Unc phenotype of the *unc-69* mutants. From a screen of over 1,000,000 haploid genomes, I isolated at least 12 strong locomotion suppressors. One of these mutants was an intragenic suppressor in the very same codon as the original *unc-69(e602)* mutation. I mapped the other 11 mutants to low resolution, and selected one of them for further characterization. I will discuss the possible nature of the suppressors, and what could they tell us when thinking about UNC-69's functions in the nervous system.

2. Materials and Methods

C. elegans Strains and Genetics

C. elegans strains were maintained as described [1]. All strains were grown at 20°C, except *lin-15(n765ts)* and some suppressor mutants, which were grown at 15°C. Wild-type worms were of the Bristol N2 strain.

Mutagenesis and the *unc-69* suppressor screen

ENU (N-nitroso-N-ethylurea) and EMS (methanesulfonate, ethyl ester) were both purchased from Sigma. Preparation of ENU stock solution and chemical mutagenesis were done following standard protocols [2, 3], except that 0.625-2.5 mM of ENU and 39 mM EMS were used. Mutant strains used for the mutagenesis screen were as

follows: *unc-69(e602), unc-69(e587)* and *unc-69(ju69); juIs1*. In brief, staged L4 or young adult hermaphrodites were soaked in 0.625-2.5 mM ENU or 39 mM EMS in 4 mL M9 [4] and incubated at room temperature for 4 hours. Following four washes in 4 mL M9, P0 worms were transferred to plates to recover overnight at 15°C, then transferred to new plates and kept at 20°C. The number of F1 progeny from mutagenized P0 worms was estimated visually. The F2 worms were starved at 15°C, chunked to new plates and grown at 20°C for 36-48 hours before actual screening. Worms that showed improved locomotion were singled out and backcrossed with respective *unc-69* mutant strains six times before further characterization.

Mapping suppressors to a chromosome (bulked segregant analysis)

Bulked segregant analysis was done following standard protocols [5]. *unc-69* mutants were crossed at least 10 times into the Hawaii isolate CB4856, a polymorphic *C. elegans* strain, until the *unc-69* mutants were homozygous for the Hawaii background except for regions linked to the *unc-69* locus on chromosome III. In general, *suppressor/+; unc-69* males were crossed into the Hawaiianized *unc-69* mutant strain WS2656, and suppressed or Unc mutant adult hermaphrodites were pooled and analyzed by restriction enzyme digestions following PCR.

Mapping suppressors to a chromosome (2-factor mapping)

suppressor/+; unc-69(ju69); juIs1 males were crossed into mapping strains homozygous for *unc-69(ju69)*, followed by selecting suppressed F1 cross progeny. Individual F2s homozygous for each recessive chromosomal marker were singled out

and the non-Unc phenotype scored in the F3 progeny to avoid maternal-effect suppression. Genotypes of the mapping strains were as follows: WS2510 – *dpy-5(e61)* I*; rol-6(e187)* II*; unc-69(ju69)* III, WS2511 – *unc-69(ju69)* III*; bli-6(sc16)* IV*; dpy-11(e224)* V*; lon-2(e678)* X.

Mapping suppressors to an interval (3-factor mapping)

The strategy for 3-factor mapping was the same as that for 2-factor mapping, except that two visible markers from the same chromosome were used to map the suppressor into an interval. Genotypes of the mapping strains were as follows: WS2663 – *bli-3(e767) dpy-5(e61)* I*; unc-69(ju69)* III, WS2901 – *dpy-5(e61) lin-11(n566)* I*; unc-69(ju69)* III, WS2902 – *dpy-10(e128) lin-29(n482)* II*; unc-69(ju69)* III, WS2904 – *lin-31(n301) dpy-10(e128)* II*; unc-69(ju69)* III.

Germline transformations

For high copy overexpression of $P_{unc\text{-}69}$*::unc-69(M1I)::gfp*, the pSU86 plasmid was injected into the germline of adult *unc-69(e587); lin-15(n765ts)* hermaphrodites [6] at 50 ng/μl together with 150 ng/μl rescuing pL15-EK *lin-15(+)* plasmid. Transgenic progeny of injected animals were selected as non-Muv animals at 25°C.

Behavioral assays

Wild-type or mutant adult hermaphrodites were placed on a seeded plate, and assayed for complete sine wave movement per minute. Results were represented as mean ± S.D.

3. Results

ENU and EMS are two commonly used mutagens for the generation of new point mutations. Whereas EMS preferentially causes G/C → A/T transitions, ENU in addition also causes A/T → T/A and A/T → C/G transversions [3]. Since previous EMS-based screen did not generate satisfying results, I started with ENU and mutagenized *unc-69(e602)* and *unc-69(e587)* mutant worms. The basic idea of the screen was to look for *unc-69* mutants worms that, when harboring a second-site mutation, could effectively crawl from one side of the plate to the other (Figure 1). I screened 29,000 haploid genomes with different concentrations of ENU, but did not find any suppressor.

I performed a second screen using EMS to mutagenize *unc-69(e602)* mutant worms. I isolated one strong suppressor allele, *op329,* by screening over 10,000 haploid genomes. I discovered by outcross that *op329* was very tightly linked to *unc-69*. Sequencing of the *unc-69* ORF revealed a T-to-A transversion at position 77 in *op329 unc-69(e602)* mutants. The point mutation changed the premature Amber stop codon (TAG) into a lysine (AAG) (Figure 2A). Therefore, *op329* is an intragenic suppressor. Interestingly, compared to the wild-type sequence, *unc-69(e602 op329)* still caused a leucine (TTG) to lysine (AAG) missense mutation at position 77 (Figure 2A). Since L77 lies in the coiled-coil domain of UNC-69 and is a constituent of the heptad repeat that is important for forming the α-helix, the L77K missense mutation should, in principle, destabilize the coiled-coil structure. However, the movement of *unc-69(e602 op329)* mutants was indistinguishable from wild-type (Figure 2B),

suggesting that L77K mutation possibly does not interfere with protein-protein interaction, and that the mutant UNC-69(L77K) protein still retains its functions.

To evaluate the ability of mutant UNC-69(L77K) protein to form coiled-coil structure, I analyzed primary amino acid sequence of UNC-69(L77K) protein using two programs, COILS (http://www.ch.embnet.org/software/COILS_form.html) [7] and PAIRCOIL (http://paircoil.lcs.mit.edu/cgi-bin/paircoil) [8], respectively. COILS is a general program commonly used to predict coiled-coil structure. PAIRCOIL uses pairwise residue correlations to predict dimeric coiled-coil structure. Both programs suggested that L77K mutation would have little to no effect on the capability of UNC-69 to form coiled-coil structure, and therefore likely causes no significant change in overall protein structure (Figure 2C-D).

The isolation of the *op329* suppressor demonstrates the feasibility of EMS mutagenesis as a mean to uncover *unc-69* suppressors. Unfortunately, the probability to uncover such mutations (1 in 10,000 haploid genomes) was relatively low compared to standard (1 in 4000 haploid genomes) [2]. Since *unc-69(e602)* is a strong loss-of-function allele, suppressors that only partially improve locomotion of *unc-69(e602)* mutants might not be easily detected by visual inspection. In addition, both *unc-69(e587)* and *un-69(e602)* mutations are premature Amber stop codons; a screen for suppressors would thus likely lead to the isolation of informational suppressors. Indeed, while I could show that neither *unc-69(e587)* nor *unc-69(e602)* were suppressed by *smg-1(cc546ts),* a dominant *smg* suppressor that affects nonsense-mediated mRNA decay [9], I found that *unc-69(e602)* could be significantly suppressed by *sup-7(st5),* a strong semidominant Amber suppressor [10, 11]. Thus,

screening of *unc-69(e602)* suppressors may, most likely, result in uncovering Amber informational suppressors.

To avoid isolating informational suppressors and to ease the screening process, I switched to the use of the *unc-69(ju69)* allele for my subsequent screens. *unc-69(ju69)* is a hypomorphic allele resulting in an ATG to ATA (Met to Ile) missense mutation at the start codon (Chapter 2). I mutagenized *unc-69(ju69); juIs1 (P_{unc-25}::snb-1::gfp)* worms and isolated at least 11 strong locomotion suppressors by screening over 1,000,000 haploid genomes. These suppressors not only improved locomotion of *unc-69(ju69)* mutants to nearly wild-type (Figure 3A-B), but also restored the SNB-1::GFP mislocalization defect in the *unc-69(ju69)* mutants to nearly wild-type level, although some SNB-1::GFP puncta occasionally clustered abnormally in *mIn1/op349; unc-69(ju69)* mutant hermaphrodites (Figure 4A-C; also see below). The frequency of these suppressors (roughly 1 every 100,000 haploid genomes) was again extremely low. Intriguingly, all of these 11 suppressors were dominant (C. Rhiner, personal communication). Furthermore, initial attempts to map many of these suppressors by bulked segregant analysis [5] failed, suggesting that these suppressors could not be readily kept in the homozygous state. Indeed, many of these mutants did not suppress *unc-69(ju69)* when homozygous, and the *suppressor; unc-69(ju69)* double homozygotes were Unc (Figure 3B). In addition, many of these suppressors also showed a weak maternal effect rescue, as some suppressed F1 progeny from a *suppressor/+; unc-69(ju69)* hermaphrodite gave rise to 100% Unc F2 progeny.

All of these 11 suppressors were mapped to a chromosome by classical 2-factor mapping (Table 1). I obtained unambiguous chromosome assignments for 8 suppressors: *op332, op334, op348* and *op351* mapped to LG I, whereas *op333, op345, op349* and *op350* showed linkage to chromosome II. I have not yet determined whether the mutations that map to the same chromosome are allelic with each other. The other three suppressors, *op346, op363* and *op377,* are likely located on chromosome III or at the end of one of the chromosomes. Sequencing of the *unc-69* ORF in these three mutants suggested that they were not intragenic reversions of the *unc-69(ju69)* allele. I did not pursue mapping of these three suppressors further due to their dominant nature and technical difficulties.

I chose *op348* and *op349* – one representative allele on each of chromosome I and II – and mapped them further into an interval between two genetic markers (Tables 2-3). From *op348/bli-3(e767) dpy-5(e61); unc-69(ju69)* hermaphrodites, 28/41 Bli non-Dpy and 0/25 Dpy non-Bli recombinant progeny were suppressed, suggesting that *op348* is not on the left of *bli-3,* and is very close to or to the right of *dpy-5.* Indeed, 2/4 Dpy non-Lin progeny from *op348/dpy-5(e61) lin-11(n566); unc-69(ju69)* hermaphrodites were suppressed, thus likely placing *op348* between *dpy-5* and *lin-11,* on the right arm of chromosome I. For mapping *op349,* initial 3-factor mapping data suggest that *op349* is very close to or on the left of *dpy-10*: 0/12 Dpy non-Lin and 19/19 Lin non-Dpy recombinants from *op349/dpy-10(e128) lin-29(n482); unc-69(ju69)* hermaphrodites were suppressed. Moreover, 18/27 Lin non-Dpy and 4/16 Dpy non-Lin recombinants from *op349/lin-31(n301) dpy-10(e128); unc-69(ju69)* hermaphrodites were suppressed. These data suggest that *op349* likely lies between *lin-31* and *dpy-10,* at approximately -2 map units on the left arm of chromosome II.

To characterize *op348* and *op349* in more detail, I removed *unc-69(ju69)* mutation from their backgrounds, and isolated *op348* and *op349* homozygote hermaphrodites alone. Interestingly, both *op348* and *op349* homozygotes showed a unique Sleepy phenotype: the adult hermaphrodites ceased moving after a period of time, and gradually became motionless on the plates. However, both *op348* and *op349* hermaphrodites were sensitive to vibration and touch, as they resumed moving upon mechanical stimuli. These observations suggest that the Sleepy phenotype might result from a defect in synaptic transmission. In addition, *op349* mutants were temperature-sensitive embryonic lethal at 25ºC. Although some of the embryos could develop into the 3-fold stage (J. Kinchen, observations), none of them survived. *op349* also showed a synthetic phenotype in the *unc-69(ju69)*; *juIs1* [SNB-1::GFP] background, as the *op349; unc-69(ju69); juIs1* hermaphrodites were sick and hard to maintain at both 15ºC and 20ºC. Both *op348* and *op349* mutants showed a mild constitutive dauer formation (Daf-c) phenotype. However, these dauers could exit their dauer state and continued development into adulthood. Both *op348* and *op349* mutants also showed other minor defects including larval head deformation, protruding vulva, and even multiple vulva.

The most striking phenotype of *op348* and *op349* mutants, however, is the defect in distribution of the SNB-1::GFP puncta in the D-type GABAergic motor neurons: in both *op348; juIs1* and *op349; juIs1* mutants, several SNB-1::GFP puncta often clustered dorsal-ventrally and juxta-positioned in a stretch of axon, both in the DNC and the VNC (Figure 4D-F). When viewed dorsal-ventrally, the SNB-1::GFP puncta often appeared as large clumps along the DNC and the VNC (Figure 4G). The defect

of SNB-1::GFP clustering was stronger in the *op349* mutants than that in the *op348* mutants, both in penetrance and severity. Some puncta in the *op349* mutants were themselves contained within a region of diffused SNB-1::GFP in the VNC (Figure 4F). Thus, the Sleepy locomotion behavior of both *op348* and *op349* mutants could be a consequence of abnormal presynaptic differentiation, possibly an outcome of defective presynaptic vesicle clustering. Interestingly, the SNB-1::GFP clustering defect could also be seen in the *op349/+; unc-69(ju69); juIs1* mutants (Figure 4C), implying that this defect arise independently of *op349*'s ability to suppress *unc-69(ju69)*. Both *op348* and *op349* mutants did not show dendritic targeting defect, as ODR-10::GFP was still properly localized to the cilia of the AWB neurons (data not shown). In addition, SNB-1::GFP was not mislocalized to the DNC in L1 *op348* mutant larvae (0/30 showed SNB-1::GFP in the DNC; n=30).

The phenotypic similarities between *op348* and *op349* mutants, as well as their dominant suppression of *unc-69(ju69),* indicate that they possibly affect two loci that are required together for the same set of cellular functions.

To address whether these suppressors could also dominantly suppress the other strong loss-of-function *unc-69* alleles as well as possibly *un-76* mutants, I crossed *op349* into *unc-69(e602)* and *unc-76(e911)* mutants (due to technical reasons I did not test *op348* for suppression). Unfortunately, *op349* did not dominantly or recessively suppress either the *unc-69(e602)* or the *unc-76(e911)* mutants (Figure 5), suggesting that *op349* is only specific for the *unc-69(ju69)* allele. In addition, *op349; unc-69(e602)* double mutants were unusually sick, and were hard to maintain even at 15ºC. Since *op349* is allele-specific, I did not pursue mapping and cloning of it any further.

The allele-specificity of *op349* raises an important question: could *op349* simply suppress *unc-69(ju69)* by facilitating translational initiation at the mutated start codon? In other words, could increase of level of UNC-69(M1I) mutant protein in the suppressor background rescue the Unc phenotype? To directly test this idea, I created several transgenic *unc-69(e587)* mutant strains carrying the $P_{unc\text{-}69}$*::unc-69(M1I)::gfp* transgene as extrachromosomal arrays. The construct was microinjected at 50 ng/μL, and therefore the UNC-69(M1I)::GFP fusion protein should be overexpressed in the nervous system of the *unc-69(e587)* mutants. I found that in all four transgenic lines, the UNC-69(M1I)::GFP protein expression level was low judging by fluorescent intensity in the nervous system, however the locomotion defect of the *unc-69(e587)* mutants was completely rescued (Figure 6). Thus, an increase in UNC-69(M1I) protein can indeed suppress the Unc phenotype of the *unc-69* mutants. As an alternative, *op349* could also increase the amount of a truncated UNC-69 protein getting translated starting at the methionine at position 49. This truncated protein could possibly also restore most of the UNC-69-dependent cellular processes. It is thus possible that *op349* acts as a novel class of information suppressor that increases translational initiation from the *unc-69* mRNA. Alternatively, *op349* could act as a regulator of chromatin structure which functions in chromatin remodeling and gene transcription, whose loss of function facilitates transcription from the *unc-69* loci. Finally, it is still quite possible that *op349* does affect aspects of nervous system development.

4. Discussion

In this chapter I detailed my efforts to isolate *unc-69* locomotion suppressors. As described above, the frequency with which I isolated such suppressors was extremely low compared to the frequency with which genes are knocked out following standard ENU- or EMS-based mutagenesis. Nevertheless, from a screen of over 10^6 haploid genomes, I was able to isolate 12 suppressor mutations. One of these, *op329*, is an intragenic suppressor. The nature of the others remains to be determined. Preliminary results suggest that at least one of them might be an informational suppressor. My data suggest that strong *unc-69* suppressors might be difficult to isolate, and are possibly embryonic or larval lethal when combined with the *unc-69* mutations. Also, some suppressors that partially rescue the locomotion defects of the *unc-69* mutants might not be isolated in such screens. A similar *unc-76* suppressor screen of 96,000 haploid genomes was carried out previously by Dr. Laird Bloom in the laboratory of Dr. H. Robert Horvitz in MIT. All of the *unc-76(e911)* suppressors Dr. Bloom isolated were confirmed to be *smg* suppressors, and both *unc-76(n2398)* and *unc-76(e911)* mutants were suppressed by *smg-1(e1228)* [12]. These results imply that loss of UNC-69 and UNC-76 can not easily be compensated by activating or deactivating other loci that are required for the same cellular processes.

op348 and *op349* share many phenotypic similarities and likely affect two proteins that have similar functions. *op349* only suppresses the weak *unc-69* allele *unc-69(ju69)*, and does not suppress either *unc-69(e602)* or *unc-76(e911)* mutants. It is plausible that *op348* also suppresses *unc-69* in an allele-specific manner, but there is still no evidence to support this notion. It would be interesting to investigate the exact cause of the Sleepy phenotype, as it has not been observed or reported before by other research groups. The Sleepy phenotype seen in *op348* and *op349* mutants implies

that both mutants affect synaptic transmission. The defects in synaptic transmission could be explained in several ways. First, *op348* and *op349* could affect synaptic vesicle exocytosis under normal conditions, but are not required for synaptic vesicle exocytosis upon mechanical stimuli. Second, *op348* and *op349* could affect replenishment of synaptic vesicles into the presynaptic readily releasable pool (RRP). In *op348* and *op349* mutants, the synaptic vesicles are readily released upon mechanical stimuli, but the rate of RRP replenishment is decreased, resulting in smaller RRPs and decreased synaptic transmission. To test this hypothesis, paired-pulse facilitation could be used to record excitatory post-synaptic currents (EPSCs) in *op348* and *op349* mutants. Last but not least, it is possible that both *op348* and *op349* indirectly contribute to the synaptic transmission defects by tipping the balance of the amount of unknown synaptic proteins, reflecting in abnormal presynaptic SNB-1::GFP clusters. It remains to be examined by ultrastructural analysis whether the SNB-1::GFP puncta in the *op348* and *op349* mutants are near the active zones, next to the active zones, or are just floating around in the presynaptic terminals. Cloning of either *op348* or *op349* in the future may elucidate some basic mechanisms controlling presynaptic differentiation.

As a way to improve future *unc-69* suppressor screens, it might be worth to do a visual screen by following neuronal morphology or SNB-1::GFP puncta localization instead of locomotion. Considering the inherent difficulties to isolate *unc-69* and *unc-76* suppressors, a clonal screen might be necessary to uncover recessive suppressors that, when homozygous, are sterile. Conversely, a screen for enhancement of the axonal outgrowth phenotype of the *unc-69(ju69)* mutants will be another possibility,

but it will certainly run the risk to isolate previously characterized axonal guidance mutants.

5. Acknowledgements

First of all, I would like to thank Dr. Michael Hengartner's encouragement in the beginning when initial small-scale screens failed. I also thank Dr. Yishi Jin for her permission of letting me use the *unc-69(ju69); juIs1* strain for the mutagenesis screens. I would also like to thank Dr. Erik Jorgensen for providing me with the mapping strains EG1000 and EG1020 as starting materials of my 2-factor mapping.

References

1. Brenner S: **The genetics of *Caenorhabditis elegans***. *Genetics* 1974, **77**(1):71-94.
2. Anderson P: **Mutagenesis**. *Methods Cell Biol* 1995, **48**:31-58.
3. De Stasio EA, Dorman S: **Optimization of ENU mutagenesis of *Caenorhabditis elegans***. *Mutat Res* 2001, **495**(1-2):81-88.
4. Sulston J, Hodgkin J: **Methods**. In: *The Nematode Caenorhabditis elegans.* Edited by Wood WB. Cold Spring Harbor, New York: Cold Spring Harbor Laboratory Press; 1988: 587-606.
5. Wicks SR, Yeh RT, Gish WR, Waterston RH, Plasterk RH: **Rapid gene mapping in *Caenorhabditis elegans* using a high density polymorphism map**. *Nat Genet* 2001, **28**(2):160-164.
6. Mello CC, Kramer JM, Stinchcomb D, Ambros V: **Efficient gene transfer in *C.elegans*: extrachromosomal maintenance and integration of transforming sequences**. *Embo J* 1991, **10**(12):3959-3970.
7. Lupas A, Van Dyke M, Stock J: **Predicting coiled coils from protein sequences**. *Science* 1991, **252**(5010):1162-1164.
8. Berger B, Wilson DB, Wolf E, Tonchev T, Milla M, Kim PS: **Predicting coiled coils by use of pairwise residue correlations**. *Proc Natl Acad Sci U S A* 1995, **92**(18):8259-8263.
9. Hodgkin J, Papp A, Pulak R, Ambros V, Anderson P: **A new kind of informational suppression in the nematode *Caenorhabditis elegans***. *Genetics* 1989, **123**(2):301-313.

10. Bolten SL, Powell-Abel P, Fischhoff DA, Waterston RH: **The *sup-7(st5)* X gene of *Caenorhabditis elegans* encodes a tRNATrpUAG amber suppressor**. *Proc Natl Acad Sci U S A* 1984, **81**(21):6784-6788.

11. Wills N, Gesteland RF, Karn J, Barnett L, Bolten S, Waterston RH: **The genes *sup-7* X and *sup-5* III of *C. elegans* suppress amber nonsense mutations via altered transfer RNA**. *Cell* 1983, **33**(2):575-583.

12. Bloom L: **Genetic and molecular analysis of genes required for axon outgrowth in *Caenorhabditis elegans***. *Ph.D. Thesis*. Cambridge, Massachusetts: Massachusetts Institute of Technology; 1993.

Figures

Figure 1. *unc-69* suppressor screen.

3-5 mutagenized worms were put on one side of a large 100mm plate and allowed to lay eggs. F1 or F2 generation of worms with improved locomotion were identified based on their ability to crawl to the other side of the plate. Candidate mutants were singled out and transferred to a new plate.

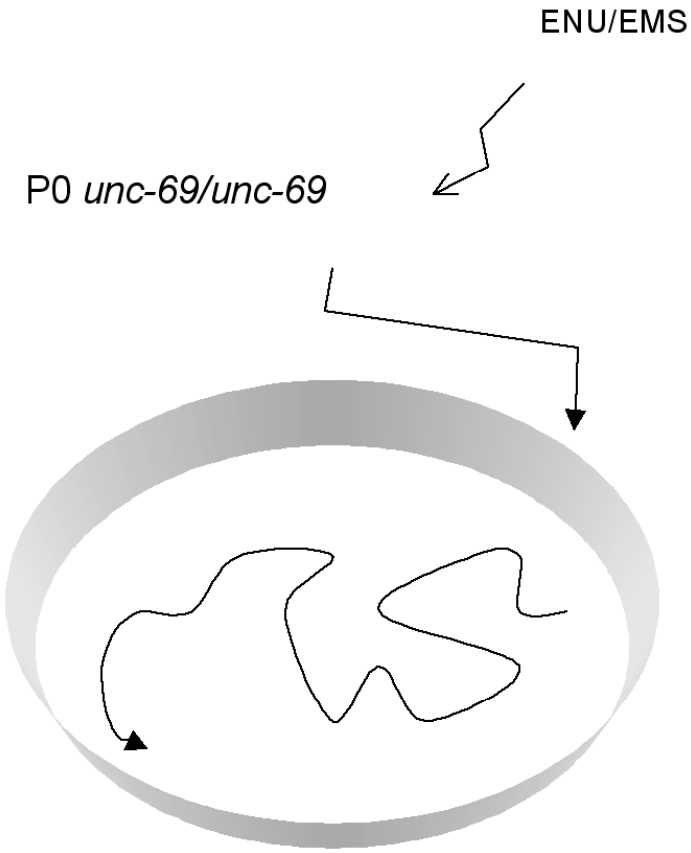
ENU/EMS
P0 *unc-69/unc-69*

Figure 2. *op329* is an intragenic suppressor of *unc-69(e602).*

(A) Sequencing data from wild-type, *unc-69(e602)* and *unc-69(e602 op329)* animals. Note the TTG to TAG nonsense mutation in *unc-69(e602)* mutants, and the TTG to AAG missense mutation in *unc-69(e602 op329)* mutants. (B) Quantitation of locomotion suppression by *op329*. Adult hermaphrodites were assayed for complete sine wave movement per minute. *op329* suppressed locomotion defect of the *unc-69(e602)* mutants to nearly wild-type. For wild type, n=14. For the other genotypes, n=10. Data shown are mean±S.D. (C-D) The L77K mutation has little or no effect on the capability of UNC-69 to form coiled-coil structure. The probability of forming coiled-coil structure was shown for residue 40-100 of the UNC-69(wt) and the UNC-69(L77K) proteins. (C) Coiled-coil structure prediction using the COILS program with a MTIDK matrix. For each calculation, two windows (window=14 and window=28) were used. Primary amino acid sequences in all predictions were of the same register. (D) Coiled-coil structure prediction using the PAIRCOIL program. Primary amino acid sequences in both predictions were of the same register.

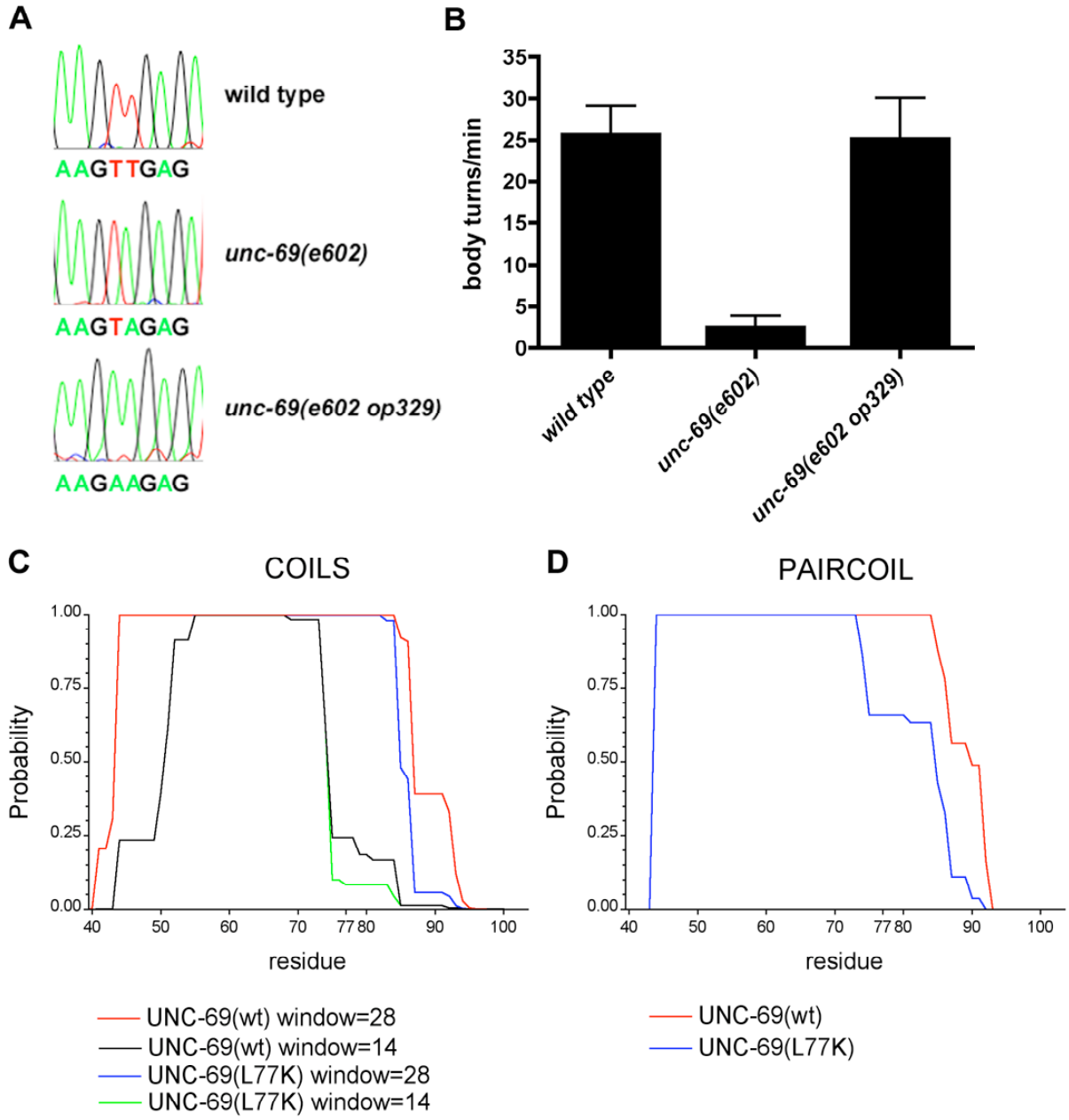
A
wild type
AAGTTGAG
unc-69(e602)
AAGTAGAG
unc-69(e602 op329)
AAGAAGAG
B
body turns/min
35
30
25
20
15
10
5
0
wild type
unc-69(e602)
unc-69(e602 op329)
C
COILS
Probability
1.00
0.75
0.50
0.25
0.00
40
50
60
70
77 80
90
100
residue
UNC-69(wt) window=28
UNC-69(wt) window=14
UNC-69(L77K) window=28
UNC-69(L77K) window=14
D
PAIRCOIL
Probability
1.00
0.75
0.50
0.25
0.00
40
50
60
70
77 80
90
100
residue
UNC-69(wt)
UNC-69(L77K)

Figure 3. *op348* and *op349* dominantly suppress *unc-69(ju69).*

(A) Restoration of locomotion in *op349*/+ heterozygotes. (B) Quantitation of locomotion suppression by *op348* and *op349*. Adult hermaphrodites were assayed for complete sine wave movement per minute. Both *op348* and *op349* dominantly suppressed locomotion defect of the *unc-69(ju69)* mutants to nearly wild-type. However, both *op348* and *op349* failed to suppress *unc-69(ju69)* when homozygous. For wild type, n=14. For *op348/+; unc-69(ju69),* n=7. For the other genotypes, n=10. Data shown are mean±S.D.

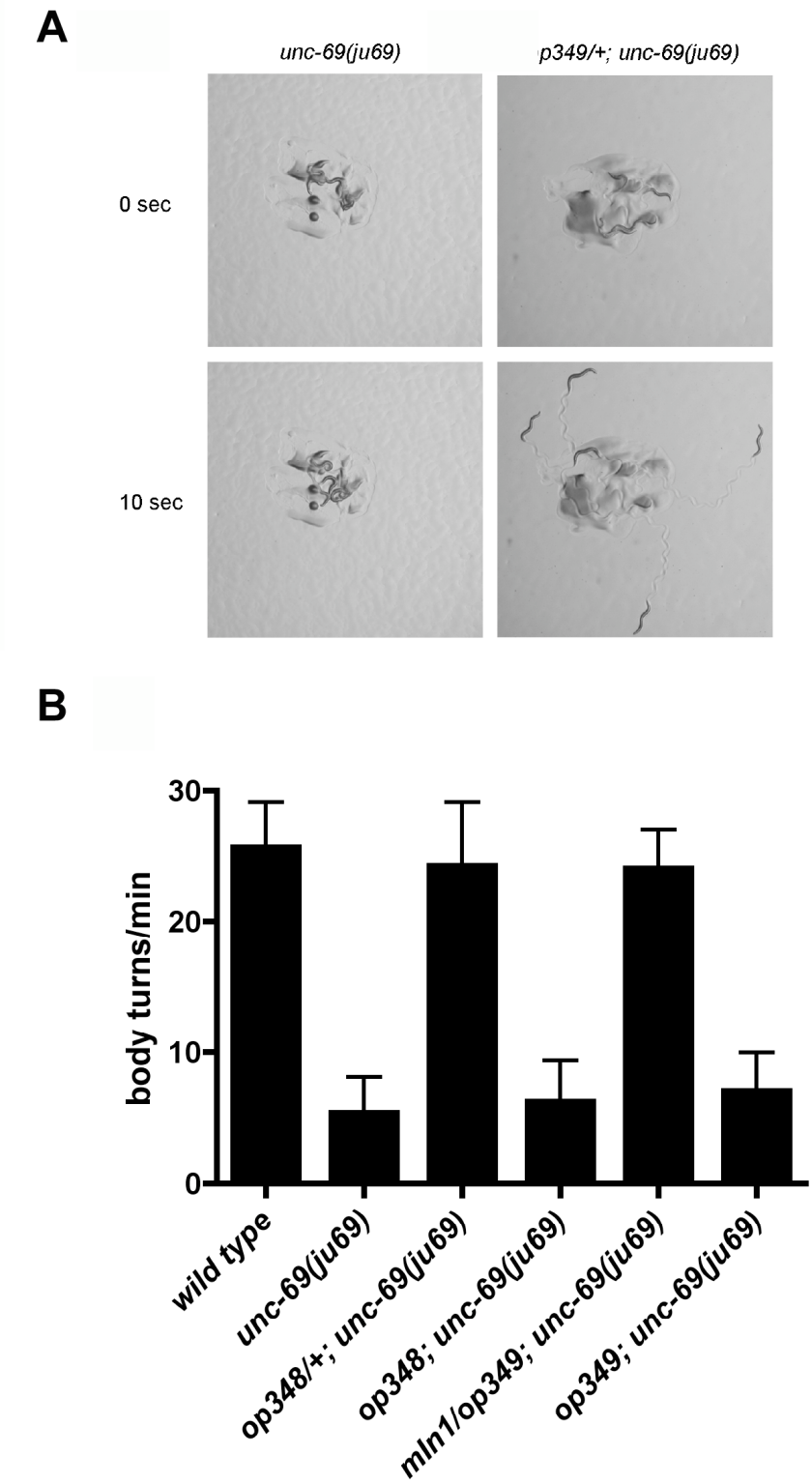
A
unc-69(ju69)
p349/+; unc-69(ju69)
0 sec
10 sec
B
body turns/min
30
20
10
0
wild type
unc-69(ju69)
op348/+; unc-69(ju69)
op348; unc-69(ju69)
mln1/op349; unc-69(ju69)
op349; unc-69(ju69)

Figure 4.

The *op348* and *op349* mutations alter SNB-1::GFP localization. (A) A wild-type hermaphrodite carrying *juIs1* (*P_{unc-25}::snb-1::gfp*). The SNB-1::GFP expressed in the D-type GABAergic motor neurons is evenly distributed in the DNC as equal sized puncta. (B) In a *unc-69(ju69)* mutant, SNB-1::GFP is often missing completely from a stretch of DNC. (C) In a *mIn1/op349; unc-69(ju69)* hermaphrodite, the SNB-1::GFP mislocalization defect is greatly suppressed. However, the distribution of the puncta is not completely normal. Occasionally, some SNB-1::GFP could be seen clustered together in the DNC (arrow). Some puncta on the left are out of the focus plane. (D) In a *op348l unc-69(ju69)* animal, the defect of SNB-1::GFP puncta clustering becomes more pronounced and severe in the DNC (arrow). (E-G) *op349; unc-69(ju69)* mutants. (E) Lateral view of the DNC of a *op349; unc-69(ju69)* hermaphrodite. SNB-1::GFP puncta frequently form abnormal clusters in a stretch of DNC (arrows). (F) Lateral view of the VNC of a *op349; unc-69(ju69)* hermaphrodite. Note that some SNB-1::GFP puncta are contained within a stretch of diffused SNB-1::GFP (arrowhead). (G) Ventral view of the VNC of a *op349; unc-69(ju69)* hermaphrodite. SNB-1::GFP can be seen as large and diffused puncta along the VNC (asterisk). Scale bar = 10 μm.

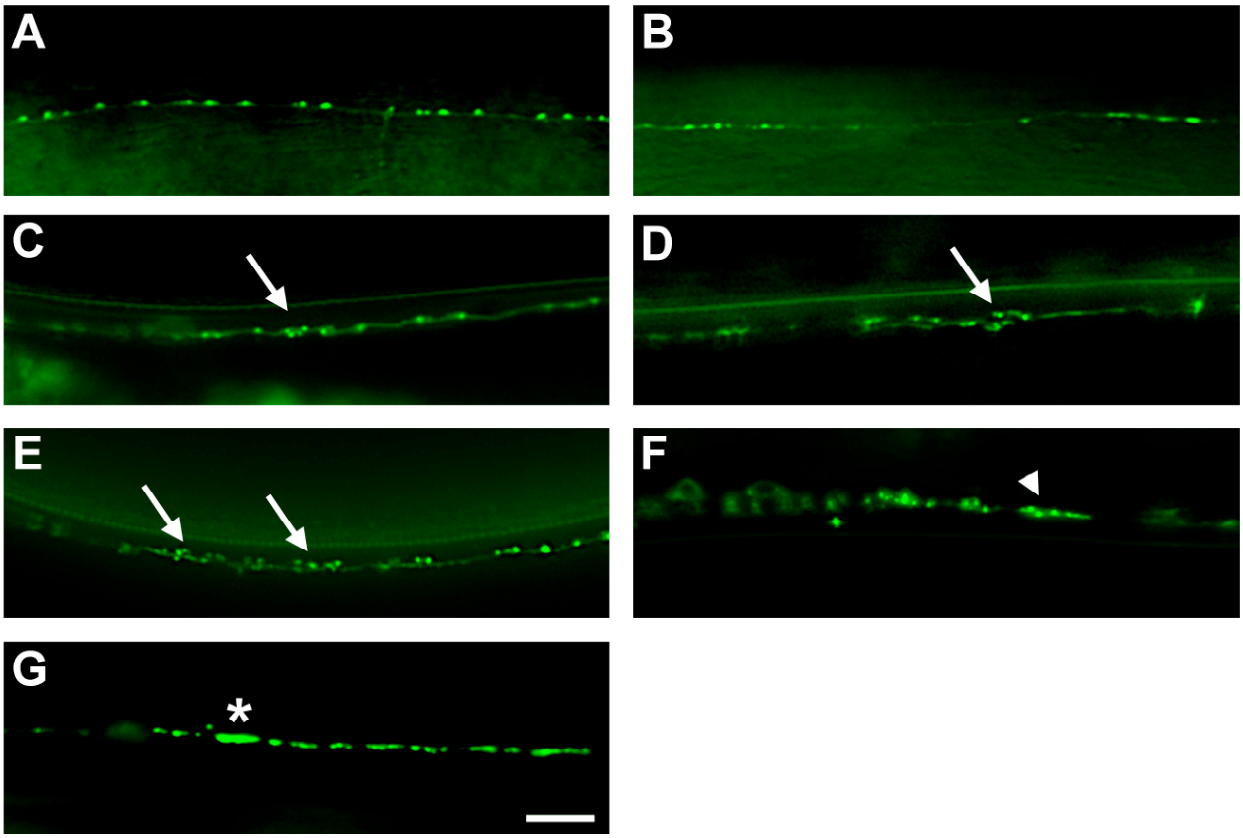
A
B
C
D
E
F
G
*

Figure 5

op349 does not dominantly or recessively suppress locomotion defects of either the *unc-69(e602)* or the *unc-76(e911)* mutants. Adult hermaphrodites were assayed for complete sine wave movement per minute. For wild type, n=14. For the other genotypes, n=10. Data shown are mean±S.D.

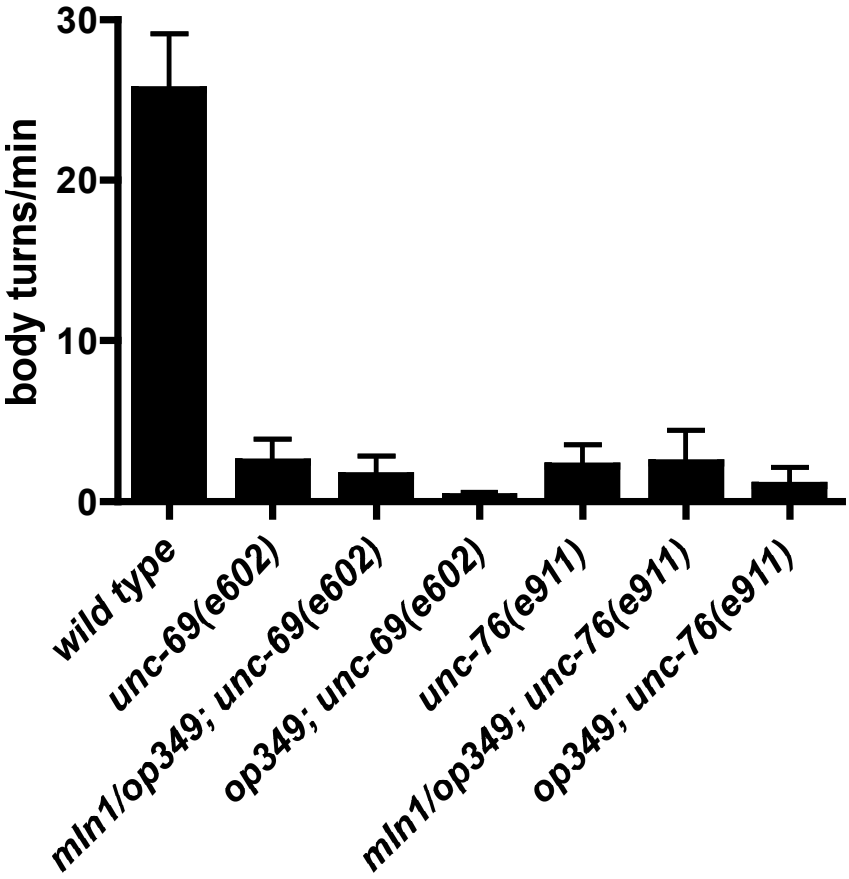
body turns/min
30
20
10
0
wild type
unc-69(e602)
mln1/op349; unc-69(e602)
op349; unc-69(e602)
unc-76(e911)
mln1/op349; unc-76(e911)
op349; unc-76(e911)

Figure 6

Overexpression of a full-length UNC-69(M1I)::GFP protein rescues locomotion defects of the *unc-69(e587)* mutants. pSU86 (*Punc-69::unc-69(M1I)::gfp)* was microinjected at 50 ng/μL into *unc-69(e587); lin-15(n765ts)* mutant hermaphrodites. Non-Muv transgenic hermaphrodites were selected for further characterization. Three independent transgenic lines were assayed for locomotion improvement. For wild type, n=14. For the other genotypes, n=10. Data shown represent mean±S.D. Note that all transgenic lines also carry the *lin-15(n765ts)* mutation in the background.

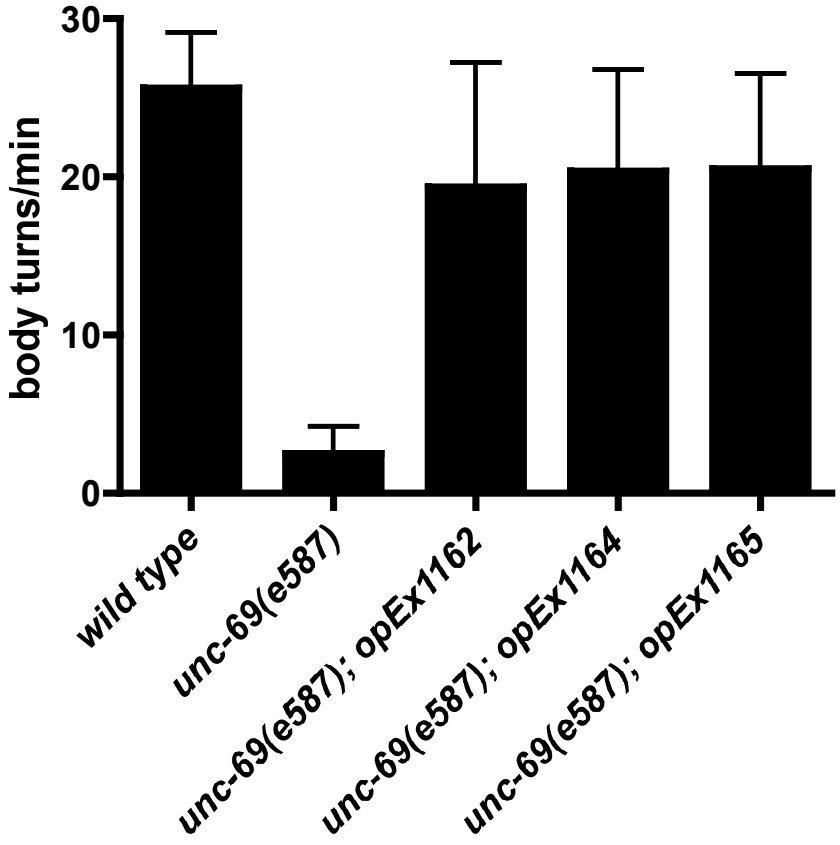
30
20
10
0
body turns/min
wild type
unc-69(e587)
unc-69(e587); opEx1162
unc-69(e587); opEx1164
unc-69(e587); opEx1165

Chapter 4

Future Directions

Part I:

What signaling pathways regulate the activity of the UNC-69/UNC-76 protein complex in *C. elegans*?

1. Preface

The genetic analysis in *C. elegans* has failed to assign *unc-69* and *unc-76* into either Netrin- or Slit-signaling pathways (see Chapter 2). It has also been shown previously that the *unc-76(e911)* mutation does not suppress exuberant axon outgrowth phenotype caused by overexpressing MYR::UNC-40, a constitutively active form of UNC-40, in the AVM mechanosensory neuron [1]. However, the possibility that both UNC-69 and UNC-76 could function downstream of Ephrins remains to be explored. Nevertheless, alternative pathways might exist which can transduce signals that are necessary for UNC-69/UNC-76 protein complex activation (see below).

2. Lessons from mammals: Cdk5 and the NUDEL protein complex

In mammals, a growing number of evidence has put cyclin-dependent kinase 5 (Cdk5) at the center stage as a regulator of cytoskeletal rearrangements and membrane traffic. Cdk5 regulates axonal pathfinding, establishment of the neuromuscular junction, as well as synaptic vesicle exocytosis and endocytosis through phosphorylation of various intracellular substrates [2]. Cdk5 seems to couple cytoskeletal dynamics with the membrane traffic system, as it has been shown to contribute to both anterograde and retrograde axonal transport as well as growth cone collapse elicited by semaphorin3A (Sema3A) in dorsal root ganglion (DRG) neurons [3].

Cdk5 also affects axonal morphology of cultured embryonic cortical neurons via its phosphorylation on NUDEL (NUDE-Like), a mammalian protein similar to *Aspergillus nidulans* NudE protein [4]. As NudE functions in nuclear migration

during hyphal growth in *Aspergillus*, mammalian NUDEL regulates neuron migration by association with cytoplasmic dyneins and LIS1, whose haploinsufficiency in humans causes type I lissencephaly [5]. Dynein is a retrograde motor sliding toward the microtubule minus ends, and it has been suggested that NUDEL modulates activity of the dynein complex as a consequence of Cdk5 phosphorylation. NUDEL is also required for neurofilament assembly and axonal morphogenesis in adult central nervous system (CNS) [6]. Thus, NUDEL appears to be a key protein involved in both neuronal migration and cell shape integrity.

Interestingly, *Drosophila* Lis1 and cytoplasmic dynein are required for axonal transport, in addition to their roles in axonal and dendritic development [7-9]. Genetic analysis in *C. elegans* also suggests that LIS-1 and cytoplasmic dynein function in vesicular transport [10, 11]. It appears that NUDEL might execute its functions in part by regulating axonal transport. As discussed below, emerging evidence starts to argue for a possible role of NUDEL in intracellular trafficking events.

3. DISC1 functions as a link between NUDEL and FEZ1

Recently NUDEL has been found as a binding partner of DISC1 (for Disrupted-In-Schizophrenia 1), and this interaction is essential for neurite outgrowth [12-14]. Although the mechanism of DISC1-mediated neurite outgrowth is not yet clear, some evidence hinted at axonal transport as one of the possible means. In addition to NUDEL, DISC1 physically interacts with fasciculation and elongation protein, zygin/zeta 1 (FEZ1), the mammalian homologue of *C. elegans* axonal transport

protein UNC-76 [15]. DISC1 enhances neurite outgrowth through FEZ1 in NGF-treated PC12 cells, and both DISC1 and FEZ1 colocalize in axonal shafts as puncta and in growth cones of cultured rat hippocampal neurons. Moreover, FEZ1 binds F-actin [15]. In rats, FEZ1 is a substrate of PKCζ and enhances neurite outgrowth upon PKCζ activation [16]. Thus, phophorylated FEZ1 might cooperates with DISC1 to control membrane addition and actin polymerization at the growing tip of the axons.

To date, at least 50 proteins are found to associate with DISC1 (Table 1) [12-15, 17]. They include proteins associated with various organelles, cytoskeletal components, and proteins implicated in synapse formation, signal transduction, chromatin remodeling and transcription. Thus, DISC1 likely acts as an adaptor by integrating a variety of signaling pathways. Alternatively, DISC1 might shuttle between different protein complex to execute its functions. For example, DISC1 may facilitate KIF5-dependent targeting of GRIP1 (Glutamate Receptor Interacting Protein 1) and its associated protein GRIPAP1 into dendrites ([18, 19], and reviewed in [20]). On the other hand, DISC1 could also facilitate transport and/or activation of the UNC-69/UNC-76 protein complex in the axons.

4. From Golgi to centrosome: how are these two subcellular compartments coupled?

So far, it is not known if NUDEL plays any role in FEZ1-dependent transport regarding axonal outgrowth and fasciculation. It is also totally unclear if Cdk5 or NUDEL-modulated dynein activity is essential for any intracellular transport events that are relevant to FEZ1-mediated growth cone extension and cell adhesion. If FEZ1

is an effector of the NUDEL-signaling pathway, then it would be reasonable to predict that FEZ1 and NUDEL would localize to the same organelles and/or subcellular compartments.

DISC1 and NUDEL puncta are both centromeric and axonal, suggestive of a function in microtubule biogenesis [4, 5, 12]. Indeed, DISC1 can be found biochemically in the same subcellular fraction with γ-tubulin [12]. In addition, both DISC1 and NUDEL colocalize in puncta in transiently transfected human neuroblastoma SH-SY5Y cells [12].

Interestingly, FEZ1 is also shown to associate with the centrosome. In mice, two proteins, Necdin and Magel2, physically interact with FEZ1 and FEZ2 [21]. Both Necdin and Magel2 stabilize FEZ1 and FEZ2 by preventing proteasome-dependent degradation. Necdin and Magel2 are two members of the MAGE (stands for Melanoma Antigen Gene Expression) domain-containing proteins whose genes are deleted in patients suffering from the Prader-Willi syndrome, a neurodevelopmental disease characterized by hypothalamic dysfunctions. Some symptoms of the Prader-Willi syndrome are similar to that of another disease, the Bardet-Biedl syndrome (BBS). The Bardet-Biedl syndrome is thought to arise from basal body and cilia dysfunctions, and many of the BBS proteins function in recruitment of centrosomal proteins, microtubule anchoring or intraflagellar transport (IFT) [22-26]. Both Necdin and FEZ1 colocalize near the centrosome in HEK293 cells, and both of them physically interact with the pericentriolar protein BBS4 [21, 24]. In addition, FEZ1 associates with γ-tubulin physically in the presence of Necdin [21]. However, it is also reported that rat FEZ1 subcellularly localizes to the plasma membrane in cultured

COS-7 cells, but is translocated into the cytosol upon PKCζ activation [16]. Thus, the subcellular distribution of FEZ1 might depend on the physiological context and its secondary modifications.

Despite accumulation of evidence supporting a possible role for FEZ1 in centrosomal functions, the molecular analysis of subcellular localization of UNC-76 as well as UNC-76's interaction with UNC-69 in *C. elegans* argue against such centrosomal roles. Our data suggest, although not fully establish, that the UNC-69/UNC-76 protein complex could function in regulating transport of vesicles derived from the Golgi apparatus: both UNC-69 and UNC-76 colocalize as round, perinuclear dots in the soma, and the homologues of UNC-69, Slo1p and SCOCO, interact with the Golgi-tethering proteins Arl3p and ARL1 [27, 28]. However, counterevidence also exists. For example, *C. elegans* UNC-69 is found to be a binding protein of SPD-2 in a large-scale Y2H screen [29]. SPD-2 is involved in centrosome maturation and duplication, and is localized to both the centrioles and the pericentriolar material (PCM) in *C. elegans* [30, 31].

In sum, it is tempting to speculate that the Golgi and the centrosome are not morphologically static, functionally discrete, separate subcellular compartments, but rather are dynamically coupled. Perhaps one of the mediators for this Golgi-centrosome interaction is the cytoplasmic dynein. Cytoplasmic dynein is shown to localize Golgi apparatus near to the centrosome [32]. RNAi knock-down of NUDEL, a potential regulator of dynein activity, as well as overexpression of a DHC-binding defective form of NUDEL, result in Golgi fragmentation [33]. Interestingly, UNC-69 binds DLC-1, the worm homologue of dynein light chain ([29] and Table 3). Golgi-

derived vesicles might require interaction between the UNC-69/UNC-76 protein complex and the centrosomal proteins, possibly through the bridge of cytoplasmic dynein, to be loaded onto the microtubules, which emanate from the centrosome, before embarking on their journey into the axons in a Kinesin-1-dependent manner.

Part II:

How does the UNC-69/UNC-76 protein complex execute its function in the axons?

1. Preface

Based on my observation of distinct subcellular localizations of UNC-69 and UNC-76 in *unc-116(lf)* mutants, I propose that an unknown activity associated with UNC-69 (named activity X) could possibly regulate the shape of UNC-76-associated membranous structure. What could be the identity of this activity X?

2. Could UNC-69 use cytoplasmic dynein to regulate axonal transport?

A possible cue comes from the Y2H screen: UNC-69 is identified as a binding partner of the worm dynein light chain DLC-1 [29]. Since cytoplasmic dynein is possibly required for Cdk5 and NUDEL-mediated vesicular transport, UNC-69 could potentiate the interaction between dynein and NUDEL, or upregulate dynein's activities. However, *C. elegans* LIS-1 and cytoplasmic dynein mutants do not have neuronal morphology defects [10, 11]. Thus, simply loss of dynein activity is not equivalent to complete loss of UNC-69 functions in the nervous system. Additional proteins might be required to mediate UNC-69's functions.

3. What are the roles of UNC-76′s secondary modifications?

On the other hand, it is known that PKCζ-mediated phosphorylation and E4B-mediated polyubiquitination of FEZ1 contribute to its neurite outgrowth activity in mammals [16, 34]. It is likely that some unknown proteins recognize these secondary modifications of FEZ1. Indeed, FEZ1 is found to bind NBR1 (Next to BRCA1), a protein whose functions remain elusive [35]. NBR1 has an ubiquitin-associated

(UBA) domain at its C-terminus, in addition to an octicosapeptide repeat (OPR), a zinc finger (ZZ) domain and a coiled-coil domain. However, the FEZ1-interacting region in NBR1 is mapped outside of the UBA and the coiled-coil domains. Thus, the UBA domain of NBR1 may serve additional functions than simply recruiting NBR1 to polyubiquitinated FEZ1.

Evidence for UNC-76 phosphorylation in *C. elegans* is lacking. PKCζ is an atypical PKC. The *Drosophila* atypical PKC (DaPKC) does not seem to play a role in axonal transport [36]. The only *C. elegans* atypical PKC, PKC-3, is not expressed in the nervous system [37]. Therefore, a different kinase in the invertebrates might fulfill the role of atypical PKC in phosphorylating UNC-76.

4. The choice between fission and fusion

In *unc-69* mutants the SNB-1::GFP puncta are in general bigger than in wild-type worms. This observation, together with the observations that many ectopic branches are sprouting from the soma and axons in the *unc-69* and *unc-76* mutants, suggest that failure of UNC-69/UNC-76 protein complex formation results in inappropriate membrane fusion. In other words, the normal function of the UNC-69/UNC-76 protein function possibly lies in (1) its ability to promote proper fission of the (synaptic) vesicle precursors, and (2) to prevent site-nonspecific fusion of the axonogenic vesicles.

The UNC-69/UNC-76 protein complex is implicated in regulating post-Golgi vesicular transport or maturation in *C. elegans* axons. This model seems to be

compatible with the fission-fusion hypothesis, and is self-explanatory for the observed increase of SNB-1::GFP puncta size in *unc-69* mutants. However, it does not fully explain why a Golgi-associated protein complex could be responsible for preventing vesicular fusion at the plasma membrane. The most parsimonious explanation would be that the ectopic branches seen in the *unc-69* and *unc-76* mutants arise from simply stalled but free-moving vesicles that are in close proximity to the plasma membrane. This explanation also implies that the axonogenic vesicles would have acquired all machinery necessary for fusion with the plasma membrane, however, at a wrong site. The UNC-69/UNC-76 protein complex may, to a less extent, associate with the axonogenic vesicles and prevent their untimely fusion with the plasma membrane by recruiting inhibitory factors. Alternatively, the UNC-69/UNC-76 protein complex might directly inhibit activity of the membrane fusion machinery. Finally, it is possible that UNC-69/UNC-76 prevent excessive somatic and axonal sprouting simply by efficiently transporting mature vesicles to the axon tip, thereby minimizing the time that these vesicles spend near "inappropriate" membranes.

5. A comparison between the exocyst and the UNC-69/UNC-76 protein complexes in regulating membrane transport and exocytosis

Interestingly, mammalian FEZ1 binds Synaptotagmin (Syt) [38]. Syt mediates synaptic vesicle exocytosis upon extracellular Ca^{2+} influx [39]. Since Syt is a synaptic vesicle protein, it could be one of the cargoes that FEZ1 is transporting. Alternatively, FEZ1 might act antagonistically to Syt-mediated synaptic vesicle fusion. To test this idea, I built double mutants between *unc-76* and *snt-1*, the worm homologue of Syt, and could not observe any improvement of the Unc phenotype of

either the *unc-76* or the *snt-1* mutants. Indeed, the observation that Syt is accumulated in axonal clogs in *Drosophila unc-76* mutants [36] strengthens the belief that FEZ1 transports Syt but does not participate in its enzymatic action. Thus, UNC-76 appears to control membrane fusion other than synaptic vesicle exocytosis, although this hypothesis needs to be tested experimentally. For example, a first step would be to use electron microscopy or established electrophysiological methods [40, 41] to determine if constant number of synaptic vesicles is still present in the readily releasable pool (RRP) of the presynaptic terminal in *unc-76* or *unc-69* mutants.

If the prediction is true, then the function of the UNC-69/UNC-76 protein complex might be analogous to that of the exocyst protein complex (Y. Jin, personal communications). Exocyst, as its name implies, is involved in Golgi-plasma membrane transport and exocytosis in budding yeast and is composed of eight subunits [42, 43]. In *Drosophila,* one of the subunits, Sec5, is required for transporting a variety of membrane components in neurons that are important for muscle growth, neurite extension, and maturation of the synaptic boutons at the motor axon terminals [44]. In the absence of Sec5, surface expression of CD8 is reduced, but synaptic transmission is not abrogated, suggestive of functions in membrane fusion events other than synaptic vesicle exocytosis [44]. The mammalian exocyst complex is also involved in neurite outgrowth, and is localized into growing neuronal growth cones [45]. Although both *Sec5* and *Unc-76* mutants are larval lethal in *Drosophila*, several differences between fly *Sec5* and *Unc-76* mutants have to be pointed out: Sec5 exists as puncta whereas endogenous Unc-76 appears diffused in fly neurons [36, 44]. Second, Sec5 is not required for transporting Syt into the axons, although newly synthesized Syt is not carried into the synaptic boutons in Sec5

mutants [44]. Taken together, these data from *Drosophila* studies suggested that the exocyst and Unc-76 protein complexes might target separate or overlapping sets of vesicles to the membrane. To elucidate the mechanism of Unc-76-mediated vesicular trafficking in *Drosophila*, further examination of the role of fly Unc-69 will be essential. Further analysis might also clarify the subcellular localization differences of UNC-76 between flies and worms.

Outlook

Previous attempt to isolate *unc-76* was not successful [46]. In contrast, many *unc-69* suppressors have been isolated (Chapter 3), and further characterizations of these suppressors would be a good way to learn more about the pathway in which UNC-69 participates. Nevertheless, since many of our current ideas about possible functions of the UNC-69/UNC-76 complex comes from the Y2H screens (Tables 1-3) [47], one could in the future address some of the above mentioned questions using a candidate gene approach. However, I still believe that *C. elegans* genetics will provide us with additional insight in parallel. The discovery of *unc-69* in *C. elegans* proves the power of genetics in elucidating basic membrane traffic mechanisms that are relevant to the etiology of human diseases like lissencephaly, schizophrenia and the Prader-Willi syndrome. The tiny worms may still keep us busy, and surprised, for another few years to come.

References

1. Gitai Z, Yu TW, Lundquist EA, Tessier-Lavigne M, Bargmann CI: **The netrin receptor UNC-40/DCC stimulates axon attraction and outgrowth through enabled and, in parallel, Rac and UNC-115/AbLIM**. *Neuron* 2003, **37**(1):53-65.
2. Smith DS, Tsai LH: **Cdk5 behind the wheel: a role in trafficking and transport?** *Trends Cell Biol* 2002, **12**(1):28-36.
3. Li C, Sasaki Y, Takei K, Yamamoto H, Shouji M, Sugiyama Y, Kawakami T, Nakamura F, Yagi T, Ohshima T *et al*: **Correlation between semaphorin3A-induced facilitation of axonal transport and local activation of a translation initiation factor eukaryotic translation initiation factor 4E**. *J Neurosci* 2004, **24**(27):6161-6170.
4. Niethammer M, Smith DS, Ayala R, Peng J, Ko J, Lee MS, Morabito M, Tsai LH: **NUDEL is a novel Cdk5 substrate that associates with LIS1 and cytoplasmic dynein**. *Neuron* 2000, **28**(3):697-711.
5. Sasaki S, Shionoya A, Ishida M, Gambello MJ, Yingling J, Wynshaw-Boris A, Hirotsune S: **A LIS1/NUDEL/cytoplasmic dynein heavy chain complex in the developing and adult nervous system**. *Neuron* 2000, **28**(3):681-696.
6. Nguyen MD, Shu T, Sanada K, Lariviere RC, Tseng HC, Park SK, Julien JP, Tsai LH: **A NUDEL-dependent mechanism of neurofilament assembly regulates the integrity of CNS neurons**. *Nat Cell Biol* 2004, **6**(7):595-608.
7. Murphey RK, Caruccio PC, Getzinger M, Westgate PJ, Phillis RW: **Dynein-dynactin function and sensory axon growth during *Drosophila***

metamorphosis: A role for retrograde motors. *Dev Biol* 1999, **209**(1):86-97.

8. Liu Z, Steward R, Luo L: ***Drosophila* Lis1 is required for neuroblast proliferation, dendritic elaboration and axonal transport**. *Nat Cell Biol* 2000, **2**(11):776-783.

9. Reuter JE, Nardine TM, Penton A, Billuart P, Scott EK, Usui T, Uemura T, Luo L: **A mosaic genetic screen for genes necessary for *Drosophila* mushroom body neuronal morphogenesis**. *Development* 2003, **130**(6):1203-1213.

10. Koushika SP, Schaefer AM, Vincent R, Willis JH, Bowerman B, Nonet ML: **Mutations in *Caenorhabditis elegans* cytoplasmic dynein components reveal specificity of neuronal retrograde cargo**. *J Neurosci* 2004, **24**(16):3907-3916.

11. Williams SN, Locke CJ, Braden AL, Caldwell KA, Caldwell GA: **Epileptic-like convulsions associated with LIS-1 in the cytoskeletal control of neurotransmitter signaling in *Caenorhabditis elegans***. *Hum Mol Genet* 2004, **13**(18):2043-2059.

12. Morris JA, Kandpal G, Ma L, Austin CP: **DISC1 (Disrupted-In-Schizophrenia 1) is a centrosome-associated protein that interacts with MAP1A, MIPT3, ATF4/5 and NUDEL: regulation and loss of interaction with mutation**. *Hum Mol Genet* 2003, **12**(13):1591-1608.

13. Ozeki Y, Tomoda T, Kleiderlein J, Kamiya A, Bord L, Fujii K, Okawa M, Yamada N, Hatten ME, Snyder SH *et al*: **Disrupted-in-Schizophrenia-1 (DISC-1): mutant truncation prevents binding to NudE-like (NUDEL)**

and inhibits neurite outgrowth. *Proc Natl Acad Sci U S A* 2003, **100**(1):289-294.

14. Millar JK, Christie S, Porteous DJ: **Yeast two-hybrid screens implicate DISC1 in brain development and function**. *Biochem Biophys Res Commun* 2003, **311**(4):1019-1025.

15. Miyoshi K, Honda A, Baba K, Taniguchi M, Oono K, Fujita T, Kuroda S, Katayama T, Tohyama M: **Disrupted-In-Schizophrenia 1, a candidate gene for schizophrenia, participates in neurite outgrowth**. *Mol Psychiatry* 2003, **8**(7):685-694.

16. Kuroda S, Nakagawa N, Tokunaga C, Tatematsu K, Tanizawa K: **Mammalian homologue of the *Caenorhabditis elegans* UNC-76 protein involved in axonal outgrowth is a protein kinase C zeta-interacting protein**. *J Cell Biol* 1999, **144**(3):403-411.

17. Miyoshi K, Asanuma M, Miyazaki I, Diaz-Corrales FJ, Katayama T, Tohyama M, Ogawa N: **DISC1 localizes to the centrosome by binding to kendrin**. *Biochem Biophys Res Commun* 2004, **317**(4):1195-1199.

18. Setou M, Seog DH, Tanaka Y, Kanai Y, Takei Y, Kawagishi M, Hirokawa N: **Glutamate-receptor-interacting protein GRIP1 directly steers kinesin to dendrites**. *Nature* 2002, **417**(6884):83-87.

19. Ye B, Liao D, Zhang X, Zhang P, Dong H, Huganir RL: **GRASP-1: a neuronal RasGEF associated with the AMPA receptor/GRIP complex**. *Neuron* 2000, **26**(3):603-617.

20. Hirokawa N, Takemura R: **Molecular motors and mechanisms of directional transport in neurons**. *Nat Rev Neurosci* 2005, **6**(3):201-214.

21. Lee S, Walker CL, Karten B, Kuny SL, Tennese AA, O'Neill M A, Wevrick R: **Essential role for the Prader-Willi syndrome protein necdin in axonal outgrowth**. *Hum Mol Genet* 2005, **14**(5):627-637.

22. Ansley SJ, Badano JL, Blacque OE, Hill J, Hoskins BE, Leitch CC, Kim JC, Ross AJ, Eichers ER, Teslovich TM *et al*: **Basal body dysfunction is a likely cause of pleiotropic Bardet-Biedl syndrome**. *Nature* 2003, **425**(6958):628-633.

23. Blacque OE, Reardon MJ, Li C, McCarthy J, Mahjoub MR, Ansley SJ, Badano JL, Mah AK, Beales PL, Davidson WS *et al*: **Loss of *C. elegans* BBS-7 and BBS-8 protein function results in cilia defects and compromised intraflagellar transport**. *Genes Dev* 2004, **18**(13):1630-1642.

24. Kim JC, Badano JL, Sibold S, Esmail MA, Hill J, Hoskins BE, Leitch CC, Venner K, Ansley SJ, Ross AJ *et al*: **The Bardet-Biedl protein BBS4 targets cargo to the pericentriolar region and is required for microtubule anchoring and cell cycle progression**. *Nat Genet* 2004, **36**(5):462-470.

25. Li JB, Gerdes JM, Haycraft CJ, Fan Y, Teslovich TM, May-Simera H, Li H, Blacque OE, Li L, Leitch CC *et al*: **Comparative genomics identifies a flagellar and basal body proteome that includes the BBS5 human disease gene**. *Cell* 2004, **117**(4):541-552.

26. Kulaga HM, Leitch CC, Eichers ER, Badano JL, Lesemann A, Hoskins BE, Lupski JR, Beales PL, Reed RR, Katsanis N: **Loss of BBS proteins causes anosmia in humans and defects in olfactory cilia structure and function in the mouse**. *Nat Genet* 2004, **36**(9):994-998.

27. Panic B, Whyte JR, Munro S: **The ARF-like GTPases Arl1p and Arl3p act in a pathway that interacts with vesicle-tethering factors at the Golgi apparatus**. *Curr Biol* 2003, **13**(5):405-410.

28. Van Valkenburgh H, Shern JF, Sharer JD, Zhu X, Kahn RA: **ADP-ribosylation factors (ARFs) and ARF-like 1 (ARL1) have both specific and shared effectors: characterizing ARL1-binding proteins**. *J Biol Chem* 2001, **276**(25):22826-22837.

29. Li S, Armstrong CM, Bertin N, Ge H, Milstein S, Boxem M, Vidalain PO, Han JD, Chesneau A, Hao T *et al*: **A map of the interactome network of the metazoan *C. elegans***. *Science* 2004, **303**(5657):540-543.

30. Kemp CA, Kopish KR, Zipperlen P, Ahringer J, O'Connell KF: **Centrosome maturation and duplication in *C. elegans* require the coiled-coil protein SPD-2**. *Dev Cell* 2004, **6**(4):511-523.

31. Pelletier L, Ozlu N, Hannak E, Cowan C, Habermann B, Ruer M, Muller-Reichert T, Hyman AA: **The *Caenorhabditis elegans* centrosomal protein SPD-2 is required for both pericentriolar material recruitment and centriole duplication**. *Curr Biol* 2004, **14**(10):863-873.

32. Corthesy-Theulaz I, Pauloin A, Pfeffer SR: **Cytoplasmic dynein participates in the centrosomal localization of the Golgi complex**. *J Cell Biol* 1992, **118**(6):1333-1345.

33. Liang Y, Yu W, Li Y, Yang Z, Yan X, Huang Q, Zhu X: **Nudel functions in membrane traffic mainly through association with Lis1 and cytoplasmic dynein**. *J Cell Biol* 2004, **164**(4):557-566.

34. Okumura F, Hatakeyama S, Matsumoto M, Kamura T, Nakayama KI: **Functional regulation of FEZ1 by the U-box-type ubiquitin ligase E4B contributes to neuritogenesis**. *J Biol Chem* 2004, **279**(51):53533-53543.

35. Whitehouse C, Chambers J, Howe K, Cobourne M, Sharpe P, Solomon E: **NBR1 interacts with fasciculation and elongation protein zeta-1 (FEZ1) and calcium and integrin binding protein (CIB) and shows developmentally restricted expression in the neural tube**. *Eur J Biochem* 2002, **269**(2):538-545.

36. Gindhart JG, Chen J, Faulkner M, Gandhi R, Doerner K, Wisniewski T, Nandlestadt A: **The Kinesin-associated protein UNC-76 is required for axonal transport in the *Drosophila* nervous system**. *Mol Biol Cell* 2003, **14**(8):3356-3365.

37. Wu SL, Staudinger J, Olson EN, Rubin CS: **Structure, expression, and properties of an atypical protein kinase C (PKC3) from *Caenorhabditis elegans*. PKC3 is required for the normal progression of embryogenesis and viability of the organism**. *J Biol Chem* 1998, **273**(2):1130-1143.

38. Bloom L, Horvitz HR: **The *Caenorhabditis elegans* gene *unc-76* and its human homologs define a new gene family involved in axonal outgrowth and fasciculation**. *Proc Natl Acad Sci U S A* 1997, **94**(7):3414-3419.

39. Sudhof TC: **The synaptic vesicle cycle**. *Annu Rev Neurosci* 2004, **27**:509-547.

40. Raizen DM, Avery L: **Electrical activity and behavior in the pharynx of *Caenorhabditis elegans***. *Neuron* 1994, **12**(3):483-495.

41. Koushika SP, Richmond JE, Hadwiger G, Weimer RM, Jorgensen EM, Nonet ML: **A post-docking role for active zone protein Rim**. *Nat Neurosci* 2001, **4**(10):997-1005.

42. TerBush DR, Maurice T, Roth D, Novick P: **The Exocyst is a multiprotein complex required for exocytosis in *Saccharomyces cerevisiae***. *Embo J* 1996, **15**(23):6483-6494.

43. Guo W, Grant A, Novick P: **Exo84p is an exocyst protein essential for secretion**. *J Biol Chem* 1999, **274**(33):23558-23564.

44. Murthy M, Garza D, Scheller RH, Schwarz TL: **Mutations in the exocyst component Sec5 disrupt neuronal membrane traffic, but neurotransmitter release persists**. *Neuron* 2003, **37**(3):433-447.

45. Vega IE, Hsu SC: **The exocyst complex associates with microtubules to mediate vesicle targeting and neurite outgrowth**. *J Neurosci* 2001, **21**(11):3839-3848.

46. Bloom L: **Genetic and molecular analysis of genes required for axon outgrowth in *Caenorhabditis elegans***. *Ph.D. Thesis*. Cambridge, Massachusetts: Massachusetts Institute of Technology; 1993.

47. Tharin SA: **Molecular and genetic analyses of the axon guidance gene *unc-69***. *Ph.D. Thesis*. Stony Brook, New York 11743, USA: State University of New York at Stony Brook; 2000.

Tables

Table 1. Potential human DISC1-interacting proteins identified in various yeast two-hybrid screens

Name	*Note*	*Cellular functions*	*Ref.*
Organelle-associated			
GM130		Transports and/or processes proteins through Golgi.	[12]
MGAT3		Protein glycosylation in Golgi.	[12]
IMMT	Mitofilin	Unknown mitochondria inner membrane protein.	[12]
NUDE		Cortical neuron migration.	[12]
NUDEL		LIS1-interacting protein; cortical neuron migration; centrosomal.	[10, 11, 12]
kendrin	Pericentrin-B	Centrosomal protein, anchor γ-tubulin complex to centrosomes.	[15]
HRIHFB2072	Similar to SCOCO	*trans*-Golgi-associated protein?	[12]
FEZ1		Axonal transport related to synapse formation and axonal outgrowth.	[13]
Nucleoporin-like			[11]
SYNE-1	Synaptic Nuclei Expressed gene 1	Nuclear envelope protein hypothesized in nuclear maintenance.	[10]
RanBPM	Ran GTPase-binding protein		[10]
Cytoskeleton-related			
Myosin			[10]
MAP1A		Microtubule-binding protein.	[10]
MIP-T3		Microtubule-binding protein.	[10]
Dynactin		Cytoplasmic dynein motor protein complex.	[11]
MGC2599	Similar to KATNA1	Possibly in microtubule-severing.	[12]
Actin-binding protein-like			[11]
ACTN1		Actin bundling and anchoring, neurite extension and adhesion.	[12]
DMT	Dematin	Actin bundling.	[12]
TENC1	Tensin 2	Actin binding, signal transduction and cell migration.	[12]
α-Actinin2		Actin-binding protein, links NR1 and NR2B to PSD; localized to GABAergic interneurons, mediates Ca^{2+}-dependent inactivation of NMDA receptor.	[11]
Spectrin			[11]
SPTAN1	α-Fodrin (spectrin family)		[12]
β4-Spectrin			[10]
Synaptic and signal transduction			
KCNQ5	Potassium chancel		[11]
AKAP9	A-kinase anchoring protein 9/AKAP450	Interacts with NMDA receptor.	[12]
PPFIA4	Liprin alpha 4	Possibly synaptogenesis.	[12]
APLP1		Neurite outgrowth.	[12]

Table 1. Potential human DISC1-interacting proteins identified in various yeast two-hybrid screens (continued).

Name	*Note*	*Ceuular functions*	*Ref.*
GRIPAP1	Glutamate receptor-interacting protein-associated protein/GRASP1	Ras-GEF, interacts with AMPA receptor.	[12]
HAPIP	Huntingtin-associated protein-interacting protein/kalirin	Rho-GEF; Rac-GEF; neurite oiutgrowth and dendritic morphology; inducible nitric oxide synthase regulation.	[12]
ARHGEF11	PDZ-RhoGEF	Axonal outgrowth, interacts with EAAT4 glutamate transporter.	[12]
14-3-3 γ			[11]
Citron		PSD-95 and Rho-binding protein, enriched in glutamatergic synapses.	[11]
FLJ13386		Homology to Citron, Rho-binding protein. Weakly similar to *Drosophila* D-CLIP-190.	[10]
DNA binding/chromatin remodeling			
Est		Transcription factor.	[11]
ATF4	CREB2	Transcription factor.	[10, 12]
ATF5	ATFx	Interacts with GABA-B1 and PTP4A1/CAAX1.	[10]
ATF7ip			[10]
SMARCE1	SNF-related, matrix-associated, actin-dependent regulator of chromatin E1	Chromatin remodeling.	[12]
Others			
FLJ39502			[10]
ITSN			[10]
Collagen type IV			[10]
EIF3	Eukaryotic translation initiation factor 3		[10]
HRC1			[10]
KIAA1377			[10]
KIAA0373			[12]
WKL1		Previously associated with catatonic schizophrenia (questionable) and megalencephalic leukoencephalopathy with subcortical cysts (MLC).	[12]
APAP2		A protein with multiple ankyrin repeats.	[10]
Uncharacterized sequences			[11]

Table 2. Potential candidate proteins interacting with UNC-76/Unc-76/FEZ1/FEZ2.

Name	*Organism*	*Methods*	*Cellular functions*	*Ref.*
UNC-69	*C. elegans*	Y2H; pull down	Synaptic vesicle trafficking, axonal outgrowth and fasciculation.	[45]
KHC	*D. melanogaster*	Y2H; pull down	Kinesin heavy chain.	[34]
PKCζ C1 regulatory subunit	*R. norvegicus*	Y2H; coIP	Atypical protein kinase C that could phosphorylate FEZ1/FEZ2.	[14]
Synaptotagmin	*R. norvegicus*	biochemical	v-SNARE, synaptic vesicle fusion.	[36]
E4B	*M. musculus*	Y2H (human-mouse); coIP	U-box-type ubiquitin ligase that polyubiquitinates human FEZ1; neuritogenesis.	[32]
Necdin	*M. musculus*	Y2H; coIP	Prader-Willi syndrome protein, induces neuronal differentiation.	[19]
Magel2	*M. musculus*	Y2H; coIP	Prader-Willi syndrome protein.	[19]
BBS4	*M. musculus*	coIP	Bardet-Biedl syndrome protein; centrosomal protein involved in centrosome and basal body/cilia functions.	[19]
γ-tubulin	*M. musculus*	coIP	Centrosomal protein.	[19]
DISC1	*H. sapiens*	Y2H; coIP	Disrupted in Schizophrenia 1; neurite outgrowth.	[13]
NBR1	*H. sapiens*	Y2H; coIP	Next to BRCA1; function unknown, possibly neural development. Contains a ubiquitin-associated domain.	[33]
CIB	*H. sapiens*	Y2H	Calcium and integrin binding protein; associated with Fnk/Snk and presenilin 2.	[33]
F-actin	*R. norvegicus; H. sapiens*	Pull down (rat); coIP (human-rat); subcellular fractionation (human)		[13]

Table 3. Potential candidate proteins interacting with Slo1p/UNC-69/SCOCO

Name	*Organism*	*Methods*	*Cellular functions*	*Ref.*
Arl3p	*S. cerevisiae*	Y2H; pull down	Vesicular trafficking	[25]
UNC-76	*C. elegans*	Y2H; pull down	Synaptic vesicle trafficking, axonal outgrowth and fasciculation.	[45]
Y116A8C.36	*C. elegans*	Y2H	Similar to Intersectin.	[45]
RFP-1	*C. elegans*	Y2H	Ring finger protein, E3 ubiquitin ligase involved in syntaxin degradation.	[45]
K02D10.1	*C. elegans*	Y2H	Similar to SNAP-29.	[45]
F12F6.5	*C. elegans*	Y2H	Similar to Rho-GAP hematopoietic protein C1 (p115).	[45]
K09F6.7	*C. elegans*	Y2H	Similar to ARD-1; also predicted as E3 ubiquitin ligase .	[45]
F25H2.5	*C. elegans*	Y2H	Similar to nucleoside diphosphate kinase	[45]
UNC-15	*C. elegans*	Y2H	Paramyosin.	[45]
UNC-54	*C. elegans*	Y2H	Myosin heavy chain.	[45]
IFD-1	*C. elegans*	Y2H	Intermediate filament.	[45]
MUA-6/IFA-2	*C. elegans*	Y2H	Intermediate filament; muscle attachment.	[45]
IFA-4	*C. elegans*	Y2H	Intermediate filament.	[45]
IFP-1	*C. elegans*	Y2H	Nonessential intermediate filament protein.	[45]
IFD-2	*C. elegans*	Y2H	Nonessential intermediate filament protein.	[45]
F37A4.5	*C. elegans*	Y2H	C6.1A/MPR1/PAD-1/F37A4.5 family, similar to proteasome regulatory subunit S12.	[45]
F56F11.4	*C. elegans*	Y2H	Similar to proteasome regulatory subunit 8.	[45]
HCP-1	*C. elegans*	Y2H	Homologous to mammalian CENP-F; mitotic chromosome segregation.	[45]
K07C11.9	*C. elegans*	Y2H	Unknown.	[45]
C27H5.2	*C. elegans*	Y2H	Unknown.	[45]
LAM-1	*C. elegans*	Y2H	Laminin.	[45]
W10G11.19	*C. elegans*	Y2H	Unknown.	[45]
F21H11.2	*C. elegans*	Y2H	Unknown.	[45]
F41H10.4	*C. elegans*	Y2H	Unknown.	[45]
T24H7.4	*C. elegans*	Y2H	Unknown.	[45]
DLC-1	*C. elegans*	Y2H	Dynein light chain.	[27]
SPD-2	*C. elegans*	Y2H	Centrosome maturation and duplication; locates in both centrioles and PCM (pericentriolar material).	[27]
ARL1	*H. sapiens*	Y2H; pull down	post-Golgi membrane trafficking.	[26]

Appendix I

Design of a conditional, tissue-specific RNAi-mediated gene knock down system in *C. elegans*

1. Introduction

In mammals and *Drosophila*, it is possible to selectively knock out a gene of interest in a specific tissue at a specific time (e.g., Cre-loxP in mice and FRT/UAS-GAL4 in *Drosophila*). In contrast, it is not yet possible to do this in worms. Some research groups have attempted to apply both systems in worms (e.g. the groups of Drs. Julie Ahringer and Barbara Conradt), but none of them has yet reported satisfying results.

It is well documented that double-stranded RNA (dsRNA) is a potent inducer of RNAi response. Long dsRNA molecules are recognized by a Dicer-containing complex and digested to generate 21-23 nucleotide small interfering RNAs (siRNAs). These siRNAs then associate with the RISC (RNAi-induced silencing complex). These recognize through base pairing mRNAs with complementary sequences and degrade them. In *C. elegans*, the RNAi scenario is further helped by the action of RNA-dependent RNA polymerases that extend the siRNA-mRNA duplex in a 5' to 3' manner, generating new dsRNA molecules that serve as additional substrates for Dicer and hence amplifies the RNAi response [1]. One way of conditionally producing dsRNAs in the cell is to clone part of the gene of interest as an inverted repeat under the control of a heat shock promoter. In animals transgenic for such a construct, a short heat shock will lead to the generation of the hairpin dsRNA and hence activation of RNAi [2]. The disadvantage of this method is that it is not tissue-specific.

I have tried to develop an alternative method, based on the particular properties of RNAi in *C. elegans*, to overcome this problem. In my design, I use a stretch of

foreign DNA as the priming sequence (i.e. ribulose biphosphate carboxylase or Rubisco, a gene involved in photosynthesis in plants), and append it to the 3' end of the gene of interest. The hybrid transcript is transcribed from a tissue-specific promoter. The second construct contains an inverted priming sequence driven by a heat shock promoter. Worms carrying these two constructs will only have both strands of priming sequence expressed in the specific tissue, and only after heat shock (Figure 1). Thus, this treatment should result in the tissue-specific generation of dsRNA of the priming sequence in the tissue of interest. Because of the presence of RNA-dependent RNA polymerases, new dsRNA molecules will eventually be generated that also include the gene of interest (located 5' of the priming sequence), and result in the knock down of that gene. If successful, this technique would greatly facilitate our understanding of gene function within a subset of cells, e.g. neurons at a given time.

2. Materials and Methods

Plasmid subclonings were done following standard procedures [3]. A barley Rubisco cDNA fragment of about 500 bp was kindly provided by Dr. Catherine Feuillet in the laboratory of Dr. Beat Keller, Institut für Pflanzenbiologie, University of Zurich, Switzerland. The Rubisco cDNA was PCR amplified and inserted into pCZ245 ($P_{unc\text{-}25}$*::unc-25*$_{a.a.\ 1\text{-}13}$*::gfp*; provided by Dr. Yishi Jin, University of California, Santa Cruz, USA*)* immediately after the stop codon of the ORF to create pSU14. The same Rubisco cDNA was inverted subcloned into pPD49.78 (provided by Dr. Andrew Fire, Carnegie Institute of Washington, USA) downstream of the heat shock promoter *hsp16-2* to create pSU13. The structure of both pSU13 and pSU14 was confirmed by

sequencing. The coelomocyte-expressing *ofm-3::gfp* plasmid [4] was provided by Dr. Piali Sengupta (Brandeis University, USA) as a coinjection marker. Dr. H. Robert Horvitz (Massachusetts Institute of Technology, USA) provided me with the pL15-EK plasmid containing the *lin-15* genomic fragment as an additional coinjection marker.

Two separate transgenic strains were created using germ line transformation [5]. The genotype of these two strains are as follows: strain #1 (WS3676) – *kyIs156 [AWB::odr-10::gfp]; opEx1167 [pSU14; rol-6(su1006)]*; strain #2 (WS3764) – *lin-15(n765); opEx1179 [pSU13; ofm-3::gfp; lin-15(+)]*. For creating strain #1, pSU14 was injected at 50 ng/μL together with 150 ng/μL pRF4 into the *kyIs156* strain. For creating strain #2, pSU13 and *ofm-3::gfp* plasmids were coinjected at 24 ng/μL and 30 ng/μL respectively, together with 150 ng/μL of pL15-EK into the *lin-15(n765)* mutant strain. Transgenic lines were selected at 20°C following injection, and maintained at 20°C. The presence of Rubisco was confirmed by PCR in both transgenic strains.

Prior to experiments, these two strains (WS3676 and WS3764) were crossed to generate a strain (WS3768) carrying both extrachromosomal arrays (*kyIs156; opEx1167; opEx1179)*, and kept at 20°C before heat shock. Adult transgenic worms carrying both $P_{unc\text{-}25}$*::gfp* and *ofm-3::gfp* were heat shocked in a 33°C water bath for 30 min, then kept at 20°C before examination using a dissecting microscope equipped with epifluorescence (M_2Bio, Zeiss).

3. Results

According to my design, Rubisco-specific dsRNA will form upon heat shock in the D-type GABAergic neurons in which *unc-25* promoter is active, but not in any other tissue. However, I did not observe a dramatic decrease in GFP fluorescence intensity in the D-type GABAergic neurons following heat shock. The GFP in the D-type GABAergic neurons was still present even 48 hours after heat shock (data not shown), suggesting that no or very little RNA interference occurred in these neurons.

4. Discussion

There are several possible reasons for my failure to observe a reduction in GFP fluorescence in the D-type GABAergic neurons. First, the Rubisco sequence in transcripts derived from pSU14 might be spliced out by the spliceosomes when the pre-mRNAs are incorporated into the hnRNP particles in the nuclei of the GABAergic neurons. Second, the extrachromosomal array *opEx1179* may be excluded from the *opEx1167*-carrying, P_{unc-25}::GFP-positive D-type GABAergic neurons due to chromosomal nondisjunction during cell division. Last, and perhaps least likely, the *hsp16-2* promoter might not be potent enough to generate adequate amount of transcripts containing the inverted Rubisco sequence during a 30 min course of heat shock, and these transcripts might be regarded as toxic and are quickly degraded.

To address these issues and to improve efficacy of the technique, RT-PCR could be used to assay for presence of the Rubisco-containing transcripts in the transgenic

worms after heat shock. In addition, an extrachromosomal array containing both pSU13 and pSU14 can be generated by co-injection to ensure expression of both transcripts in the same neurons upon heat shock. A decrease in DNA concentration for generation of the extrachromosomal arrays may be helpful to bring down the threshold for detection of the RNAi effect in the GABAergic neurons. Finally, a heat shock-inducible double-strand Rubisco hairpin RNA may trigger the RNAi response more effectively in the neurons of interest. Shifting the heat shock time earlier to the L1 larval stage could possibly overcome the problem of GFP perdurance.

References

1. Tijsterman M, Ketting RF, Plasterk RH: **The genetics of RNA silencing**. *Annu Rev Genet* 2002, **36**:489-519.
2. Tavernarakis N, Wang SL, Dorovkov M, Ryazanov A, Driscoll M: **Heritable and inducible genetic interference by double-stranded RNA encoded by transgenes**. *Nat Genet* 2000, **24**(2):180-183.
3. Sambrook J, Fritsch EF, Maniatis T: **Molecular cloning: a laboratory manual.** Cold Spring Harbor, New York: Cold Spring Harbor Laboratory Press; 1989.
4. Miyabayashi T, Palfreyman MT, Sluder AE, Slack F, Sengupta P: **Expression and function of members of a divergent nuclear receptor family in *Caenorhabditis elegans***. *Dev Biol* 1999, **215**(2):314-331.
5. Mello CC, Kramer JM, Stinchcomb D, Ambros V: **Efficient gene transfer in *C.elegans*: extrachromosomal maintenance and integration of transforming sequences**. *Embo J* 1991, **10**(12):3959-3970.

Figure

Figure 1. Schematic of tissue-specific and conditional knock-down using RNAi

unc-25 is the *C. elegans* homologue of the vertebrate glutamate decarboxylase, and is only expressed in the GABAergic motor neurons, including 13 DD and 6 VD neurons. After heatshock, the efficiency of RNAi is monitored by disappearance of GFP from the D-type neurons and by scoring the percentage of Unc worms.

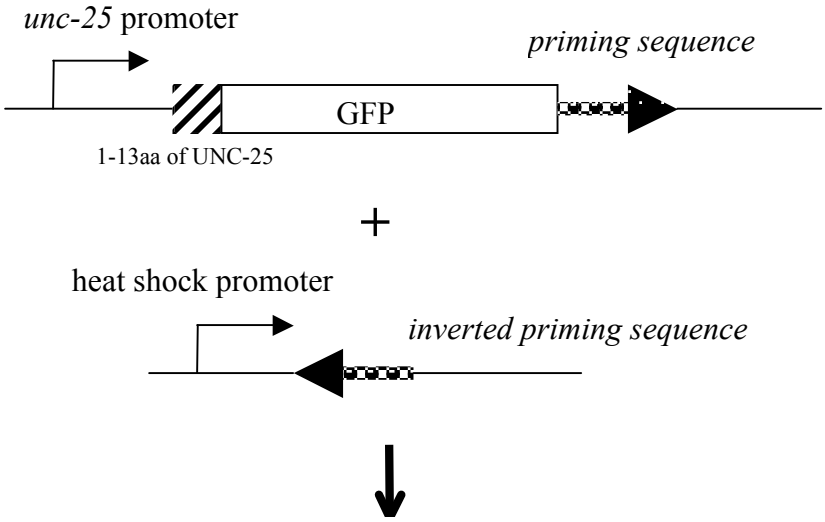

Conditional knockdown in D type GABAergic neurons